



**VERIFICATION OF METEOROLOGICAL DATA REPORTS
FROM THE RQ-4A GLOBAL HAWK UNMANNED AERIAL VEHICLE**

THESIS

Steven M. Callis, Captain, USAF

AFIT/GM/ENP/04-03

**DEPARTMENT OF THE AIR FORCE
AIR UNIVERSITY**

AIR FORCE INSTITUTE OF TECHNOLOGY

Wright-Patterson Air Force Base, Ohio

APPROVED FOR PUBLIC RELEASE; DISTRIBUTION UNLIMITED

The views expressed in this thesis are those of the author and do not reflect the official policy or position of the United States Air Force, Department of Defense, or the United States Government.

AFIT/GM/ENP/04-03

VERIFICATION OF METEOROLOGICAL DATA REPORTS
FROM THE RQ-4A GLOBAL HAWK UNMANNED AERIAL VEHICLE

THESIS

Presented to the Faculty

Department of Engineering Physics

Graduate School of Engineering and Management

Air Force Institute of Technology

Air University

Air Education and Training Command

In Partial Fulfillment of the Requirements for the

Degree of Master of Science in Meteorology

Steven M. Callis, BS

Captain, USAF

March 2004

APPROVED FOR PUBLIC RELEASE; DISTRIBUTION UNLIMITED

VERIFICATION OF METEOROLOGICAL DATA REPORTS
FROM THE RQ-4A GLOBAL HAWK UNMANNED AERIAL VEHICLE

Steven M. Callis, BS

Captain, USAF

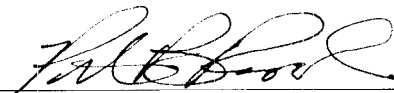
Approved:



Ronald P. Lowther (Chairman)

8 MAR 04

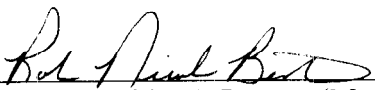
date



Peter B. Roohr (Member)

8 MAR 04

date



Robin N. Benton (Member)

8 Mar 04

date

Abstract

Unmanned aerial vehicles (UAVs) have onboard sensors that continuously record weather data during their missions. This information is extremely valuable to both the meteorological and UAV communities with numerous potential benefits, which include improved weather forecast products and additional weather intelligence for military planners. The value of any dataset is directly related to its accuracy and this research determined the accuracy of weather data obtained from a particular UAV, the RQ-4A Global Hawk. This was accomplished through statistical analysis and comparisons with upper-air data and Atmospheric Slant Path Analysis Model (ASPAM) profiles of the atmosphere. Recommendations are provided for the use of this valuable environmental intelligence source to multiple user communities.

Similar sensors exist on commercial aircraft using the Aircraft Communications Addressing and Reporting System (ACARS). Data from ACARS-equipped aircraft are compiled and quality controlled by the National Weather Service Forecast Systems Laboratory, then processed and made available to numerous agencies. Personnel use the information not only to enhance their forecast products but also as a data source for ingest into numerical weather prediction models. ACARS data are more spatially and temporally available than rawinsonde data, thus potentially having a more significant impact on upper-air analysis models. Forecasters also use this near-real-time data to

enhance their products such as weather warnings and advisories. ACARS information is a proven asset to the weather community as well as mission planners.

Methods analogous to the implementation and quality control of ACARS data can also be applied to the information obtained from UAVs since its accuracy is demonstrated in this research. This study illustrates the utility of the UAVs to create on-demand upper-air soundings for any location worldwide, whereas ACARS data are limited to commercial aircraft routes. The use of this data can greatly enhance forecast models and products especially in data-sparse regions, as well as provide a weather reconnaissance capability to military planners.

Acknowledgments

I would like to thank the Lord for getting me through this experience. His ultimate wisdom, guidance, and love helped me remain focused and pushed me through the more difficult times. I am truly indebted to my faculty advisor, Lt Col Ron Lowther, for his guidance, support, and patience throughout this endeavor. I am also grateful to Lt Col Pete Roohr and Maj Nicole Benton for their assistance as members of my committee. The support provided by Professor Dan Reynolds is appreciated, as well. I will always cherish the love and support of my wife and daughter. This assignment was a true test of our relationship and I am thankful for their patience and understanding.

I would also like to thank my sponsors, the 88th Weather Squadron and the Global Hawk SPO. I am grateful to the SPO for its support and funding, which was vital to this research. The assistance provided by Capt Harm Visser, Mr. John Polander, Mr. Jim Crouch, Ms. Betty Staggs, and Mr. Steve Yamaguchi is very much appreciated.

I am thankful to Mr. Chan Vong of the 452nd FLTS at Edwards AFB. His knowledge and help were essential to this research and provided a starting point for my work. The assistance of Mr. Phil Harvey of the Edwards AFB weather unit is also appreciated. I would like to thank the AFCCC personnel who aided this research, especially TSgt John Kovachich and Mr. Gary Swanson. Finally, I am grateful to my fellow classmates. Their support and camaraderie will always be treasured.

Steven M. Callis

Table of Contents

	Page
Abstract.....	iv
Acknowledgments.....	vi
List of Figures.....	x
List of Tables	xiii
1. Introduction.....	1
a. Problem statement.....	2
b. Objectives	4
c. Approach.....	5
1) Data acquisition	5
2) Data formatting.....	5
3) Data verification.....	6
2. Literature Review.....	7
a. ACARS background	7
b. ACARS data use	9
1) Thunderstorms	9
2) Turbulence	11
3) Winter weather.....	13
4) Airline mission control	15
c. ACARS accuracy and quality control.....	16
d. UAV background.....	17
e. Possible uses of UAV data.....	17
f. UAV accuracy and quality control	18
3. Data Collection and Review	19
a. Data collection	19
1) Global Hawk.....	19
2) ASPAM.....	21
3) RAOB	22
b. Data limitations.....	23
1) Global Hawk.....	23
2) ASPAM.....	23
3) RAOB	24

4. Methodology	26
a. Data acquisition	26
1) Global Hawk	26
2) ASPAM	27
3) RAOB	27
b. Data formatting	28
1) Global Hawk	28
2) ASPAM	30
3) RAOB	31
c. Data verification	31
1) Statistical overview	32
2) Wind direction techniques	38
5. Analysis and Results	40
a. Pressure	40
1) ASPAM	40
2) RAOB	44
b. Temperature	46
1) ASPAM	47
2) RAOB	49
c. Wind speed	52
1) ASPAM	53
2) RAOB	57
3) ASPAM – adjusted wind data	59
4) RAOB – adjusted wind data	63
d. Wind direction	67
1) RMS vector error	67
2) Mean difference	68
6. Conclusions and Recommendations	69
a. Conclusions	69
b. Recommendations	73
1) For Air Force Weather	73
2) For Global Hawk SPO	74
3) For future research	74
Appendix A: Acronyms	75
Appendix B: Upper-Level Wind Analyses	76
Appendix C: Global Hawk Flight Level Information	81

Appendix D: Global Hawk Data Reports & Flight Mode	99
Appendix E: Global Hawk Dimensions.....	101
Bibliography	102

List of Figures

Figure	Page
1. The RQ-4A Global Hawk	3
2. A 24-h worldwide ACARS/AMDAR plot for 27 Mar 2002	8
3. ACARS coverage over the CONUS for 27 Mar 2002.....	8
4. ACARS sounding from O'Hare at 1515 UTC.....	10
5. ACARS sounding from O'Hare at 1623 UTC.....	10
6. ACARS sounding from O'Hare at 1738 UTC.....	11
7. ACARS wind data between 25,692 and 37,008 ft, for the period 1200 UTC to 1459 UTC January 17, 1998	12
8. ACARS sounding showing above-freezing layer.....	14
9. ACARS sounding showing above-freezing layer diminishing.....	14
10. ACARS wind data between 22,000 and 39,000 ft.....	15
11. Aeronautical map of Edwards AFB military operating areas.....	20
12. Latitude versus longitude plot of Global Hawk flight routes for all five examined missions	21
13. Scatterplot of Global Hawk pressure versus ASPAM pressure.....	33
14. Simple linear regression scatterplot and fitted line of Global Hawk pressure versus ASPAM pressure.....	40
15. Regression analysis results of Global Hawk pressure versus ASPAM pressure.....	41
16. Residual versus predicted plots of ASPAM pressure for Global Hawk missions 1 through 5	43
17. Simple linear regression scatterplot and fitted line of Global Hawk pressure versus RAOB pressure	44

18.	Regression analysis results of Global Hawk pressure versus RAOB pressure	45
19.	Residual versus predicted plots of RAOB pressure for Global Hawk missions 1, 4, and 5.....	46
20.	Simple linear regression scatterplot and fitted line of Global Hawk temperature versus ASPAM temperature	47
21.	Regression analysis results of Global Hawk temperature versus ASPAM temperature	48
22.	Residual versus predicted plots of ASPAM temperature for Global Hawk missions 1 through 5.....	50
23.	Simple linear regression scatterplot and fitted line of Global Hawk temperature versus RAOB temperature.....	51
24.	Regression analysis results of Global Hawk temperature versus RAOB temperature.....	51
25.	Residual versus predicted plots of RAOB temperature for Global Hawk missions 1, 4, and 5.....	53
26.	Simple linear regression scatterplot and fitted line of Global Hawk wind speed versus ASPAM wind speed	54
27.	Regression analysis results of Global Hawk wind speed versus ASPAM wind speed	55
28.	Residual versus predicted plots of ASPAM wind speed for Global Hawk missions 1 through 5.....	56
29.	Simple linear regression scatterplot and fitted line of Global Hawk wind speed versus RAOB wind speed.....	57
30.	Regression analysis results of Global Hawk wind speed versus RAOB wind speed.....	58
31.	Residual versus predicted plots of RAOB wind speed for Global Hawk missions 1, 4, and 5.....	59
32.	Simple linear regression scatterplot and fitted line of Global Hawk wind speed versus ASPAM wind speed with adjusted wind data	61

33.	Regression analysis results of Global Hawk wind speed versus ASPAM wind speed with adjusted wind data	62
34.	Residual versus predicted plots of ASPAM wind speed for Global Hawk missions 1 through 5 with adjusted wind data	64
35.	Simple linear regression scatterplot and fitted line of Global Hawk wind speed versus RAOB wind speed with adjusted wind data	65
36.	Regression analysis results of Global Hawk wind speed versus RAOB wind speed with adjusted wind data	66
37.	Residual versus predicted plots of RAOB wind speed for Global Hawk missions 1, 4, and 5 with adjusted wind data	67
38.	Atmospheric sounding plots of temperature versus pressure from Global Hawk missions 1 through 5	72

List of Tables

Table	Page
1. Percentage of rejected data from U.S. Navy quality control methods.....	17
2. Global Hawk flight levels examined and differences from corresponding 500-foot levels	29

VERIFICATION OF METEOROLOGICAL DATA REPORTS
FROM THE RQ-4A GLOBAL HAWK UNMANNED AERIAL VEHICLE

1. Introduction

Unmanned aerial vehicles (UAVs) can provide continuous weather data during all aspects of their flight mission. This information, if made available, would be an asset not only to weather forecasters but also UAV operators and mission planners. An increase in the amount of environmental intelligence would improve weather products and aid UAV mission planners and operators in their decision-making processes. The value of any dataset is directly proportional to its accuracy. Irrelevant or inaccurate information would only amplify errors already inherent in any process. Therefore, efforts must be made to ensure the validity of available data from UAVs.

Similar sensors exist on some commercial aircraft, which transmit weather information along with other flight data by a method called Aircraft Communication Addressing and Reporting System (ACARS). The environmental intelligence obtained from these aircraft has been used successfully for the past decade to improve numerical weather prediction (NWP) models, enhance forecast products, and assist in flight planning (Moninger et al. 2003). Pressure, temperature, wind speed, and wind direction are reported by all ACARS equipped aircraft and some more advanced aircraft provide moisture and turbulence data as well. There are numerous other uses for these data and studies continue to show their value. Before this information was made available to the weather community and other agencies, it was examined to determine its accuracy. It was shown to be a valid source of environmental information and then provided for use.

Quality control is a key ingredient in the processing of the data and ensures the continued accuracy of the information. Thus, the value of products created with this information is maintained.

UAV meteorological data may be used and validated in much the same way as ACARS weather data. This study briefly describes the ACARS process and presents details on weather observations provided by the system. Some of the uses and benefits of the data are also explained. Then a short discussion on current quality control methods will illustrate the validity of these data. A comparison is then made between ACARS and UAV data, showing how environmental intelligence available on UAVs can be exploited to improve weather forecast products and support. The methodology of this research demonstrates the verification of UAV weather data and recommendations state that this information can and should be used in ways comparable to the methods applied to commercial aircraft ACARS data.

a. Problem statement

Accurate environmental information from UAV platforms is important to the meteorological community as well as mission planners and operators. Military UAVs have the ability to provide weather intelligence in data-sparse regions of combat operations, while ACARS equipped civilian aircraft are restricted from these areas. The RQ-4A Global Hawk (Figure 1) currently reports weather data but this information has never been validated. The following statement is from the 88th Weather Squadron's (2002) thesis topic proposal, which summarizes the scope of this problem:

“In an August 27, 2002, article in Federal Computer Week, the CSAF, General John P. Jumper, said the Air Force should begin to think of the YF-22 fighter jet as also being an intelligence, surveillance and reconnaissance aircraft and ‘get away from being platform-centric’ (Caterinicchia 2002). In this same spirit, specialized surveillance platforms such as the RQ-4A Global Hawk could theoretically be exploited to obtain environmental/meteorological information over data-sparse areas. These data could then be used by DoD to initialize meteorological models. There are a number of questions however that must be answered before AFWA can begin incorporating meteorological data from platforms such as RQ-4A Global Hawk into its models. Among these questions is how accurate are the data?”



Figure 1. The RQ-4A Global Hawk (Northrop Grumman 2001).

This research validates Global Hawk weather data using statistical comparisons with other available environmental information. This thesis provides recommendations for the use of this information once its accuracy has been shown. The Atmospheric Slant Path Analysis Model (ASPAM) is the primary tool used to verify the Global Hawk data. ASPAM is a model used by the Air Force Combat Climatology Center (AFCCC) and

ingests all available weather information to create a “best guess” vertical profile of the atmosphere by optimal interpolation techniques. The data used by ASPAM include surface and upper-air observations, ACARS and other aircraft reports, satellite soundings, and information from other meteorological databases, primarily the Navy Operational Global Atmospheric Prediction System (NOGAPS) model analyses.

b. Objectives

The primary objective of this research is to validate Global Hawk weather data and justify the benefits of using such information in weather prediction models, weather forecasting, and as weather intelligence for mission planning. Specific steps needed to achieve this overall goal are to:

- 1) obtain and format environmental data from several Global Hawk flights;
- 2) obtain and format vertical atmospheric profiles from ASPAM;
- 3) obtain and format rawinsonde observations (RAOBs) taken from Edwards Air Force Base (AFB) near the time of the Global Hawk flights;
- 4) compare Global Hawk weather data with ASPAM and RAOB observations;
- 5) determine the validity of Global Hawk data based on these comparisons and statistical analyses;
- 6) and, make conclusions and recommendations to users based on the validity of the Global Hawk data.

c. Approach

1) DATA ACQUISITION

Weather data were obtained from several Global Hawk flights in order to perform statistical analyses. The Global Hawk System Program Office (SPO) at Wright-Patterson Air Force Base (WPAFB) funded travel to Edwards AFB, California to gather data from Global Hawk flight tests. Unfortunately, flight tests did not occur during this temporary duty (TDY) but data were acquired from missions performed earlier in the year.

Information was also available from operational missions but the use of that data was impractical because of the sensitive nature of the operations. Data obtained from classified operations and missions flown in sensitive areas are classified and difficult to obtain and use. Weather data were also obtained from ASPAM analyses and Edwards AFB RAOBs to compare with the Global Hawk observations. The times and locations of the ASPAM profiles were provided at the medians of the Global Hawk ascent and descent times and locations, so that the data were as representative as possible. Edwards RAOB data were provided at the closest possible dates and times to the Global Hawk missions but were unavailable at the specific times of certain missions.

2) DATA FORMATTING

The Global Hawk weather information was separated and decoded from the data stream. This was initially accomplished during the Australian deployment of the Global Hawk in 2001 and similar methods were investigated during this research. Data processors of the 452nd Flight Test Squadron (FLTS) decoded and compiled data from five separate missions and provided the information for this study on CD-ROM media.

The Global Hawk, ASPAM, and RAOB data were then put into the same format and unit conversions were performed.

3) DATA VERIFICATION

All of the formatted data were entered into statistical software packages and several tests were performed. The intent of these tests was to show the accuracy of the Global Hawk weather data when compared with actual environmental observations. It was assumed that the ASPAM and RAOB data represented actual ground-truth conditions, although ASPAM interpolates available observations to a particular location and time, and RAOB data were not available at the exact time and location as the Global Hawk information. The statistical measures used include simple linear regression, analysis of variance (ANOVA), coefficient of determination (R^2), mean square error (MSE), root mean square error (RMSE), and hypothesis testing using the t -test.

2. Literature Review

a. ACARS background

Weather observations are reported by commercial aircraft in the United States (US) through the Aircraft Communications Addressing and Reporting System (ACARS) which is managed by Aeronautical Radio, Inc. (ARINC). The data are compiled, processed, quality controlled, and made available by the National Oceanic and Atmospheric Administration's (NOAA) Forecast Systems Laboratory (FSL). FSL collects over 170,000 meteorological observations daily including data from aircraft outside the US, which are known as aircraft meteorological data relay (AMDAR) reports, and displays them on an interactive website (FSL 2003, <http://www.acweb.fsl.noaa.gov/>). Pressure, temperature, wind speed, and wind direction are the primary environmental variables reported, although some aircraft provide moisture and turbulence data. The spatial coverage of the reports is shown in Figure 2 for the world and Figure 3 for the continental United States (CONUS) (Moninger et al. 2003).

The data are currently accessible only by National Weather Service Forecast Offices (NWSFO) and other government agencies. Private organizations and research groups may obtain the information and are encouraged to use it in their research and operations as long as certain criteria are met (FSL 2003, <http://acweb.fsl.noaa.gov/FAQ.html>).

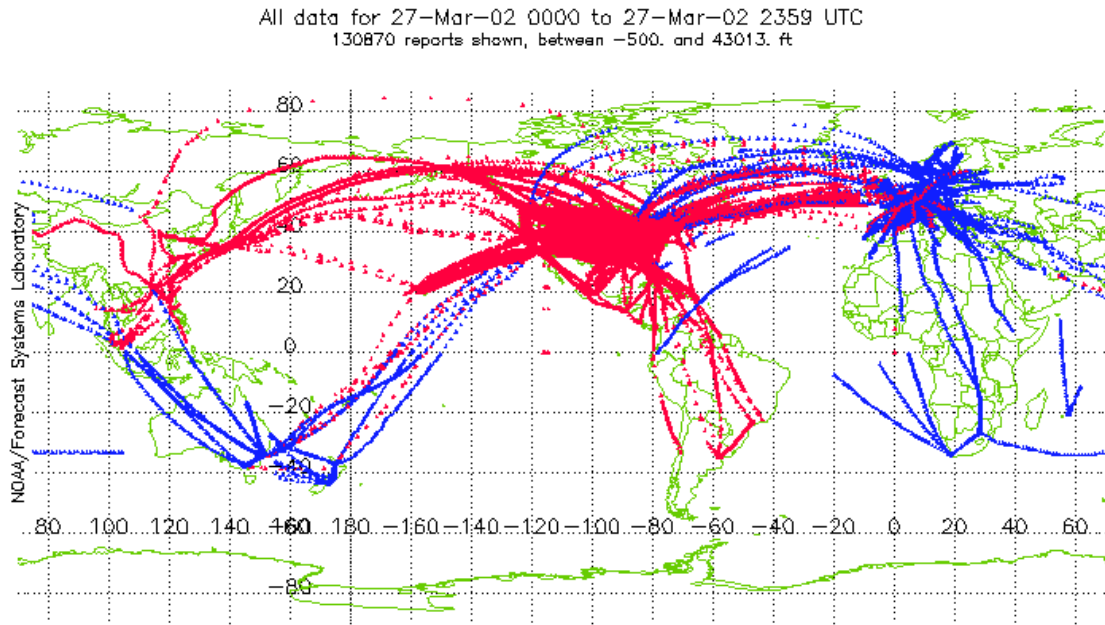


Figure 2. A 24-h worldwide ACARS/AMDAR plot for 27 Mar 2002. ACARS reports are in red and AMDAR reports are in blue (Moninger et al. 2003).

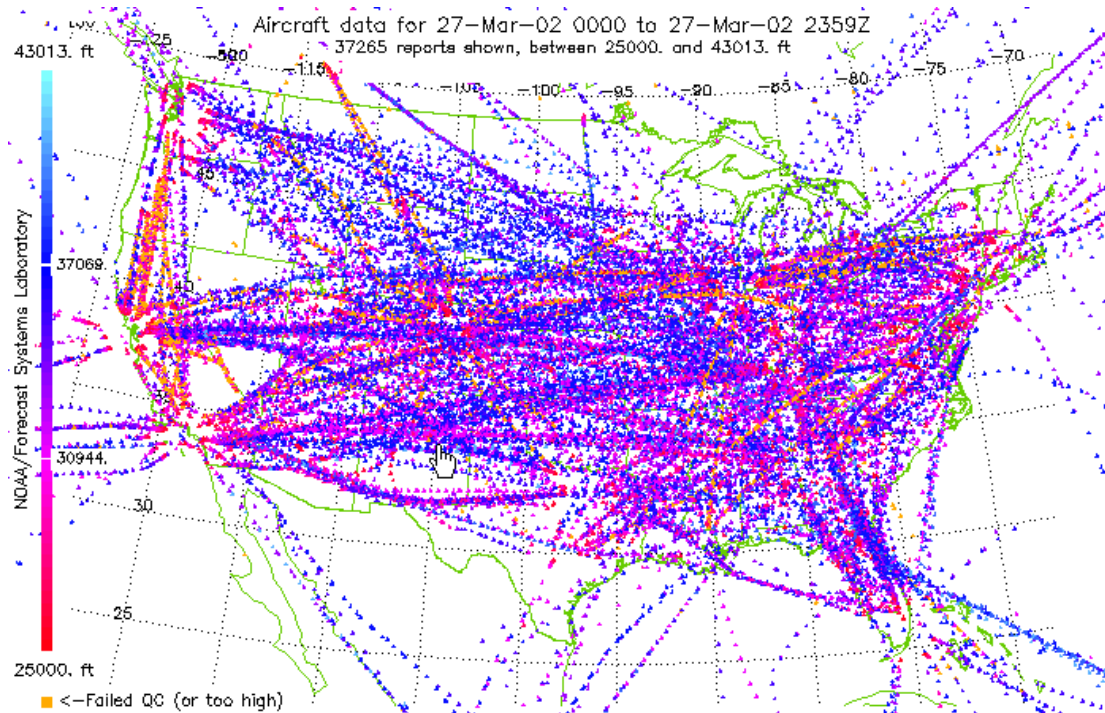


Figure 3. ACARS coverage over the CONUS for 27 Mar 2002. Reports are between 25,000 and 45,000 ft and are color coded by altitude (Moninger et al. 2003).

b. ACARS data use

ACARS and AMDAR information have numerous uses and benefits to the meteorological community such as improved NWP potential, enhanced weather forecast products, and an overall increase in available upper-air observational data. ACARS reports are also more spatially and temporally available than current rawinsonde information. Moninger et al. (2003) state the “data are the only in situ source of upper-air data at non-synoptic times, and therefore are highly valuable.” Some of the benefits of this data are illustrated in the following case studies:

1) THUNDERSTORMS

Mamrosh (1998) showed the value of ACARS data in forecasting a convective event by the Chicago NWS office. ACARS environmental information was used to determine the amount of atmospheric instability and wind shear during the day and accurately predict the timing and type of severe weather to occur.

Figure 4 is a sounding created from ACARS data at 1515 Universal Time Code (UTC), which showed an inversion indicating a stable layer in the lower atmosphere. The convective temperature was established with the data and the forecasters believed it was possible to reach this temperature due to strong warm air advection in the region. Also evident on the sounding was a low-level jet of 60 knots, which could mix down to the surface once the inversion broke. Figure 5 is an ACARS sounding about one hour later which shows the inversion had lifted and weakened and the low-level winds were still significant at 40 to 60 knots.

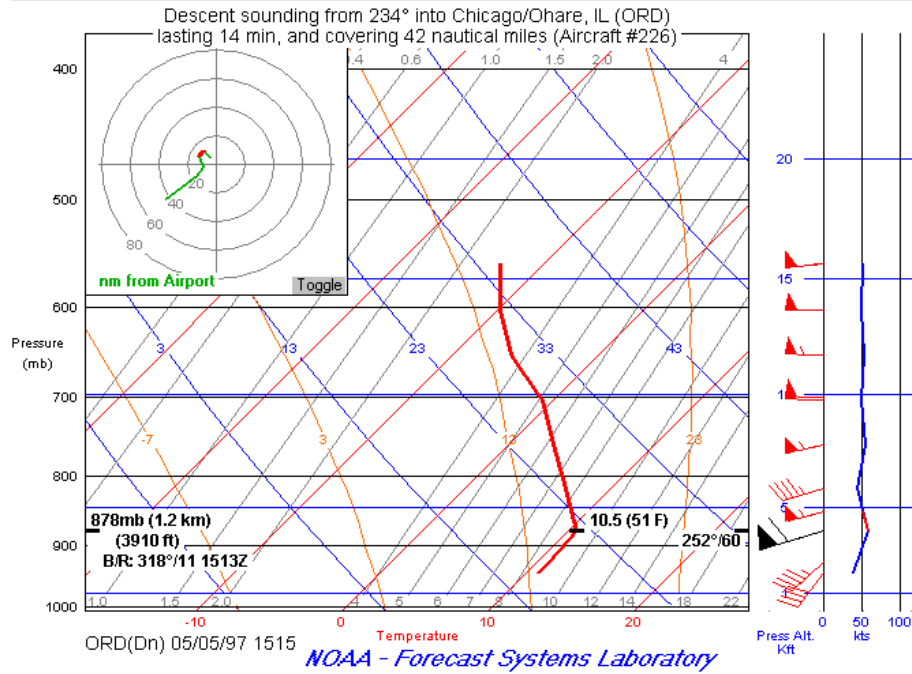


Figure 4. ACARS sounding from O'Hare at 1515 UTC (Mamrosh 1998).

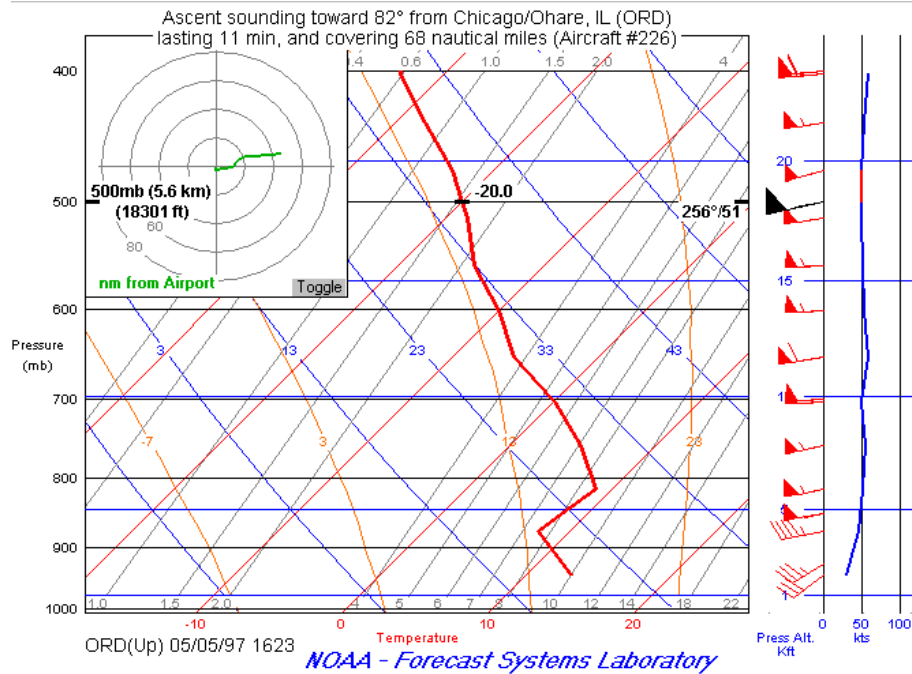


Figure 5. ACARS sounding from O'Hare at 1623 UTC (Mamrosh 1998).

A sufficient amount of instability to initiate thunderstorm activity was evident on a sounding about an hour later (Figure 6) and a Severe Thunderstorm Watch was issued by the Storm Prediction Center (SPC). Thunderstorms developed in the area shortly thereafter and several severe weather events followed such as winds of 50 to 60 knots and golfball-sized (1.75 inch) hail (Mamrosh 1998). Mamrosh (1998) stated, “the ACARS data was a very useful supplement to the usual tools found in an NWS office, for there is no other system in place to get very frequent soundings of both wind and temperature.”

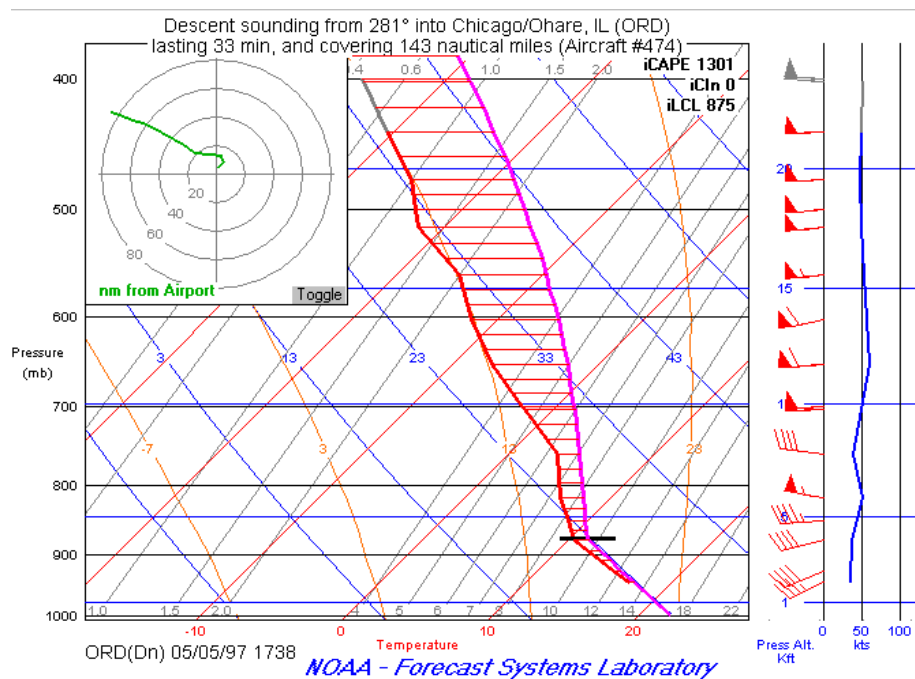


Figure 6. ACARS sounding from O’Hare at 1738 UTC (Mamrosh 1998).

2) TURBULENCE

Reports from aircraft using ACARS were extremely beneficial in verifying turbulence for the Center Weather Service Unit (CWSU) at Seattle (Mamrosh et al. 2001). The polar jet stream was located across the Pacific Northwest with maximum

winds in excess of 175 knots through Oregon (Figure 7). Rawinsonde data at the level of the jet stream were unavailable because the high winds transport the instrument far from the ground station and the signal is lost. Therefore, ACARS data were the only existing information and were used to verify the placement of the jet stream and determine areas of moderate to severe turbulence. Additional ACARS reports also allowed the Seattle CWSU to track the slow northward progression of the jet stream during the day.

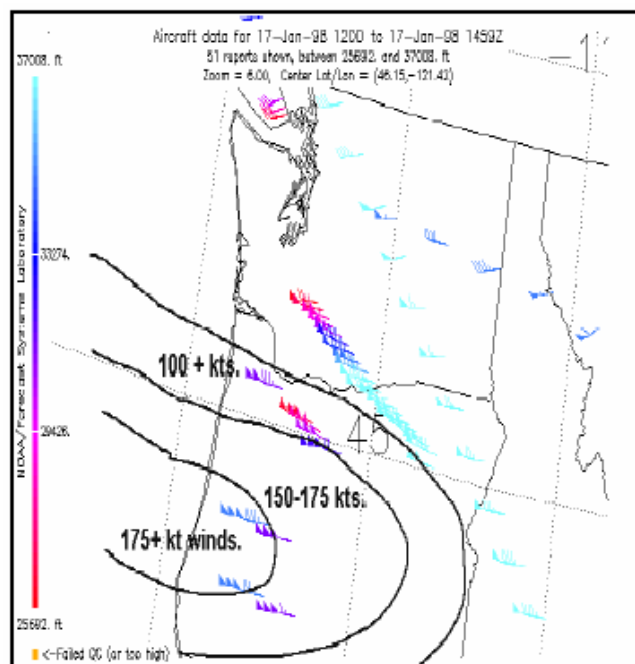


Figure 7. ACARS wind data between 25,692 and 37,008 ft, for the period 1200 UTC to 1459 UTC January 17, 1998 (Mamrosh et al. 2001).

Some aircraft also report turbulence through varying measures and algorithms including Derived Equivalent Vertical Gust (DEVG), Eddy Dissipation Rate (EDR), and measuring the vertical acceleration of aircraft (Moninger et al. 2003). Some of this information has inaccurate values and biases in the algorithms but the data are useful

nonetheless. EDR is the recommended and most valuable measure of turbulence because it relates to the atmosphere rather than the aircraft. The other two procedures rely on the weight and velocity of the aircraft to determine a value for turbulence.

3) WINTER WEATHER

Determining whether precipitation will be liquid or solid in winter storms is always a challenge, especially with minimal data. One such occasion where ACARS reports were used to improve winter forecasts was during a moderate snow event in Chicago on Christmas Eve (Mamrosh et al. 2001). Most of the NWP models predicted rain for the 24th and 25th of December, while others hinted at only a trace of snowfall during the period. Two soundings from ACARS data (Figures 8 and 9) were examined and a layer with temperatures below freezing was evident in the low levels. The soundings also showed a mid-level layer with above freezing temperatures and that its thickness was decreasing. Wind data from the soundings showed low-level easterly flow, which would advect dry air into the region causing the air to cool even more as it evaporated. This information indicated the possibility of freezing rain and snow in the area and forecasts were updated as such.

The precipitation began that evening as freezing rain and changed over to snow soon thereafter. The snow continued overnight and ended as drizzle the following evening. The amount of snowfall recorded was about 2.5 inches.

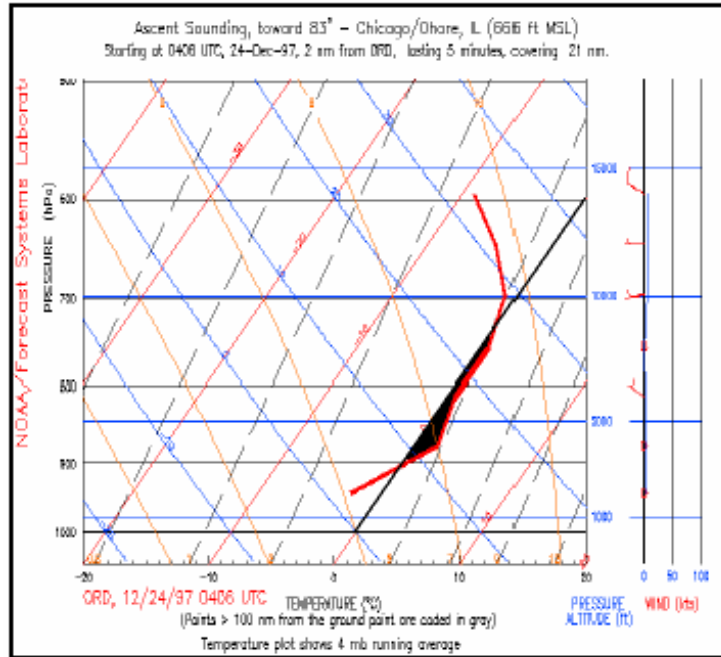


Figure 8. ACARS sounding showing above-freezing layer (Mamrosh et al. 2001).

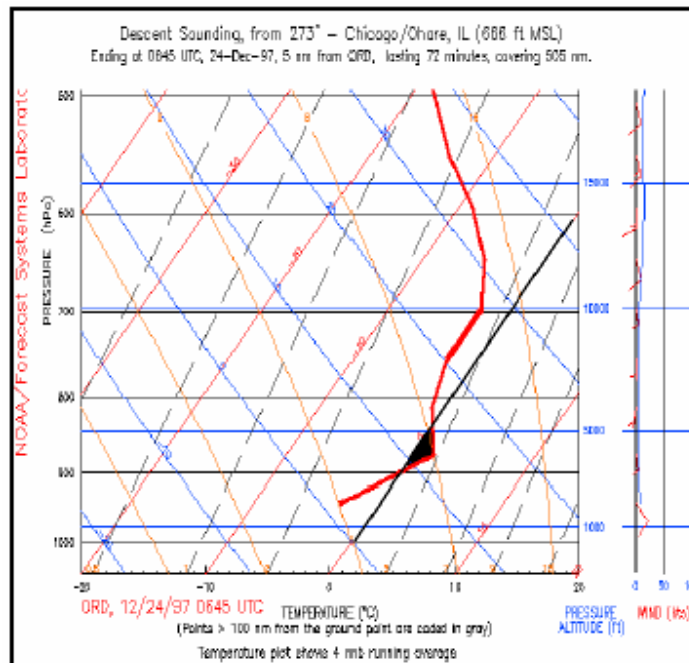


Figure 9. ACARS sounding showing above-freezing layer diminishing (Mamrosh et al. 2001).

Mamrosh et al. (2001) stated, “This was an especially useful forecast as even modest snowfalls as this has significant impact on a busy airport such as O’Hare – especially the day before Christmas!” Without the ACARS reports, this forecast might have been missed.

4) AIRLINE MISSION CONTROL

Another benefit of ACARS data is that they are near real time and can assist flight planners and mission controllers with weather related decisions. An example of this occurred when an Italian airliner encountered unexpected strong headwinds over the Atlantic Ocean and the crew unsure if the fuel supply would be sufficient to complete the flight. The Miami CWSU used ACARS wind data to determine an altitude with lighter headwinds (Figure 10), the airliner was directed there by controllers, and the flight was completed without incident (Mamrosh et al. 2001).

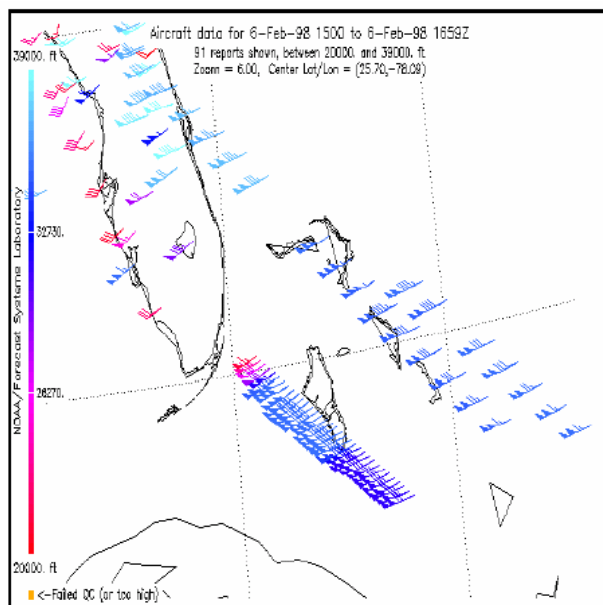


Figure 10. ACARS wind data between 22,000 and 39,000 ft (Mamrosh et al. 2001).

The case studies above demonstrate the value of ACARS data in the forecasting process, which is just a hint of the possible uses and benefits of the information. The reports are also used with NWP models both as input for enhanced model initialization and as verification for model forecasts.

c. ACARS accuracy and quality control

ACARS weather data are only valuable if they are accurate and checked for errors. Several studies have shown the accuracy of ACARS reports by comparing them with other sources, such as rawinsondes and models (Moninger et al. 2003). ACARS data were compared with rawinsonde readings by Schwartz and Benjamin (1995) and the values were shown to agree. Further statistical analysis implied ACARS reports were actually more precise than rawinsonde data. Benjamin et al. (1999) determined wind and temperature errors in the 400-300 millibar layer to be 1.1 m s^{-1} and $0.5 \text{ }^{\circ}\text{C}$, respectively. The low variability of mesoscale values was the reason this atmospheric layer was used.

Once the data were shown to be accurate, they were made available for use in forecasting and mission control. Continuous quality checks must be performed on the data to ensure sustained accuracy and value. Quality control statistics from a system used by the U.S. Navy is seen in Table 1 (Pauley 2003, in preparation). The FSL utilizes a quality control system that checks reports and notifies the airlines of possible equipment problems. When reports from an aircraft are consistently in error, the airline is advised so corrections can be made. This relationship between the data users and providers is important to guarantee continued value of ACARS information.

Table 1. Percentage of rejected data from U.S. Navy quality control methods (Moninger et al. 2003).

	ACARS	AMDAR
Duplicates	2.1%	0.8%
Bad reports	2.5%	1.1%
Bad temperature	0.5%	0.0%
Bad winds	0.8%	0.4%

d. UAV background

Unmanned aerial vehicles report environmental information much the same way as commercial aircraft but the data are not as readily accessible. Comparisons can be made between UAV and ACARS reports showing the potential value of the weather information. Unmanned systems perform a variety of missions at varying locations and altitudes and for different lengths of time. The environmental intelligence would benefit both the weather forecasters and the UAV controllers by providing much needed weather information in data-sparse regions, which is where most of the flights occur.

e. Possible uses of UAV data

Forecasters could use UAV weather information to improve their products and enhance the NWP models. The increased amount of information available to weather personnel can be utilized in ways comparable to ACARS reports, as seen in Section 2.b. Currently, the U.S. Navy uses ACARS data in their synoptic scale model NOGAPS and their mesoscale model called the Coupled Ocean/Atmospheric Mesoscale Prediction System (COAMPS) and are interested in obtaining UAV data as well (E.C. Mozley 2002, personal communication). The U.S. Air Force has also shown interest in using UAV data

in their mesoscale model called the Weather Research and Forecasting model (WRF). The data could also alert UAV controllers of possible turbulence and low temperatures, which impact the performance and stabilization of the UAV systems. Another advantage to the operators is using the data to redirect missions to areas with weather more favorable to the aircraft and its sensors and weapons.

f. UAV accuracy and quality control

Weather data from UAV sensors should be checked for accuracy similar to methods used with ACARS reports. The information should be made available for use once the validity of the data is shown. Then quality-control procedures must be established and followed to ensure the continued value of the data. Using procedures which are analogous to ACARS methods is a feasible approach. The Fleet Numerical Meteorology and Oceanography Center (FNMOC) has advanced algorithms in place to test data used in NOGAPS for accuracy and relevancy. These and other similar methods could be used with UAV weather data.

3. Data Collection and Review

a. Data collection

Three sets of data were analyzed and compared in this research. The primary dataset was from the Global Hawk, which included the environmental parameters that were evaluated. Vertical atmospheric profiles from the Atmospheric Slant Path Analysis Model (ASPAM) and upper-air rawinsonde soundings from Edwards Air Force Base (AFB) were used to simulate “ground truth” datasets that were compared with the Global Hawk data observations.

1) GLOBAL HAWK

All Global Hawk datasets used in this research were obtained within the Edwards AFB operating range area. The positions varied from 34.82 to 36.56 degrees north latitude and 116.6 to 118.6 degrees west longitude (Figures 11 and 12). Observations were obtained from five separate test flights occurring in 2003 on 29 May, 3 June, 26 June, 8 August, and 15 August. All data were from the same aircraft, Air Vehicle 7 (AV7), which is the newest airframe in the inventory. The intent was to obtain data near-real-time while on TDY to Edwards AFB during late September 2003. Flight testing, however, did not occur during this period due to weather or to be more precise, the lack of weather. The 452nd FLTS had planned to perform crosswind tests, which require wind speeds of 10 to 15 knots for takeoff and landing, but an area of high pressure dominated the region and winds were unusually calm during the week. Therefore, the only available data were from previous missions and the time at Edwards was spent working with the data-processing section to get the information that was used in this study. The desired

parameters were determined and a request was made to the 412th Test Wing Range Division at Edwards AFB, which provided the information in comma-separated text format on CD-ROM media.

Data points for each mission were provided once per second, which was more than adequate for this study. The duration of the missions ranged from one hour and 45 minutes to 10 hours and 30 minutes, but the length of time the aircraft was actually airborne ranged from 30 minutes to nine hours and 30 minutes. This research only evaluated Global Hawk data during its flight, so information provided when it was on the ground was disregarded.

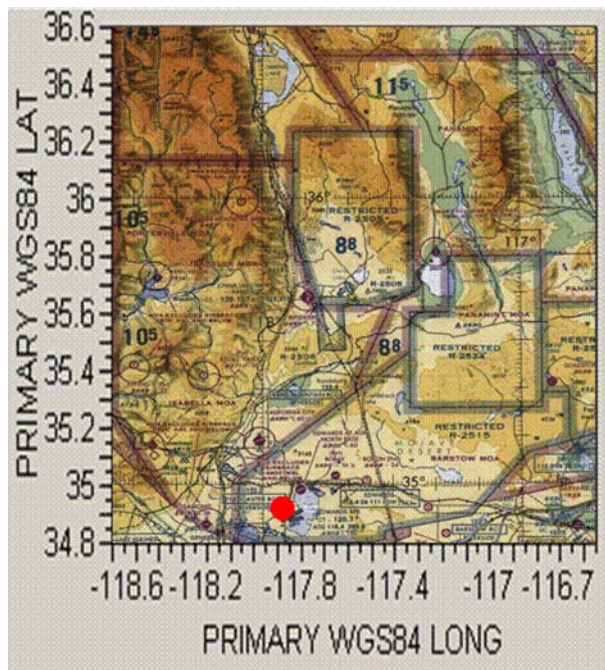


Figure 11. Aeronautical map of Edwards AFB military operating areas. The red dot indicates the Edwards AFB rawinsonde site (Maptech 2003).

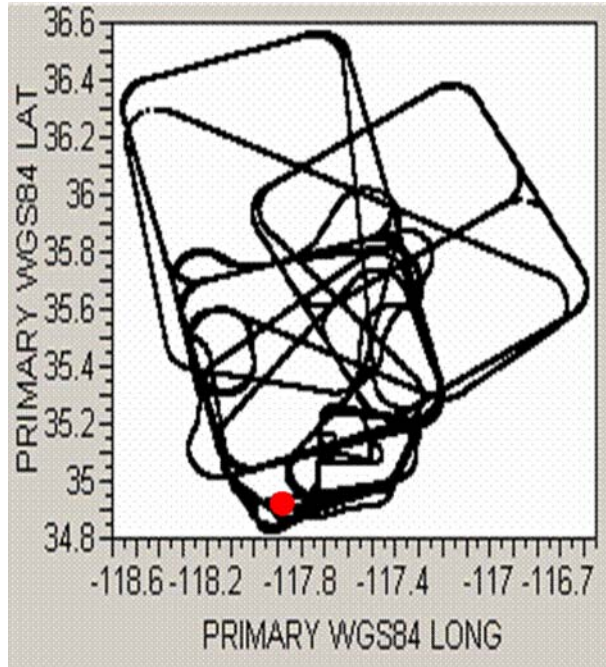


Figure 12. Latitude versus longitude plot of Global Hawk flight routes for all five examined missions. The red dot indicates the Edwards AFB rawinsonde site. The latitude/longitude range corresponds to Figure 11.

The Air Data System onboard the Global Hawk compiles, processes, and transmits all atmospheric variables to the Integrated Mission Management Computers (IMMC) onboard the aircraft. These parameters include static air pressure, outside air temperature, wind speed, and wind direction. The units of measurement for each of these variables are pounds per square foot, degrees Celsius, degrees true, and knots; respectively (Northrop Grumman 2001).

2) ASPAM

AFCCC manages an extensive database of environmental information which is used as input for ASPAM. The input consists of surface observations, upper-air soundings, satellite observations, snow and ice field data, solar and geomagnetic

information, aerosol information, Digital Terrain Elevation Data (DTED), Real-Time Nephanalysis (RTNEPH) data, NOGAPS information, aircraft reports (AIREPS), pilot reports (PIREPS), and Aircraft Communication Addressing and Reporting System (ACARS) reports. The profiles provide data from the surface to 100,000 feet in 500-foot increments for specified latitudes, longitudes, and times. Among the data in the profiles are pressure, temperature, wind direction, and wind speed in units of millibars, degrees Celsius, degrees true, and meters per second; respectively. ASPAM uses the method of Multivariate Optimal Interpolation (MVOI) to determine data values at each level. MVOI assigns a value of significance to each input data point based on its distance from the profile location, the difference between the observation time and the profile time, the accuracy of the observing equipment, and the expected accuracy of the first guess. Then all of the weighted inputs are combined to create a “best guess” vertical profile at the given position and time. Two ASPAM vertical profiles per Global Hawk mission were obtained for this research, one for the ascending segment and the other for the descending segment of the flight profiles.

3) RAOB

The weather unit at Edwards AFB supports the flight testing squadrons by providing surface and upper-air observations, as well as forecasts. The unit launches rawinsondes based on customer requirements and the corresponding upper-air data are posted to its web site and archived for future use. Data were available for three of the five Global Hawk mission dates within four hours of the flight times. Another dataset was available for one of the other mission dates but was approximately 15 to 18 hours

prior to the flight time. This dataset was not used because it was not considered to be representative of the atmospheric conditions during the Global Hawk flight. These upper-air datasets were obtained in text format and compared with the Global Hawk mission data as a second test of accuracy.

b. Data limitations

Errors and limitations are inherent in any atmospheric process or dataset. The results of this research are of value, so long as these problems are identified and taken into account.

1) GLOBAL HAWK

Data received from the Global Hawk Air Data System (ADS) are occasionally imprecise or incorrectly formatted during transmission. The ADS is a redundant system, which means another ADS processor relays data to a separate Integrated Mission Management Computer (IMMC). The Global Hawk is also equipped with a system status computer, which reports any expected problems in ADS output. Distorted information can still make it through the system, however, and all datasets must be checked for erroneous or missing data. This research will help determine if and when ADS output cannot be trusted as an accurate data source.

2) ASPAM

ASPAM interpolates data to a specific location and time and the profiles are a representation of the atmosphere based on the input. They may or may not reflect the

actual conditions. Therefore, any errors in the input will result in less accurate ASPAM profiles. Possible causes for input error include instrumentation faults, problems in data entry or transmission, and inconsistencies in equipment and reporting.

3) RAOB

Possible errors in rawinsonde data include transmission problems, incorrect data entry, and equipment faults. The upper-air datasets used in this research did not exactly coincide with the Global Hawk mission times or locations, but were as close as feasibly possible to perform statistical analyses and comparisons. The results of these tests can be used to support the evaluations based on ASPAM data and gain further insight into the validity of the Global Hawk data. Allen (2003) states, “the raw sounding data includes the temperature, dew point temperature, pressure, and wind speed and direction for the atmospheric column. This column is assumed to be directly over the station that launches the balloon. However, this assumption is not entirely accurate since the atmospheric flow will typically carry the balloon downwind away from the station as it ascends. Errors in balloon location and height can occur if the balloon is not rising at the standard ascension rate of 300 meters per minute. Errors in sounding data can also occur due to the lag time of sensors in the instrumentation package. For example, if the balloon is passing through a rapidly changing layer, some of the information will not get reported since the instruments cannot react to the changes fast enough. The typical lag for temperature sensors is 4 to 20 seconds, with the lag increasing with altitude. The pressure measurements used for determining the height have a standard error of ± 1 mb at the surface and 10 mb with an error of 2 mb at 500 mb (Golden et al. 1986).”

Edwards AFB is located in the Mojave Desert and the weather in this region is generally stable, especially during the late spring and summer. Upper-air charts were obtained coincident to the five Global Hawk missions and it was determined that the weather conditions were stable during these times. Upper-level wind speeds during the first three missions were such that the rawinsondes may not have drifted significantly far downwind. Considerably stronger upper-level wind speeds and substantial directional shear during the two August missions may have caused the rawinsondes to drift farther downstream producing RAOBs that were not representative of the atmospheric conditions in the Global Hawk flight areas. See Appendix B for the upper-level wind analyses corresponding to all five mission dates.

4. Methodology

a. Data acquisition

Three sets of data were analyzed and compared in this research. Environmental information from the Global Hawk was the focus of this research and was, therefore, the primary dataset examined. The dates, times, and locations of the Global Hawk data determined the format of the additional data requested. The additional data included vertical atmospheric profiles from the Atmospheric Slant Path Analysis Model (ASPAM) and upper-air observations from Edwards AFB rawinsondes.

1) GLOBAL HAWK

Global Hawk environmental information was obtained from flight-test databases maintained by the 452nd FLTS at Edwards AFB. The available weather data included pressure, temperature, wind direction, and wind speed in units of pounds per square foot, degrees Celsius, degrees true, and knots; respectively. Aircraft flight parameters were collected along with the weather information, including altitude in feet above mean sea level (MSL), ascent mode, descent mode, altitude hold mode, pitch angle, and roll angle. This information was used to determine if the Global Hawk environmental data were influenced by various aspects of the aircraft's flight. The data reports were available once per second for each mission but only data at specific flight levels were analyzed and compared. Data from five separate test missions of the same aircraft, Air Vehicle 7 (AV7), were provided in comma-separated format on CD-ROM media.

2) ASPAM

AFCCC provided vertical atmospheric profiles from the Atmospheric Slant Path Analysis Model (ASPAM). The profiles provided weather information from the surface to 100,000 feet MSL in 500-foot increments. The environmental data used in this research included height, pressure, temperature, wind direction, and wind speed, in units of feet MSL, millibars, degrees Celsius, degrees true, and meters per second; respectively.

A total of ten ASPAM profiles were requested from AFCCC, one for the ascending and one for the descending portion of each Global Hawk mission. The parameters of the ASPAM profiles were based on the median times, latitudes, and longitudes for each ascent and descent of the Global Hawk missions. The profiles were then created and e-mailed in text format.

3) RAOB

Rawinsonde observations were provided by the Edwards AFB weather unit. The observations provided altitude, pressure, temperature, wind direction, and wind speed in units of feet MSL, millibars, degrees true, and knots; respectively. RAOBs were available on three of the Global Hawk mission dates within four hours of the flight times. An additional RAOB was available for another mission but was 15 to 18 hours prior to the Global Hawk flight time and was, therefore, not used in this research. All Rawinsonde observations were compiled and e-mailed in text format.

b. Data formatting

Global Hawk, ASPAM, and RAOB files were imported into Microsoft Excel and SAS Institute JMP and saved in the same file format prior to quality checks. All of the datasets were then checked for errors and any faulty reports were removed prior to statistical analysis. All three data types were arranged in the same format and unit convention to simplify comparisons and tests.

1) GLOBAL HAWK

Comma-separated text files were formatted and imported into statistical software. Datasets from all five Global Hawk missions were carefully examined for obvious errors or incorrect entries. If any variable in a row of data was invalid or suspect, the entire row of data was removed. Additionally, all data reports while the aircraft was on the ground were excluded from analysis because this research focused only on verifying data during ascent and descent. Global Hawk data are reported once per second but the only data of interest were at altitudes from the surface (approximately 2,500 feet MSL) to maximum flight level (20,000 to 60,000 feet MSL) in 500-foot increments. Therefore, all data reports were removed except for those closest to a specified 500-foot flight level. Table 2 depicts a sample of the Global Hawk data analyzed and the difference between the actual altitude and the corresponding 500-foot level. The table data represent the greatest differences for the ascending and descending portions of each mission. Appendix C provides a complete listing of the entire Global Hawk dataset which was used in this research.

Table 2. Global Hawk flight levels examined and differences from corresponding 500-foot levels. Data displayed below represent the levels with the greatest differences per mission. See Appendix C for the complete dataset.

Global Hawk Mission #	Global Hawk Flight Mode	Global Hawk Flight Level (ft MSL)	500-Foot Flight Levels (ft MSL)	Difference (ft MSL)
1	Ascent	15972.29	16000	27.71
1	Descent	18528.68	18500	28.68
2	Ascent	5028.65	5000	28.65
2	Descent	60002.20	60000	2.20
3	Ascent	7527.80	7500	27.80
3	Descent	27969.59	28000	30.41
4	Ascent	12028.23	12000	28.23
4	Descent	50479.88	50500	20.12
5	Ascent	14028.72	14000	28.72
5	Descent	55038.77	55000	38.77

The Global Hawk continuously checks the Air Data System (ADS) and indicates any suspected problems in the ADS Status column. Thusly, any reports with ADS problems were removed from the datasets prior to analysis. A total of 772 rows of Global Hawk data were available for analysis once all invalid or suspect rows were removed.

Global Hawk reports of Climb Mode, Altitude Hold Mode, and Descend Mode were checked for errors and some possible system faults were identified. For example, the aircraft continued to climb, sometimes as much as 2,500 feet, while still reporting to be in Altitude Hold Mode. During other missions, the aircraft indicated to be in Altitude Hold Mode but its altitude fluctuated as much as 6,000 feet. Most of these suspect data reports were not included in the analysis but some of them had to be kept to ensure a

complete mission profile was examined. Notes pertaining to the Global Hawk data and varying flight modes are shown in Appendix D.

The wind data reported by the Global Hawk were not in the standard meteorological format and had to be converted prior to analysis. Original values of wind direction were between -180 and 180 degrees and depicted winds toward, rather than from the direction. It was also determined that negative values corresponded to winds in the western quadrants (west of north) and positive values corresponded to winds in the eastern quadrants (east of north). The method used to put the Global Hawk wind direction into the standard meteorological format was to add 180 degrees to all values. The wind speed data were reported in units of knots and were converted to meters per second by dividing all values by 1.943.

The pressure data from the Global Hawk were converted from pounds per square foot to millibars by dividing all values by 2.08854. This ensured all pressure values were consistently formatted prior to comparison.

2) ASPAM

All ASPAM data files were converted into Excel and JMP formats and combined with the Global Hawk data. The vertical profiles were created in the standard meteorological format; therefore, no unit conversions were necessary. All applicable data were reported from the surface to 100,000 feet MSL in 500-foot increments but only data with corresponding Global Hawk reports were examined. Therefore, 772 rows of ASPAM data were available for analysis and comparison with the Global Hawk data.

3) RAOB

All Edwards AFB rawinsonde observations were converted into Excel and JMP formats and combined with Global Hawk and ASPAM data. Any additional information, such as density and humidity, was removed before incorporating the observations with the other datasets. Wind speed was reported in knots and was converted to meters per second by dividing all values by 1.943. Only three RAOBs were used in this research, the dates and times of which were 29 May 03 at 1631Z, 8 Aug 03 at 1230Z, and 15 Aug 03 at 1900Z. RAOB data were provided in 500-foot increments from the surface to 15,000 feet and then in 1,000-foot increments from 15,000 feet to the end of the transmission. The final altitudes reported by each RAOB were: 29 May – 40,000 feet, 8 Aug – 57,000 feet, and 15 Aug – 48,000 feet. Available RAOB data points were significantly less than Global Hawk and ASPAM reports due to missing RAOBs for missions two and three, fewer RAOB reports above 15,000 feet, and lower maximum altitudes of the balloon datasets. Therefore, 246 rows of RAOB data were analyzed and compared with the Global Hawk and ASPAM data.

c. Data verification

Once all of the Global Hawk, ASPAM, and RAOB datasets were formatted and standardized, several statistical tests were accomplished to verify the Global Hawk data. The primary test performed was simple linear regression of Global Hawk data with ASPAM and RAOB data.

1) STATISTICAL OVERVIEW

Regression analysis, as stated by Montgomery and Runger (2003), is a useful method to determine the relationship between two or more variables. Simple linear regression was used to resolve relationships between the Global Hawk, ASPAM, and RAOB variables of pressure, temperature, wind speed, and wind direction. Global Hawk data were used as the independent, or predictor variables represented by x and ASPAM and RAOB data were used as the dependent variables, or predictands represented by y (Wilks 1995). Regression analysis provided valuable information on the accuracy of the Global Hawk data after plotting corresponding datasets on a scatter diagram. For example, a plot was created of Global Hawk pressure (x) versus ASPAM pressure (y) (Figure 13) where each (x_i, y_i) pair was shown as a single point on the graph. The data points appeared to be randomly scattered around a straight line and a simple linear regression model was developed. The model is given by the equation

$$Y = \beta_0 + \beta_1 x + \epsilon \quad (1)$$

where β_0 and β_1 are unknown regression coefficients representing the intercept and slope of the linear model, respectively. The random errors, ϵ , were assumed to be uncorrelated random variables with a mean of zero and unknown variance σ^2 (Montgomery and Runger 2003).

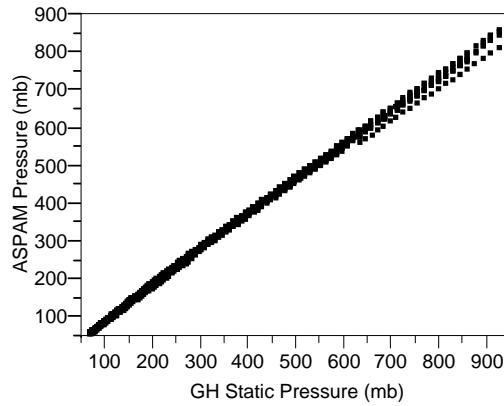


Figure 13. Scatterplot of Global Hawk pressure (x) versus ASPAM pressure (y).

This model was used to determine relationships between Global Hawk variables and ASPAM and RAOB variables. In the words of an Air Force Institute of Technology (AFIT) statistics professor, “There are good models and bad models, but no correct ones. It’s a model. If it were right, it would be scientific fact (R.N. Benton 2003, personal communication).” The estimates of β_0 and β_1 produce a “best fit” line to the data and the technique of least squares regression is performed to minimize the sum of the squares of the vertical deviations, or total spread, of the y -values from the line. The least squares estimates of the intercept and slope in the linear regression model with n observations are

$$\hat{\beta}_0 = \bar{y} - \hat{\beta}_1 \bar{x} \quad (2)$$

and

$$\hat{\beta}_1 = \frac{\sum_{i=1}^n y_i (x_i - \bar{x})^2}{\sum_{i=1}^n (x_i - \bar{x})^2} = \frac{\sum_{i=1}^n y_i x_i - \frac{\left(\sum_{i=1}^n y_i\right)\left(\sum_{i=1}^n x_i\right)}{n}}{\sum_{i=1}^n x_i^2 - \frac{\left(\sum_{i=1}^n x_i\right)^2}{n}} \quad (3)$$

where

$$\bar{y} = \left(\frac{1}{n} \right) \sum_{i=1}^n y_i \quad (4)$$

and

$$\bar{x} = \left(\frac{1}{n} \right) \sum_{i=1}^n x_i . \quad (5)$$

The numerator and denominator of Equation 3 are abbreviated as SS_{xy} and SS_{xx} , respectively. The expression SS_{xx} measures the spread of x_i , which is the sum of squares around the mean, \bar{x} . Another useful term is SS_{yy} , which measures the spread around \bar{y} , and is given by

$$SS_{yy} = \sum_{i=1}^n (y_i - \bar{y})^2 . \quad (6)$$

This value is also identified as the total sum of squares, SS_T , and is used to test the significance of regression for each model. The regression line or “best fit” becomes

$$\hat{y} = \hat{\beta}_0 + \hat{\beta}_1 x . \quad (7)$$

Each (x_i, y_i) pair of observations fit the relationship

$$\hat{y}_i = \hat{\beta}_0 + \hat{\beta}_1 x_i + e_i \quad (8)$$

where e_i is called the error or residual, which indicates the vertical distances between the points and the fitted line. This term is given by

$$e_i = y_i - \hat{y}_i . \quad (9)$$

The residuals provide information on the adequacy of each linear model and are used to determine an estimate of the corresponding variance, σ^2 . The analysis of variance

(ANOVA) table was used to determine the value of each regression model. The analysis of variance identity is

$$SS_T = \sum_{i=1}^n (y_i - \bar{y})^2 = \sum_{i=1}^n (\hat{y}_i - \bar{y})^2 + \sum_{i=1}^n (y_i - \hat{y}_i)^2 . \quad (10)$$

The first value on the right side of the equation measures the amount of variability in y_i accounted for by the regression line and is referred to as the regression sum of squares, SS_R . The second term on the right side of the equation measures the residual variation left unexplained by the regression line and is referred to as the error sum of squares, SS_E . It is used to show how much the predicted values, \hat{y}_i , differ from the true y -values and is defined as

$$SS_E = \sum_{i=1}^n (y_i - \hat{y}_i)^2 = \sum_{i=1}^n e_i^2 . \quad (11)$$

Several statistics provided information on the “goodness of fit” of the models. The first statistic of interest is the mean square error, MSE, which is an estimator of σ^2 and represents the sample variance of the residuals. It is calculated by dividing the error sum of squares by its number of degrees of freedom (Montgomery and Runger 2003), which is shown by

$$MSE = \hat{\sigma}^2 = \frac{SS_E}{n-2} . \quad (12)$$

The root mean square error, RMSE, is the square root of the mean square error and is used because it retains the units of the forecast variable. The magnitude of the error is, therefore, easier to interpret using RMSE (Wilks 1995).

A second statistic used to judge the adequacy of the regression models is the coefficient of determination, R^2 , which is defined by

$$R^2 = \frac{SS_R}{SS_T} = 1 - \frac{SS_E}{SS_T}. \quad (13)$$

It is the proportion of the variation of the predictand that is “accounted for” by the regression. A perfect linear regression model would have $R^2 = 1$ because $SS_R = SS_T$ and $SS_E = 0$ and a completely useless model would have $R^2 = 0$ because $SS_R = 0$ and $SS_E = SS_T$. Thus, higher values of R^2 indicate a more valuable model (Wilks 1995).

Another useful statistic is the F -ratio, which is listed on the ANOVA table and is used to describe the strength of regression models. It is the ratio of the regression sum of squares, SS_R , with the mean square error, MSE. Higher values of F indicate more effective regression because a strong relationship between x and y produces a large SS_R and a small MSE (Wilks 1995).

Once simple linear regression was accomplished between each Global Hawk variable and the corresponding ASPAM and RAOB variables, hypothesis tests were performed to further justify each model. These tests were performed to determine if the slope of each regression line was equal to one, $\beta_1 = 1$. If the hypothesis tests passed, then the relationships between the Global Hawk variables, x , and the ASPAM and RAOB

variables, y , could be validated. The t -test was employed to test the hypothesis of $\beta_1 = 1$ for each regression model. The test-statistic defined as

$$t_0 = \frac{\hat{\beta}_1 - \beta_{1,0}}{\sqrt{\hat{\sigma}^2 / SS_{xx}}} \quad (14)$$

follows the t -distribution with $n - 2$ degrees of freedom where $\beta_{1,0} = 1$ for the tests used in this research. The hypotheses of $\beta_1 = \beta_{1,0} = 1$ is rejected if $|t_0| > t_{\alpha/2, n-2}$, where $\alpha = 0.05$ and n represents the number of observations used in each model. Rejection of the null hypothesis occurs if the probability of observing the attained or more extreme value of the test statistic, given the null hypothesis is true, or p -value, is less than or equal to the test level of $\alpha = 0.05$. If the hypothesis tests were rejected then it could not be concluded that the slopes of the regression lines were equivalent to one. The hypothesis tests of $\beta_1 = 1$ used in this study were likely to fail because each of the linear models in this research had an extremely small variance. Models with low variance tend to have large values of t_0 based on the definition of the test statistic in Equation 14. The regression lines in this research were not invalidated based on the results of these hypothesis tests, however, because the variances were low and the fit was good for all models.

Another hypothesis test used to illustrate the significance of regression was performed by testing if the slopes of the regression lines were zero, $\beta_1 = 0$. If a test failed, meaning the hypothesis was rejected, then it was concluded that there was a significant relationship between x and y . Rejection of the null hypothesis occurs if the probability of observing the attained or more extreme value of the test statistic, given the

null hypothesis is true, or *p-value*, is less than or equal to the test level of $\alpha = 0.05$. Rejecting the hypothesis implies that x is of value in explaining the variability of y and could mean that the linear model is adequate. Failure to reject the hypothesis, $\beta_1 = 0$, means that x is of little value in explaining the variability in y and is the same as concluding that there is no linear relationship between x and y (Montgomery and Runger 2003). The tests of $\beta_1 = 0$ used in this research concluded $\beta_1 \neq 0$. Failure of these tests implied that the Global Hawk variables were of use in determining the “ground truth” variables of ASPAM and RAOB and that there was a linear relationship between them.

2) WIND DIRECTION TECHNIQUES

Wind direction verification was difficult due to the non-linearity of the data. A method of validating wind data used in meteorology is the root-mean-square or RMS vector error. The wind data were first broken down into their respective easterly (u) and northerly (v) components by

$$u = -X \sin \theta \quad (15)$$

and

$$v = -X \cos \theta \quad (16)$$

where X is the magnitude of the wind speed in m s^{-1} and θ is the direction of the wind in degrees measured clockwise from north. The wind components were obtained for all three datasets and the RMS vector errors were calculated for Global Hawk versus ASPAM and Global Hawk versus RAOB. The RMS vector error is defined as

$$V = \frac{1}{n} \sqrt{\sum [(u_1 - u_2)^2] + \sum [(v_1 - v_2)^2]} \quad (17)$$

where V represents the magnitude of the RMS vector error, n is the total number of observations, u_1 is the Global Hawk easterly component, u_2 is the ASPAM or RAOB easterly component, v_1 is the Global Hawk northerly component, and v_2 is the ASPAM or RAOB northerly component.

Another method used to verify wind direction was to determine the mean differences between Global Hawk and “ground truth” data. Two columns were created in JMP to calculate the differences of Global Hawk wind directions with ASPAM and RAOB wind directions. A formula was used for each column to guarantee the acute angle was given for the difference between the wind directions. The formula used in JMP returned the minimum of three calculations, which were

$$|X_1 - X_2| \tag{18}$$

$$|X_1 - X_2 + 360| \tag{19}$$

$$|X_1 - X_2 - 360| \tag{20}$$

where X_1 is the Global Hawk direction and X_2 is the ASPAM or RAOB direction.

Wind direction information was also examined as circular statistical data. The distributions of wind direction reports could not be considered normal because the data was non-linear. The von Mises distribution for circular data is analogous to the normal distribution for linear data (Fisher 1993). A statistical program called Oriana was used to analyze the circular datasets and the wind direction reports were shown to fit the von Mises distribution. Additional analyses using circular statistical information were possible but time constraints did not allow further investigation into this area.

5. Analysis and Results

a. Pressure

All tests and analyses of Global Hawk pressure were very successful and provided sufficient information to conclude that Global Hawk pressure reports were accurate. The linear regression of Global Hawk pressure with ASPAM and RAOB pressure produced significant linear models and extremely low values of variance and RMSE.

1) ASPAM

All five Global Hawk missions provided 772 data points used in linear regression of Global Hawk pressure (x) with ASPAM pressure (y). The JMP scatterplot and fitted line is depicted in Figure 14 and the regression analysis results are illustrated in Figure 15. The results include R^2 , RMSE, ANOVA table, F -ratio, and parameter estimates, along with the t -test values for the hypothesis test $\beta_1 = 0$. The figures show the Global Hawk is an accurate predictor of atmospheric pressure as established by ASPAM.

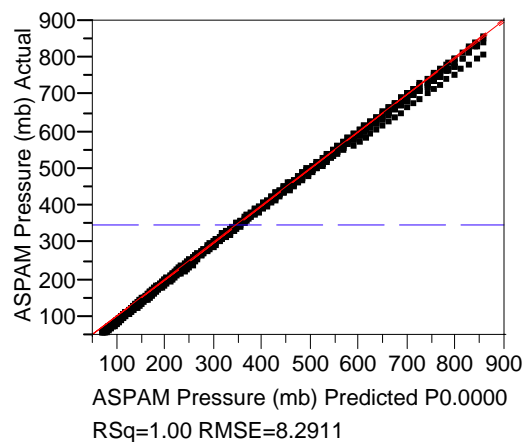


Figure 14. Simple linear regression scatterplot and fitted line of Global Hawk pressure (x) versus ASPAM pressure (y).

Summary of Fit

RSquare	0.99867
RSquare Adj	0.998668
Root Mean Square Error	8.29109
Mean of Response	347.1323
Observations (or Sum Wgts)	772

Analysis of Variance

Source	DF	Sum of Squares	Mean Square	F Ratio
Model	1	39750116	39750116	578249.4
Error	770	52931	68.742169	Prob > F
C. Total	771	39803048		0.0000

Parameter Estimates

Term	Estimate	Std Error	t Ratio	Prob> t
Intercept	9.1112201	0.535386	17.02	<.0001
GH Static Pressure (mb)	0.9157469	0.001204	760.43	0.0000

Figure 15. Regression analysis results of Global Hawk pressure (x) versus ASPAM pressure (y).

The hypothesis test for $\beta_1 = 1$ was accomplished using the JMP output from Figure 15 and calculations in Mathcad software. Recall that $\alpha = 0.05$ and the degrees of freedom are defined by $n - 2 = 770$ for Global Hawk versus ASPAM regression. The JMP values used were $\hat{\beta}_1 = 0.9157469$ and $\hat{\sigma}^2 = 68.742169$. The critical t -value and SS_{xx} were calculated as $t_{\alpha/2, n-2} = t_{0.025, 770} = 1.963$ and $SS_{xx} = 47400996.86$. The output t -value was $t_0 = -69.963$ which led to the conclusion of rejecting the null hypothesis $\beta_1 = 1$. As previously stated, this test was likely to fail because of the extremely low variance of the linear model. Therefore, all assumptions of Global Hawk pressure data quality were based on the regression analysis and hypothesis test of $\beta_1 = 0$.

Residual analysis showed there were no significant problems in the regression. The residuals were small when examined on the same scale as the regression variables. Close examination of the data revealed some possible patterns in the bias, however. Global Hawk pressure values primarily had a positive bias during ascent and a negative bias during descent. Also, the amount of bias seemed to change in relation to the rate at which the Global Hawk climbed or descended. It is possible that a time delay between measuring and transmitting atmospheric values by the Global Hawk would induce the bias observed in this study. During ascent (descent), the Global Hawk could measure the pressure at an altitude lower (higher) than the height at which it transmitted the data. This slight difference in flight level could lead to pressure values higher (lower) than those at which the data was relayed. This height difference could vary in relation to the rate at which the Global Hawk climbed or descended and the pressure bias would reflect this difference. A possible reason for this slight difference could be the vertical separation between the weather sensors at the rear of the aircraft and the altimeter during ascent and descent. See Appendix E for an illustration of the Global Hawk dimensions and location of the sensors. The residual versus predicted plots for each Global Hawk mission are depicted in Figure 16.

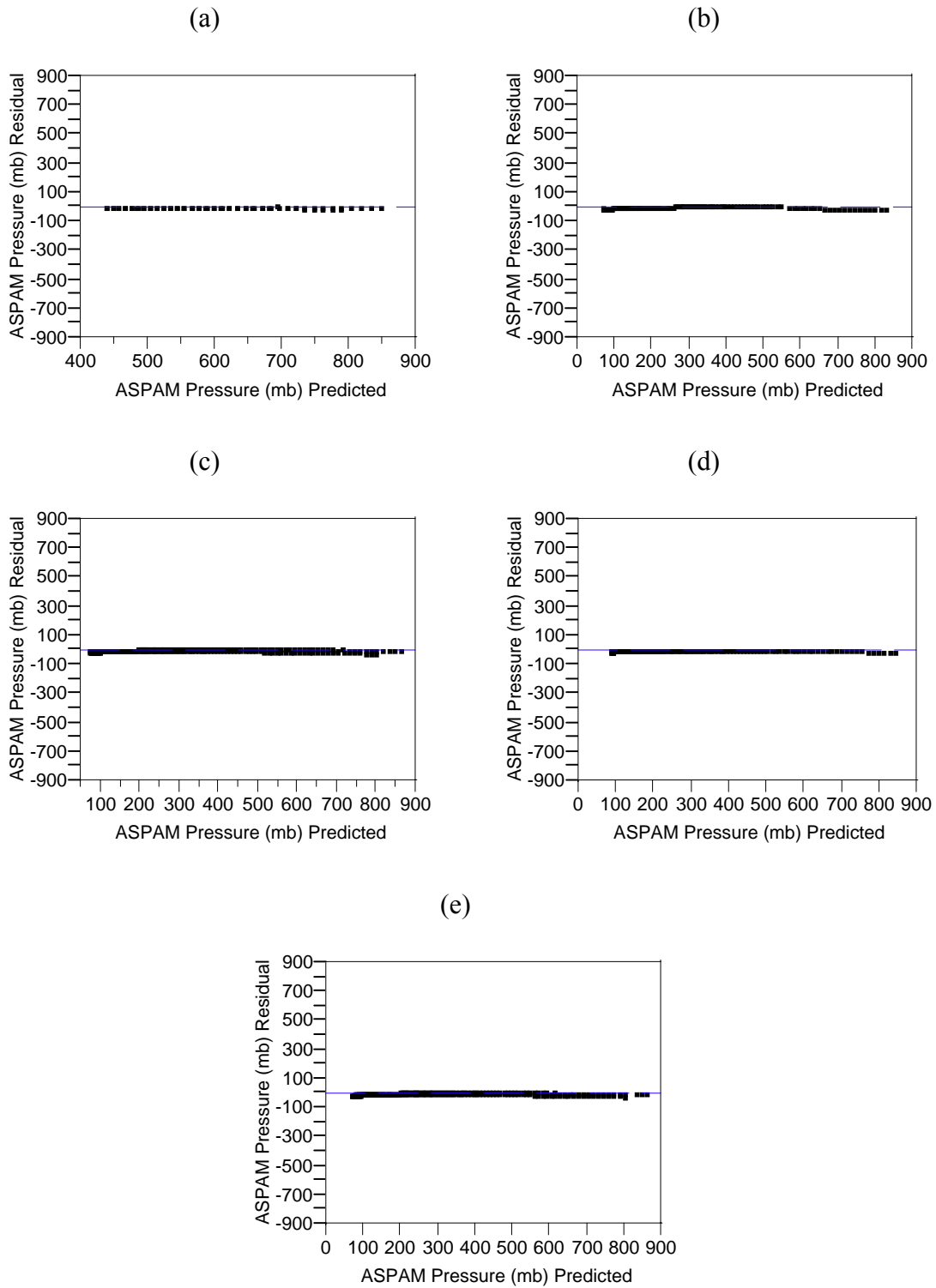


Figure 16. Residual versus predicted plots of ASPAM pressure for Global Hawk missions (a-e) 1 through 5.

2) RAOB

Only three rawinsonde observations were available for comparison with Global Hawk data and a total of 246 reports were analyzed. Global Hawk pressure was used as a predictor for RAOB pressure and the scatterplot with fitted line is shown in Figure 17.

The JMP regression analysis results are shown in Figure 18, including R^2 , RMSE, ANOVA table, F -ratio, and parameter estimates including the t -test results for the hypothesis $\beta_1 = 0$. Regression analysis showed the Global Hawk is an accurate predictor of atmospheric pressure as established by RAOBs.

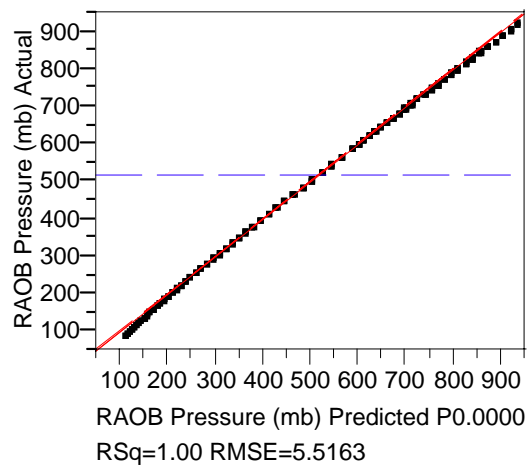


Figure 17. Simple linear regression scatterplot and fitted line of Global Hawk pressure (x) versus RAOB pressure (y).

The hypothesis test for $\beta_1 = 1$ was accomplished using the JMP output from Figure 18 and calculations in Mathcad software. Recall that $\alpha = 0.05$ and the degrees of freedom are defined by $n - 2 = 244$ for Global Hawk versus RAOB regression. The JMP values used were $\hat{\beta}_1 = 0.9874827$ and $\hat{\sigma}^2 = 30.429904$. The critical t -value and SS_{xx}

were calculated as $t_{\alpha/2, n-2} = t_{0.025, 244} = 1.9697$ and $SS_{xx} = 47400996.86$. The output t -value was $t_0 = -15.263$ which led to the conclusion of rejecting the null hypothesis $\beta_1 = 1$. As previously stated, this test was likely to fail because of the extremely low variance of the linear model. Therefore, all assumptions of Global Hawk pressure data quality were based on the regression analysis and hypothesis test of $\beta_1 = 0$.

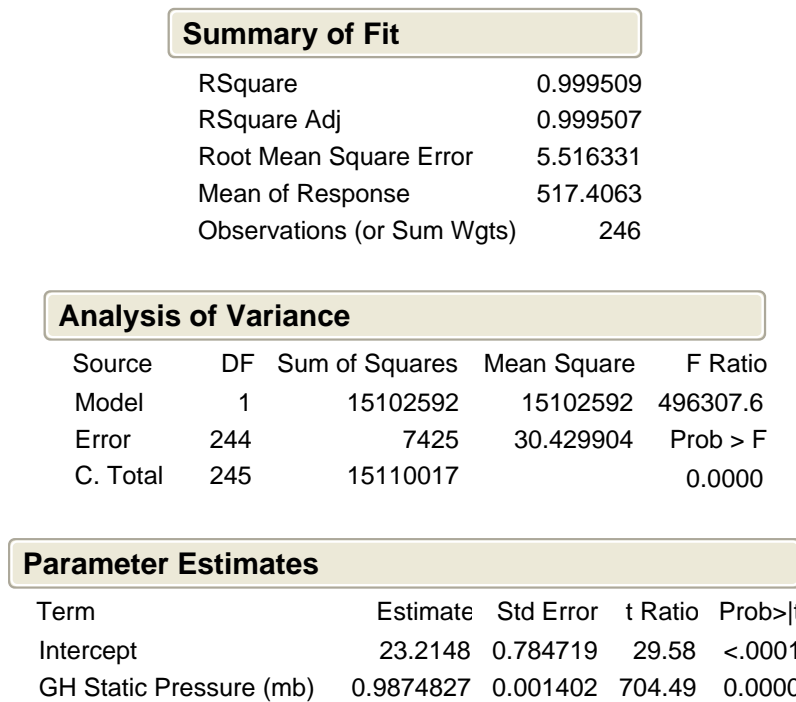


Figure 18. Regression analysis results of Global Hawk pressure (x) versus RAOB pressure (y).

Residual analysis showed there were no significant problems in the regression. The residuals were small when examined on the same scale as the regression variables. Similar patterns in the bias were observed in RAOB regression as in ASPAM regression. The residual versus predicted plots for missions 1, 4, and 5 are depicted in Figure 19.

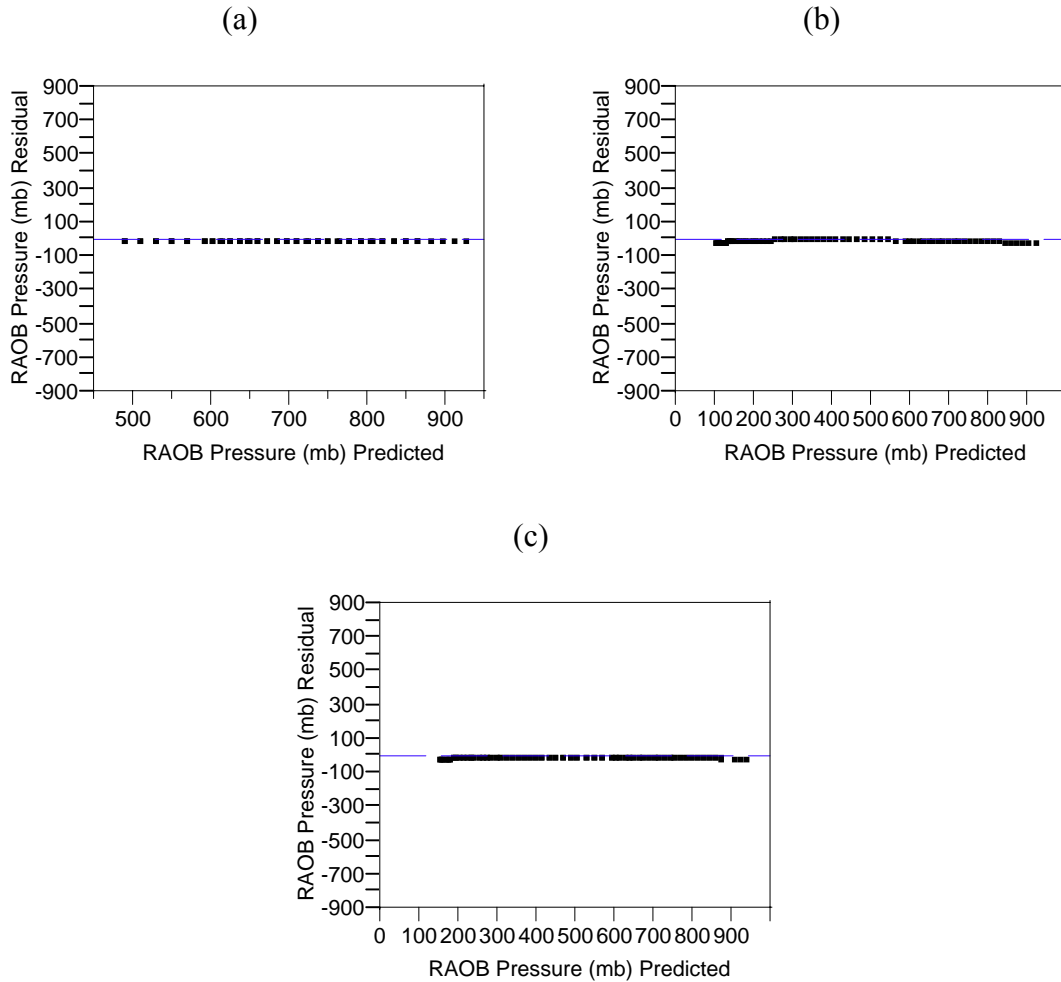


Figure 19. Residual versus predicted plots of RAOB pressure for Global Hawk missions (a) 1, (b) 4, and (c) 5.

b. Temperature

All tests and analyses of Global Hawk temperature were also successful and provided adequate results to conclude that Global Hawk temperature reports were valid. The linear regression of Global Hawk temperature with ASPAM and RAOB temperature produced significant linear models and extremely low values of variance and RMSE.

1) ASPAM

All five Global Hawk missions provided 772 data points which were used in linear regression of Global Hawk temperature (x) with ASPAM temperature (y). The JMP scatterplot and fitted line is depicted in Figure 20 and the regression analysis results are illustrated in Figure 21. The results include R^2 , RMSE, ANOVA table, F -ratio, and parameter estimates, along with the t -test values for the hypothesis test $\beta_1 = 0$. The figures show the Global Hawk is an accurate predictor of atmospheric temperature as established by ASPAM.

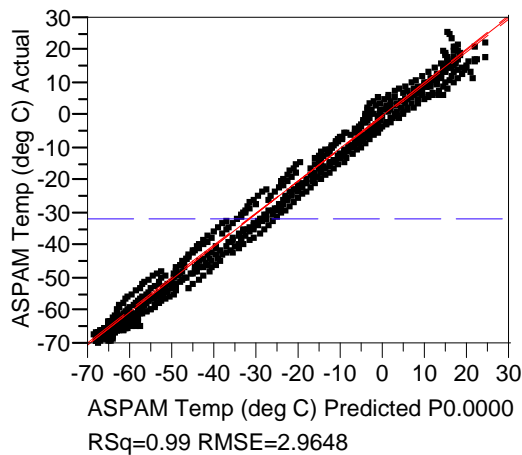


Figure 20. Simple linear regression scatterplot and fitted line of Global Hawk temperature (x) versus ASPAM temperature (y).

The hypothesis test for $\beta_1 = 1$ was accomplished using the JMP output from Figure 21 and calculations in Mathcad software. Recall that $\alpha = 0.05$ and the degrees of freedom are defined by $n - 2 = 770$ for Global Hawk versus ASPAM regression. The JMP values used were $\hat{\beta}_1 = 0.9138359$ and $\hat{\sigma}^2 = 8.79$. The critical t -value and SS_{xx}

were calculated as $t_{\alpha/2, n-2} = t_{0.025, 770} = 1.963$ and $SS_{xx} = 802047.26$. The output t -value was $t_0 = -26.027$ which led to the conclusion of rejecting the null hypothesis $\beta_1 = 1$. As previously stated, this test was likely to fail because of the extremely low variance of the linear model. Therefore, all assumptions of Global Hawk temperature data quality were based on the regression analysis and hypothesis test of $\beta_1 = 0$.

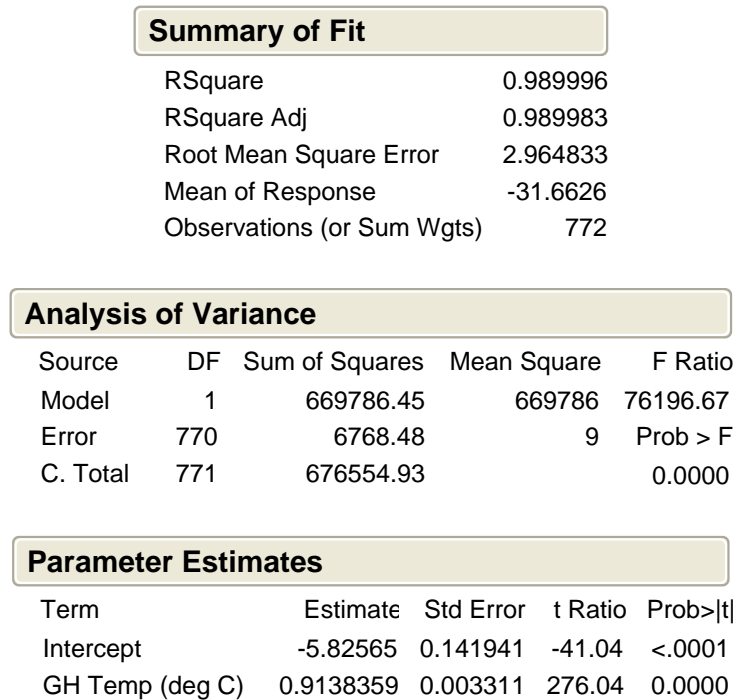


Figure 21. Regression analysis results of Global Hawk temperature (x) versus ASPAM temperature (y).

Residual analysis showed there were no significant problems in the regression. The residuals were small when examined on the same scale as the regression variables. Close examination of the data revealed some possible patterns in the bias, however. Global Hawk temperature values primarily had a positive bias during ascent and a negative bias during descent. Also, the amount of bias seemed to change in relation to

the rate at which the Global Hawk climbed or descended. It is possible that a time delay between measuring and transmitting atmospheric values by the Global Hawk would induce the bias observed in this study. During ascent (descent), the Global Hawk could measure the temperature at an altitude lower (higher) than the height at which it transmitted the data. This slight difference in flight level could lead to temperature values higher (lower) than those at which the data was relayed. This height difference could vary in relation to the rate at which the Global Hawk climbed or descended and the temperature bias would reflect this difference. The residual versus predicted plots for each Global Hawk mission are depicted in Figure 22.

2) RAOB

Only three rawinsonde observations were available for comparison with Global Hawk data and a total of 246 data points were analyzed. Global Hawk temperature was used as a predictor for RAOB temperature and the scatterplot with fitted line is shown in Figure 23. The JMP regression analysis results are shown in Figure 24, including R^2 , RMSE, ANOVA table, F -ratio, and parameter estimates with the t -test results for the hypothesis $\beta_1 = 0$. Regression analysis showed the Global Hawk is an accurate predictor of atmospheric temperature as established by RAOBs.

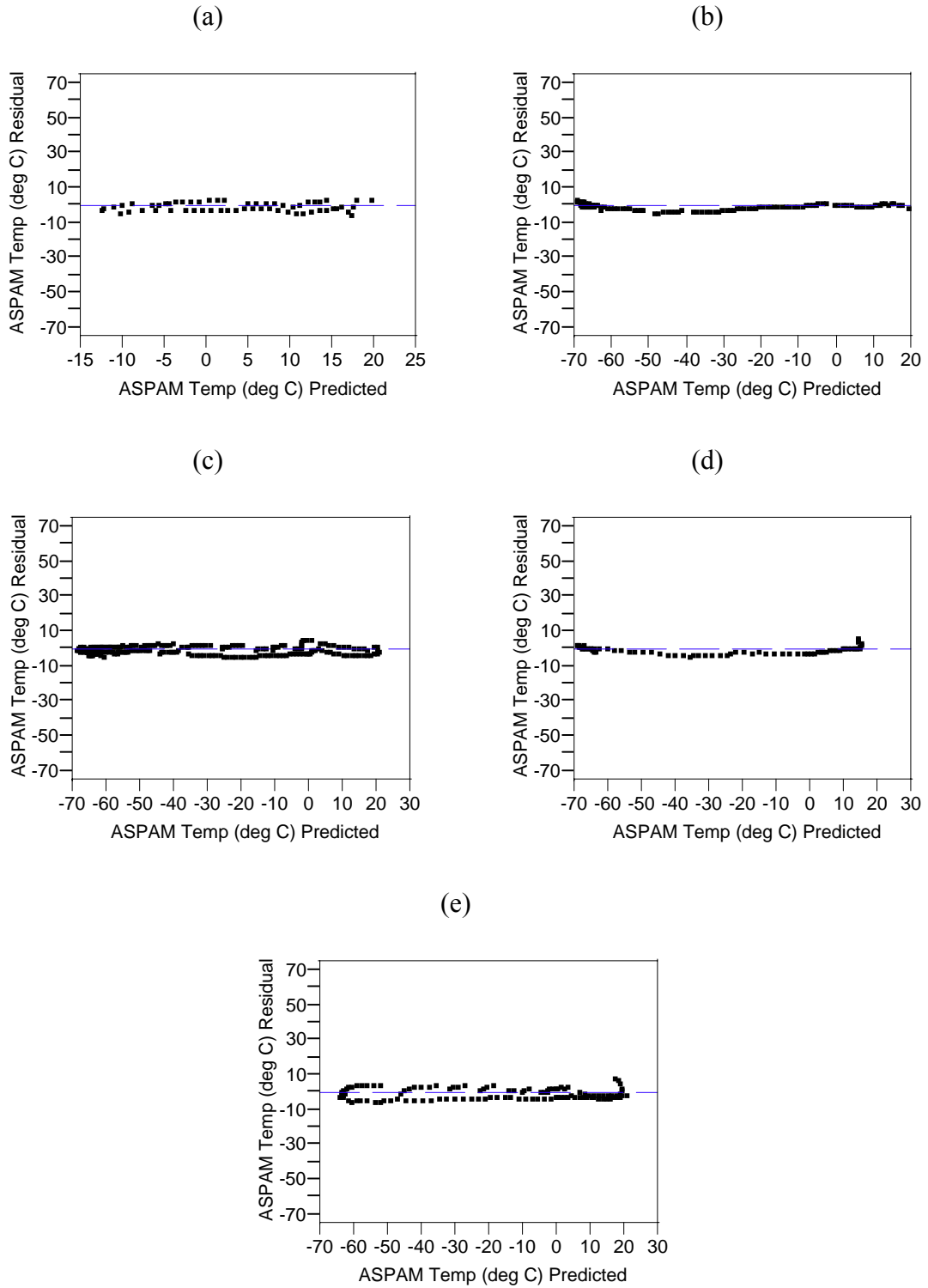


Figure 22. Residual versus predicted plots of ASPAM temperature for Global Hawk missions (a-e) 1 through 5.

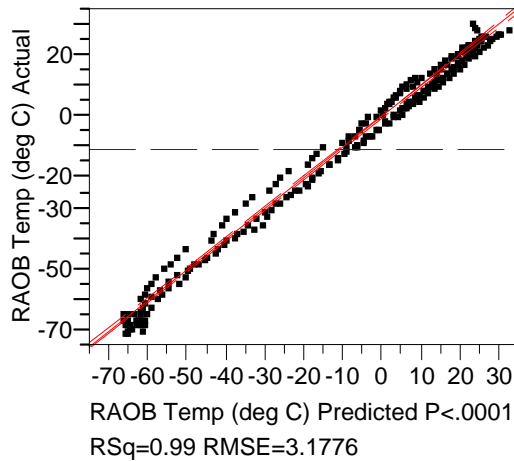


Figure 23. Simple linear regression scatterplot and fitted line of Global Hawk temperature (x) versus RAOB temperature (y).

Summary of Fit

RSquare	0.989639
RSquare Adj	0.989597
Root Mean Square Error	3.177634
Mean of Response	-10.7955
Observations (or Sum Wgts)	246

Analysis of Variance

Source	DF	Sum of Squares	Mean Square	F Ratio
Model	1	235337.71	235338	23306.86
Error	244	2463.76	10	Prob > F
C. Total	245	237801.47		<.0001

Parameter Estimates

Term	Estimate	Std Error	t Ratio	Prob> t
Intercept	0.6835406	0.216101	3.16	0.0018
GH Temp (deg C)	0.9812225	0.006427	152.67	<.0001

Figure 24. Regression analysis results of Global Hawk temperature (x) versus RAOB temperature (y).

The hypothesis test for $\beta_1 = 1$ was accomplished using the JMP output from

Figure 24 and calculations in Mathcad software. Recall that $\alpha = 0.05$ and the degrees of

freedom are defined by $n - 2 = 244$ for Global Hawk versus RAOB regression. The JMP values used were $\hat{\beta}_1 = 0.9812225$ and $\hat{\sigma}^2 = 10.097$. The critical t -value and SS_{xx} were calculated as $t_{\alpha/2, n-2} = t_{0.025, 244} = 1.9697$ and $SS_{xx} = 802047.26$. The output t -value was $t_0 = -5.292$ which led to the conclusion of rejecting the null hypothesis $\beta_1 = 1$. As previously stated, this test was likely to fail because of the extremely low variance of the linear model. Therefore, all assumptions of Global Hawk temperature data quality were based on the regression analysis and hypothesis test of $\beta_1 = 0$.

Residual analysis showed there were no significant problems in the regression. The residuals were small when examined on the same scale as the regression variables. Similar patterns in the bias were observed in RAOB regression as in ASPAM regression. The residual versus predicted plots for missions 1, 4, and 5 are depicted in Figure 25.

c. Wind speed

All tests and analyses of Global Hawk wind speed were also successful and provided adequate results to conclude that Global Hawk wind speed reports were valid. The linear regression of Global Hawk wind speed with ASPAM and RAOB wind speed produced significant linear models and extremely low values of variance and RMSE. Several studies have compared ACARS wind data with other sources, such as rawinsondes, and the amount of error ranged from 1.1 m s^{-1} to 3.1 m s^{-1} (Schwartz and Benjamin 1995; Richner and Gutermann 1987; Benjamin et al. 1999; Morone 1986; Nash 1994). Nash (1994) attributed $1\text{-}1.5 \text{ m s}^{-1}$ of the total 2.6 m s^{-1} wind error to instrument uncertainty and the rest to atmospheric variability between the locations of the compared

measurements. The Global Hawk wind error in the following tests is within this range of variability and, therefore, is assumed to be as accurate and as useful as ACARS data currently in use.

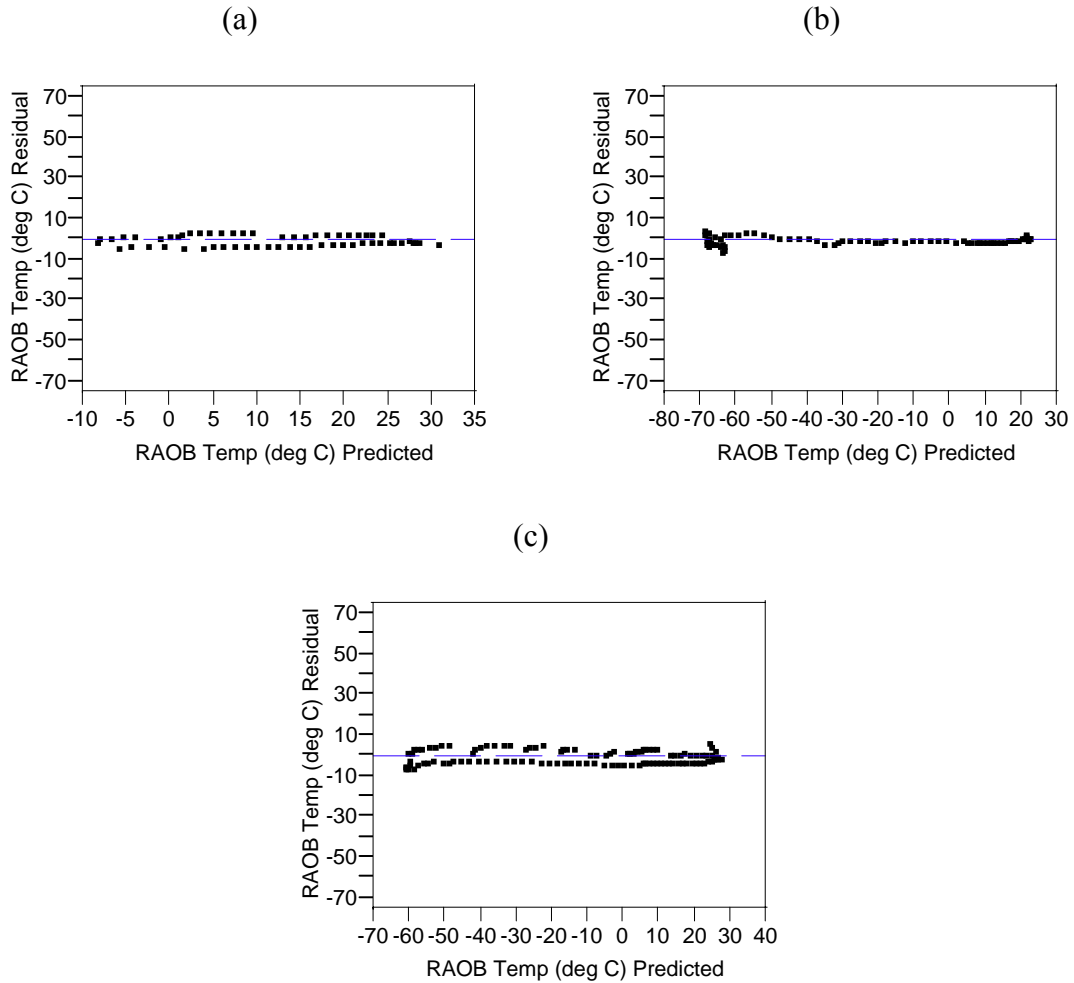


Figure 25. Residual versus predicted plots of RAOB temperature for Global Hawk missions (a) 1, (b) 4, and (c) 5.

1) ASPAM

All five Global Hawk missions provided 772 data points which were used in linear regression of Global Hawk wind speed (x) with ASPAM wind speed (y). The JMP

scatterplot and fitted line is depicted in Figure 26 and the regression analysis results are illustrated in Figure 27. The results include R^2 , RMSE, ANOVA table, F -ratio, and parameter estimates, along with the t -test values for the hypothesis test $\beta_1 = 0$. The figures show the Global Hawk is an accurate predictor of atmospheric wind speed as established by ASPAM.

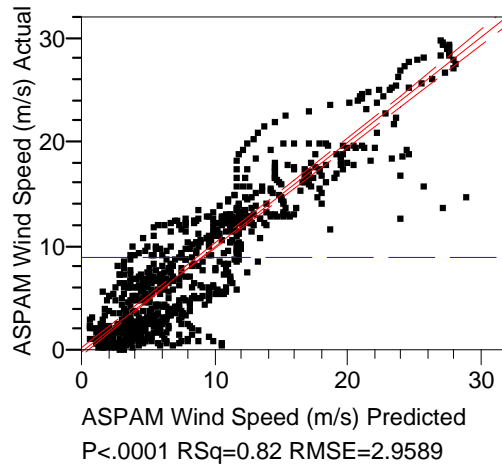


Figure 26. Simple linear regression scatterplot and fitted line of Global Hawk wind speed (x) versus ASPAM wind speed (y).

The hypothesis test for $\beta_1 = 1$ was accomplished using the JMP output from Figure 27 and calculations in Mathcad software. Recall that $\alpha = 0.05$ and the degrees of freedom are defined by $n - 2 = 770$ for Global Hawk versus ASPAM regression. The JMP values used were $\hat{\beta}_1 = 0.5581524$ and $\hat{\sigma}^2 = 33.053$. The critical t -value and SS_{xx} were calculated as $t_{\alpha/2, n-2} = t_{0.025, 770} = 1.963$ and $SS_{xx} = 95467.40$. The output t -value was $t_0 = -23.746$ which led to the conclusion of rejecting the null hypothesis $\beta_1 = 1$. As previously stated, this test was likely to fail because of the extremely low variance of the

linear model. Therefore, all assumptions of Global Hawk wind speed data quality were based on the regression analysis and hypothesis test of $\beta_1 = 0$.

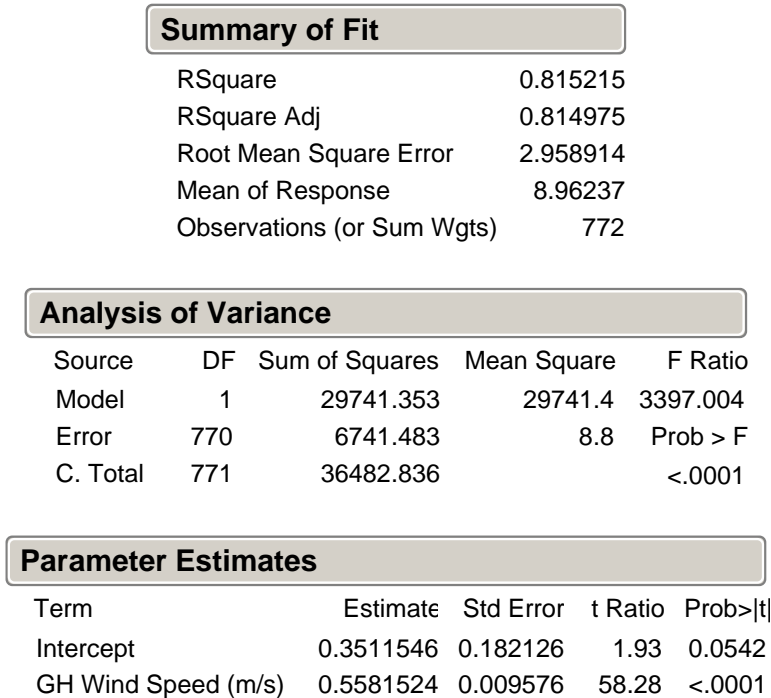


Figure 27. Regression analysis results of Global Hawk wind speed (x) versus ASPAM wind speed (y).

Residual analysis showed there were no significant problems in the regression. The residuals were small when examined on the same scale as the regression variables. Close examination of the data revealed some possible patterns in the bias, however. A majority of the extreme bias values ($-2 \text{ m s}^{-1} \geq \text{bias} \geq 2 \text{ m s}^{-1}$) were reported in the lower ($\leq 10 \text{ Kft}$) and upper ($\geq 40 \text{ Kft}$) levels of the Global Hawk missions. It is the assumption of this research that the bias was induced by the mesoscale variability of the winds in the lower levels and significantly higher wind speeds in the upper levels. Global Hawk wind measurements could be affected by higher upper-level wind speeds and these impacts

would vary with the speed and attitude of the aircraft relative to the mean flow. An additional consideration is rawinsonde balloon drift in the upper-levels, which would influence ASPAM profiles. The residual versus predicted plots are depicted in Figure 28.

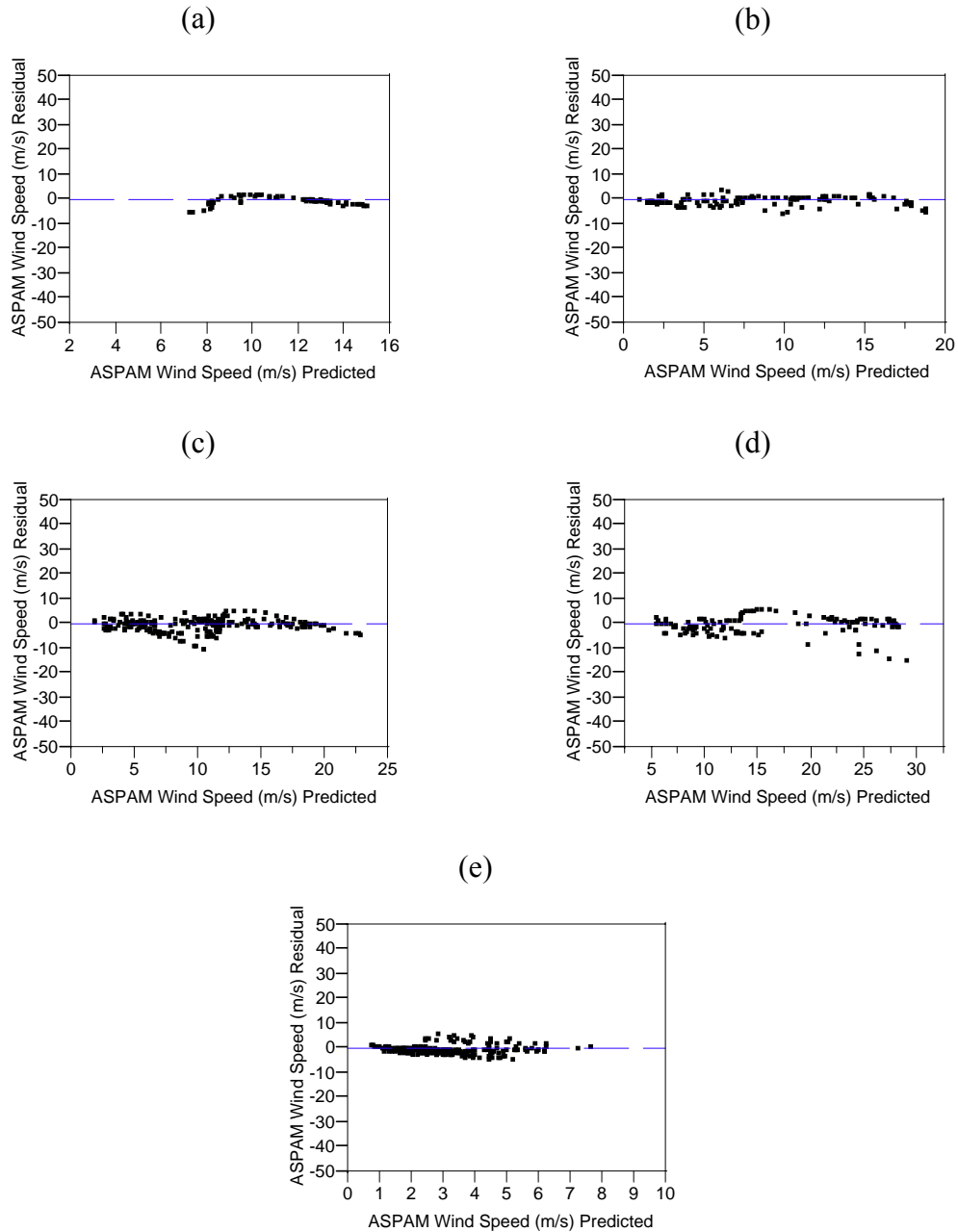


Figure 28. Residual versus predicted plots of ASPAM wind speed for Global Hawk missions (a-e) 1 through 5.

2) RAOB

Only three rawinsonde observations were available for comparison with Global Hawk data and a total of 246 data points were analyzed. Global Hawk wind speed was used as a predictor for RAOB wind speed and the scatterplot with fitted line is shown in Figure 29. The JMP regression analysis results are shown in Figure 30, including R^2 , RMSE, ANOVA table, F -ratio, and parameter estimates including the t -test results for the hypothesis $\beta_1 = 0$. Regression analysis results show the Global Hawk is an accurate predictor of atmospheric wind speed as established by RAOBs.

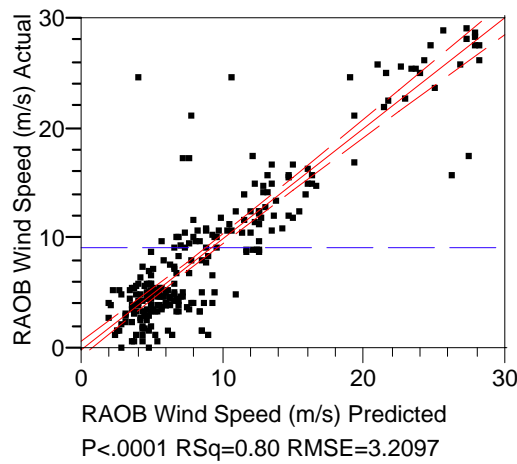


Figure 29. Simple linear regression scatterplot and fitted line of Global Hawk wind speed (x) versus RAOB wind speed (y).

The hypothesis test for $\beta_1 = 1$ was accomplished using the JMP output from Figure 24 and calculations in Mathcad software. Recall that $\alpha = 0.05$ and the degrees of freedom are defined by $n - 2 = 244$ for Global Hawk versus RAOB regression. The JMP

values used were $\hat{\beta}_1 = 0.5366051$ and $\hat{\sigma}^2 = 10.30$. The critical t -value and SS_{xx} were calculated as $t_{\alpha/2, n-2} = t_{0.025, 770} = 1.9697$ and $SS_{xx} = 95467.40$. The output t -value was $t_0 = -44.613$ which led to the conclusion of rejecting the null hypothesis $\beta_1 = 1$. As previously stated, this test was likely to fail because of the extremely low variance of the linear model. Therefore, all assumptions of Global Hawk temperature data quality were based on the regression analysis and hypothesis test of $\beta_1 = 0$.

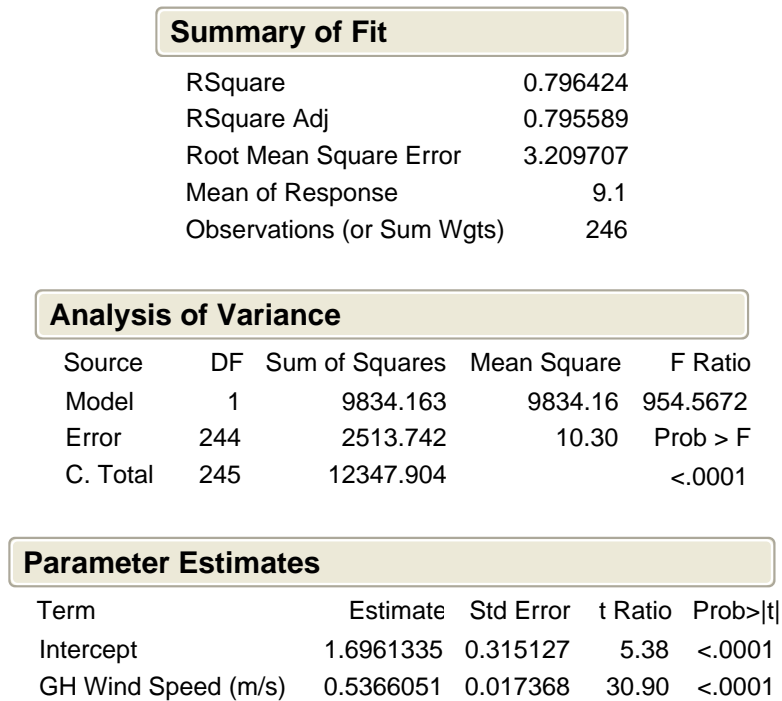


Figure 30. Regression analysis results of Global Hawk wind speed (x) versus RAOB wind speed (y).

Residual analysis showed there were no significant problems in the regression. The residuals were small when examined on the same scale as the regression variables.

Similar patterns in the bias were observed in RAOB regression as in ASPAM regression.

The residual versus predicted plots for missions 1, 4, and 5 are depicted in Figure 31.

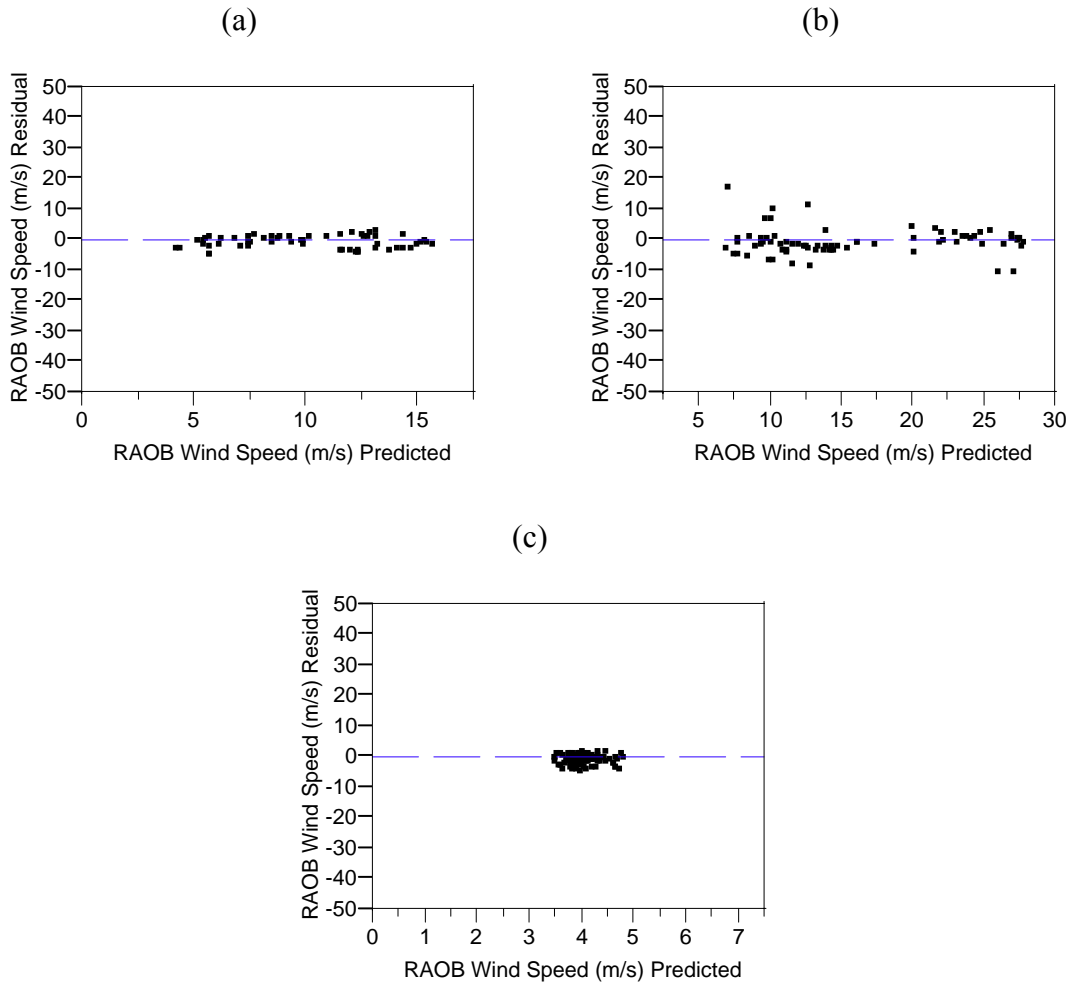


Figure 31. Residual versus predicted plots of RAOB wind speed for Global Hawk missions (a) 1, (b) 4, and (c) 5.

3) ASPAM – ADJUSTED WIND DATA

Investigation of the data revealed certain wind data points which could be excluded from analysis based on certain assumptions. The extreme outliers in the original regression were excluded due to the observation that they were grouped together

during specific periods of each of the missions. It was assumed that either the data were relayed incorrectly due to a system problem or that an unknown atmospheric occurrence corrupted the information. A total of 122 extreme outliers were excluded based on these assumptions.

Wind measurements could be degraded due to the motion and flight attitude of the measuring airframe (Axford 1968). Painting (2002) determined an uncertainty of wind data to be 2-3 m s⁻¹, which increased during aircraft maneuvers. Bisiaux et al. (1983) also calculated higher errors in wind data during aircraft maneuvers and excluded reports with roll angles greater than 5 degrees. This research excluded data points at which the aircraft was either pitching or rolling in excess of 10 degrees based on the assumptions of aircraft maneuvering impacts on wind data. A total of 129 reports were excluded for extreme pitch and 254 reports were excluded for extreme roll of the Global Hawk.

Data points were also excluded based on the assumptions of erroneous Global Hawk data as described in Section 4.b.1. The system reported to be in Altitude Hold Mode but the aircraft altitude continued to fluctuate, possibly indicating suspect data. Notes pertaining to the Global Hawk data and varying flight modes are shown in Appendix D. A total of 68 reports were excluded based on these assumptions.

In all, 440 data points were excluded from statistical analysis based on these assumptions. Some of the reports fell into two or more of the categories listed above, leading to a lower number of exclusions than expected. Of particular interest was that all but one data point from mission 1 were excluded. The regression analysis and hypothesis test results follow.

All five Global Hawk missions provided 332 data points which were used in linear regression of Global Hawk wind speed (x) with ASPAM wind speed (y). The JMP scatterplot and fitted line is depicted in Figure 32 and the regression analysis results are illustrated in Figure 33. The results include R^2 , RMSE, ANOVA table, F -ratio, and parameter estimates, along with the t -test values for the hypothesis test $\beta_1 = 0$. The figures show the Global Hawk is an accurate predictor of atmospheric wind speed as established by ASPAM.

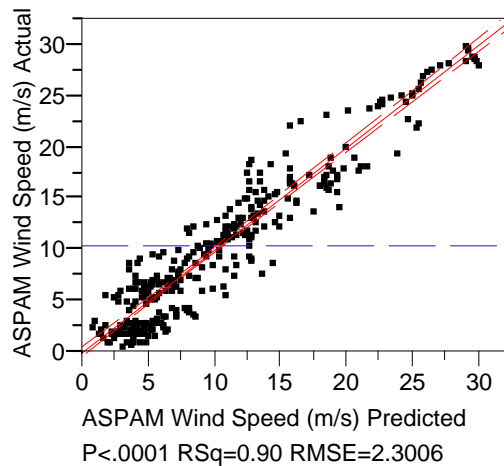


Figure 32. Simple linear regression scatterplot and fitted line of Global Hawk wind speed (x) versus ASPAM wind speed (y) with adjusted wind data.

The hypothesis test for $\beta_1 = 1$ was accomplished using the JMP output from Figure 33 and calculations in Mathcad software. Recall that $\alpha = 0.05$ and the degrees of freedom are defined by $n - 2 = 330$ for Global Hawk versus ASPAM regression. The JMP values used were $\hat{\beta}_1 = 0.5969934$ and $\hat{\sigma}^2 = 5.29$. The critical t -value and SS_{xx} were calculated as $t_{\alpha/2, n-2} = t_{0.025, 330} = 1.9672$ and $SS_{xx} = 45653.76$. The output t -value

was $t_0 = -37.439$ which led to the conclusion of rejecting the null hypothesis $\beta_1 = 1$. As previously stated, this test was likely to fail because of the extremely low variance of the linear model. Therefore, all assumptions of Global Hawk wind speed data quality were based on the regression analysis and hypothesis test of $\beta_1 = 0$.

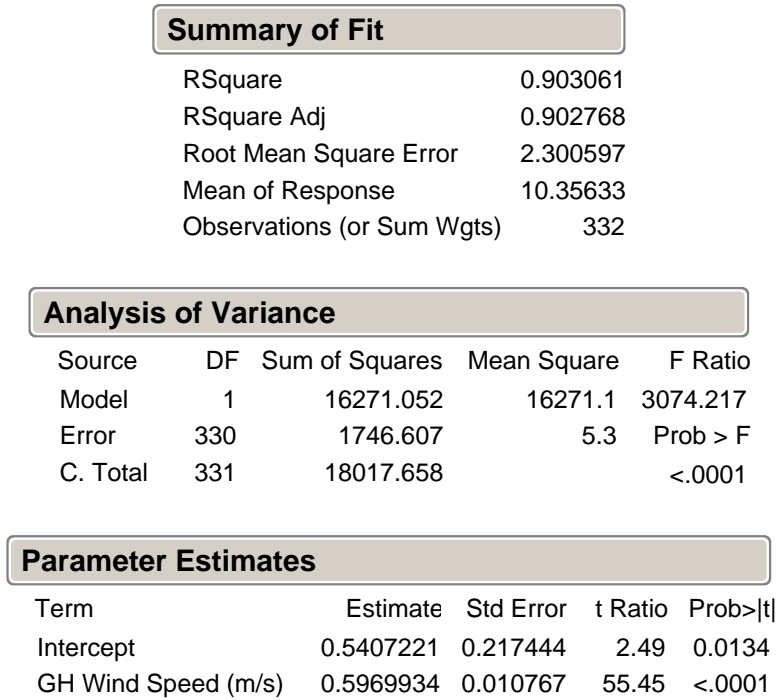


Figure 33. Regression analysis results of Global Hawk wind speed (x) versus ASPAM wind speed (y) with adjusted wind data.

Residual analysis showed there were no significant problems in the regression. The residuals were small when examined on the same scale as the regression variables. Close examination of the data revealed some possible patterns in the bias, however. A majority of the extreme bias values ($-2 \text{ m s}^{-1} \geq \text{bias} \geq 2 \text{ m s}^{-1}$) were reported in the lower ($\leq 10 \text{ Kft}$) and upper ($\geq 40 \text{ Kft}$) levels of the Global Hawk missions. It is the assumption

of this research that the bias was induced by the mesoscale variability of the winds in the lower levels and significantly higher wind speeds in the upper levels. Global Hawk wind measurements could be affected by higher upper-level wind speeds and these impacts would vary with the speed and attitude of the aircraft relative to the mean flow. An additional consideration is rawinsonde balloon drift in the upper-levels, which would influence ASPAM profiles. The residual versus predicted plots for each Global Hawk mission are depicted in Figure 34. Only one data point was available for mission 1 after excluding suspect wind data. Therefore, the residual plot for mission 1 is empty.

4) RAOB – ADJUSTED WIND DATA

The same assumptions were made and rows excluded as in Section 5.c.3. A total of 172 data rows were excluded leaving only 74 rows of data for analysis with rawinsonde observations. Global Hawk wind speed was used as a predictor for RAOB wind speed and the scatterplot with fitted line is shown in Figure 35. The JMP regression analysis results are shown in Figure 36, including R^2 , RMSE, ANOVA table, F -ratio, and parameter estimates including the t -test results for the hypothesis $\beta_1 = 0$. Regression analysis results show the Global Hawk is an accurate predictor of atmospheric wind speed as established by RAOBs.

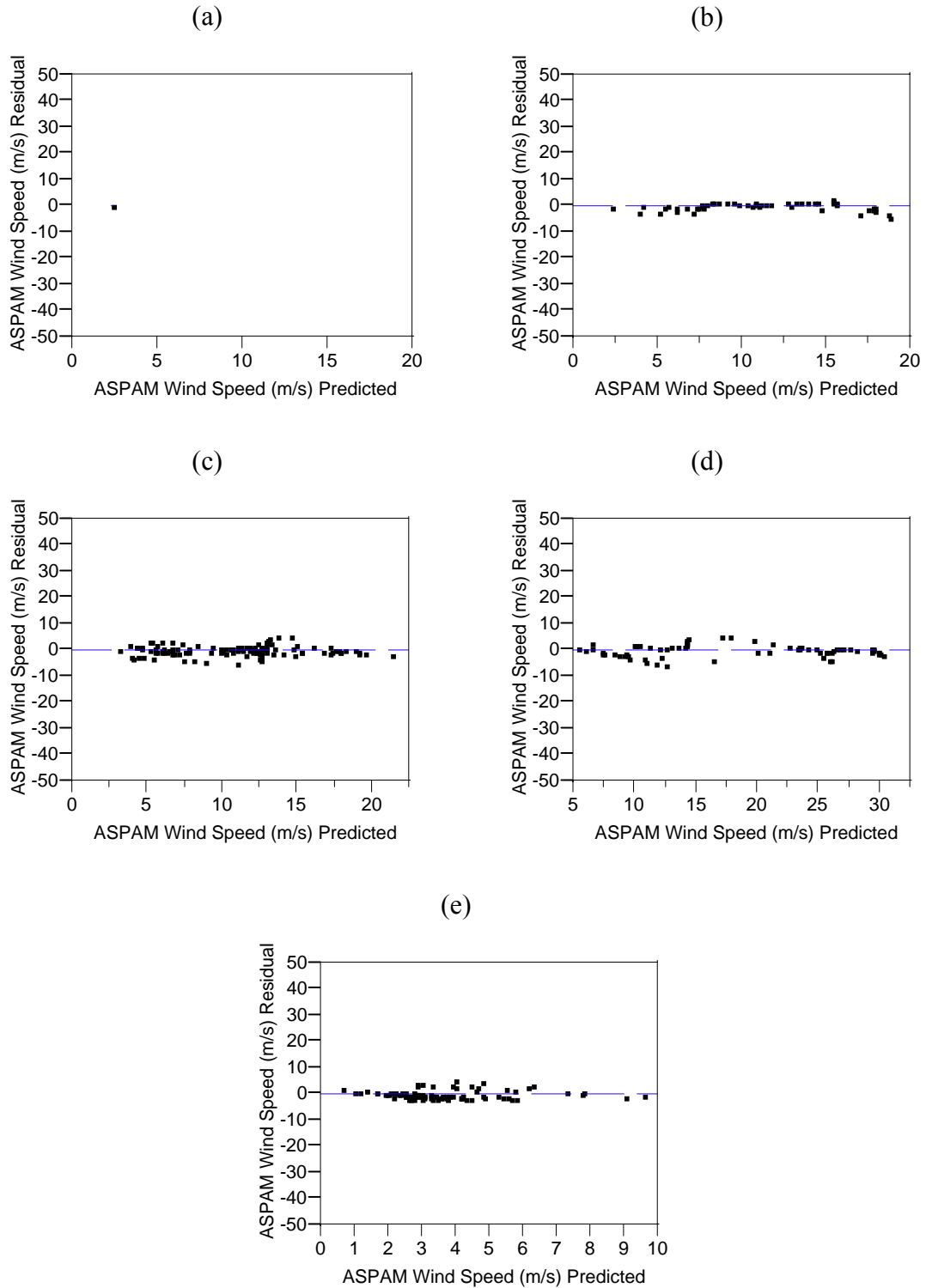


Figure 34. Residual versus predicted plots of ASPAM wind speed for Global Hawk missions (a-e) 1 through 5 with adjusted wind data.

The hypothesis test for $\beta_1 = 1$ was accomplished using the JMP output from Figure 36 and calculations in Mathcad software. Recall that $\alpha = 0.05$ and the degrees of freedom are defined by $n - 2 = 72$ for Global Hawk versus RAOB regression with adjusted wind data. The JMP values used were $\hat{\beta}_1 = 0.6029932$ and $\hat{\sigma}^2 = 4.37$. The critical t -value and SS_{xx} were calculated as $t_{\alpha/2, n-2} = t_{0.025, 72} = 1.9935$ and $SS_{xx} = 45653.76$. The output t -value was $t_0 = -40.578$ which led to the conclusion of rejecting the null hypothesis $\beta_1 = 1$. As previously stated, this test was likely to fail because of the extremely low variance of the linear model. Therefore, all assumptions of Global Hawk temperature data quality were based on the regression analysis and hypothesis test of $\beta_1 = 0$.

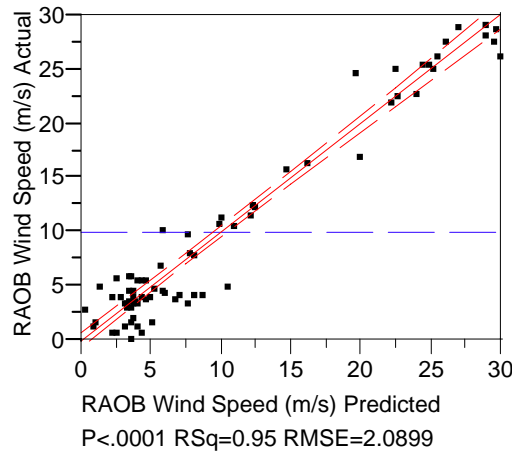


Figure 35. Simple linear regression scatterplot and fitted line of Global Hawk wind speed (x) versus RAOB wind speed (y) with adjusted wind data.

Summary of Fit

RSquare	0.950114
RSquare Adj	0.949421
Root Mean Square Error	2.089922
Mean of Response	10.02838
Observations (or Sum Wgts)	74

Analysis of Variance

Source	DF	Sum of Squares	Mean Square	F Ratio
Model	1	5989.5106	5989.51	1371.295
Error	72	314.4798	4.37	Prob > F
C. Total	73	6303.9905		<.0001

Parameter Estimates

Term	Estimate	Std Error	t Ratio	Prob> t
Intercept	0.1362796	0.361085	0.38	0.7070
GH Wind Speed (m/s)	0.6029932	0.016283	37.03	<.0001

Figure 36. Regression analysis results of Global Hawk wind speed (x) versus RAOB wind speed (y) with adjusted wind data.

Residual analysis showed there were no significant problems in the regression. The residuals were small when examined on the same scale as the regression variables. Similar patterns in the bias were observed in RAOB regression as in ASPAM regression. The residual versus predicted plots for missions 1, 4, and 5 are depicted in Figure 37. Only one data point was available for mission 1 after excluding suspect wind data. Therefore, the residual plot for mission 1 is empty.

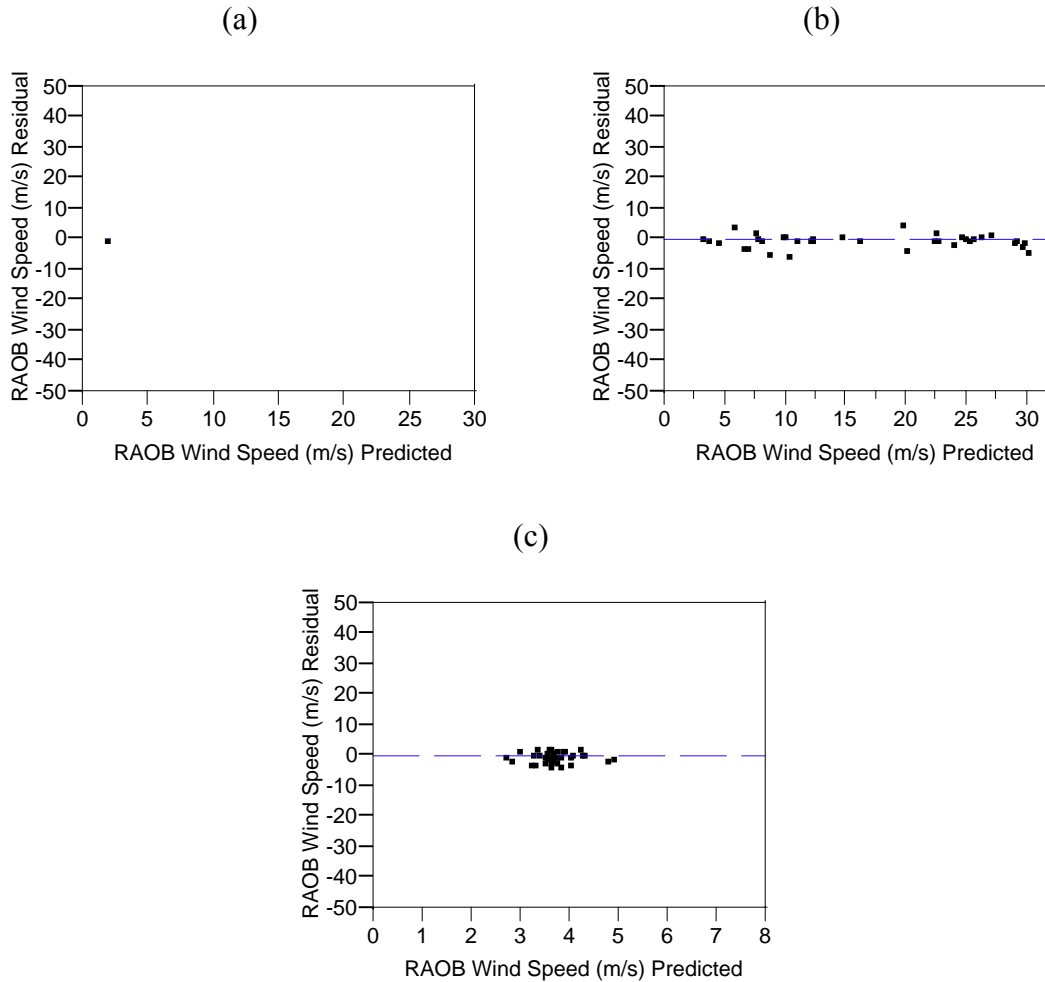


Figure 37. Residual versus predicted plots of RAOB wind speed for Global Hawk missions (a) 1, (b) 4, and (c) 5 with adjusted wind data.

d. Wind direction

1) RMS VECTOR ERROR

The root mean square vector error of the Global Hawk winds versus the ASPAM and RAOB winds was calculated using both the original and the adjusted datasets. The wind direction and wind speed were taken into account using this method. The RMS vector error of Global Hawk versus ASPAM winds was 0.806 m s^{-1} with the original dataset and 0.566 m s^{-1} using the adjusted data. The RMS vector error of Global Hawk

versus RAOB winds was 1.403 m s^{-1} with the original dataset and 0.988 m s^{-1} using the adjusted data.

2) MEAN DIFFERENCE

The ASPAM and RAOB wind direction values were subtracted from the Global Hawk wind direction measurements using the technique illustrated in Section 4.c.2. The mean differences between Global Hawk and ASPAM data were 31.4° for the original dataset and 26.3° for the adjusted data. The mean differences between the Global Hawk and RAOB data were 36.5° for the original dataset and 42.4° for the adjusted data. The degradation in the RAOB difference with the adjusted dataset was most likely due to the significantly lower number of observations available after the suspect information was eliminated.

A significant portion of the wind direction error can be attributed to light wind conditions, which were determined as 5 m s^{-1} or less for this research. Light winds occurred about 64% of the time with ASPAM and RAOB reports and 14% of the time for Global Hawk reports. Schwartz and Benjamin (1995) determined a mean directional difference of 35.1° when comparing ACARS and rawinsonde wind data, which is comparable to the results of this research.

6. Conclusions and Recommendations

a. Conclusions

The Global Hawk Air Data System is an accurate predictor of the atmospheric variables of pressure, temperature, wind speed, and wind direction. The statistical tests performed in this research show an almost perfect fit of Global Hawk pressure and temperature data with both ASPAM and RAOB values. The linear fit for wind data was also significant, especially after some assumptions and exclusions were made. The results demonstrate environmental intelligence gathered by the Global Hawk is precise and, therefore, of value to both the intelligence and meteorological communities.

The linear fit of Global Hawk pressure with ASPAM and RAOB data was virtually exact with R^2 values of 0.999. The RMSE values were exceptionally low with 8.29 mb for ASPAM regression and 5.52 mb for RAOB regression.

Simple linear regression revealed Global Hawk temperature comparisons with ASPAM and RAOB reports were also very precise with R^2 values of 0.990. The RMSE values were also small with 2.96 °C for ASPAM regression and 3.18 °C for RAOB regression.

The statistical analysis of Global Hawk wind speed data was informative and the outcome was comparable to accuracy tests performed on ACARS data. Initial regression with ASPAM and RAOB data provided R^2 values of 0.815 and 0.796, respectively. The RMSE values were 2.96 m s⁻¹ for ASPAM regression and 3.21 m s⁻¹ for RAOB regression. After adjusting the data and making exclusions based on certain assumptions, the results improved drastically. The excluded data consisted of extreme outliers that were grouped together, excessive pitch and roll of the Global Hawk, and possible

erroneous Global Hawk reports. The new R^2 values were 0.903 for ASPAM and 0.950 for RAOB. The adjusted RMSE values for ASPAM and RAOB regression were 2.30 m s^{-1} and 2.09 m s^{-1} , respectively. This typical error magnitude of the Global Hawk wind speed data is similar to the results of numerous quality assessments of ACARS data.

Wind direction data could not be analyzed by normal methods due to its non-linearity but useful information was obtained by calculating the RMS vector errors and mean differences. Analysis with the original datasets produced RMS vector errors of 0.806 m s^{-1} for Global Hawk versus ASPAM and 1.403 m s^{-1} for Global Hawk versus RAOB. The mean differences in direction between the initial Global Hawk and “ground truth” datasets were 31.4° with ASPAM and 36.5° with RAOB. After assumptions were made and the data were adjusted, RMS vector errors improved to 0.566 m s^{-1} for Global Hawk versus ASPAM and 0.988 m s^{-1} for Global Hawk versus RAOB. The adjusted data produced different results for the mean difference in wind direction. The mean difference improved to 26.3° for the ASPAM data but worsened to 42.4° for the RAOB data.

Independent verification of ACARS wind data has produced RMS vector errors ranging from 1.1 m s^{-1} to 3.1 m s^{-1} and mean differences between 30° and 40°. Mean difference values this large should raise some doubt as to the accuracy of the wind data. An assumption was made that light winds ($\leq 5 \text{ m s}^{-1}$) would introduce variability in the wind direction data. RMS vector error calculations alleviate any problems due to light and variable winds because both wind direction and wind speed are taken into account. The Global Hawk RMS vector errors produced in this research are analogous with those of ACARS data found in previous studies (Schwartz and Benjamin 1995; Richner and Gutermann 1987; Benjamin et al. 1999; Morone 1986; Nash 1994). Even so, the

accuracy of ACARS wind information has been deemed adequate to successfully enhance forecast products and NWP models for the past decade.

The results above demonstrate the accuracy of the Global Hawk environmental information. Several assumptions were made in this research but the overall results provided sufficient justification that this UAV would serve well as a meteorological sensing platform. Alterations to the Global Hawk aircraft configuration or mission profile are not required in order to obtain and exploit this data. Therefore, steps should be taken to ensure this source of environmental information is made available to military weather agencies as well as UAV operators and planners. An increase in accurate weather data would lead to improved mission effectiveness, especially over data-sparse regions. The Global Hawk has the ability to provide atmospheric soundings during its ascent and descent and its near real time data could benefit mission operators, planners, and weather forecasters alike. Sample soundings from all five Global Hawk missions are depicted in Figure 38, illustrating just one of the many possible benefits of acquiring and utilizing this accurate and timely information. Dual lines on some of the plots indicate two soundings were created, one during ascent and the other during descent. The tropopause, stratospheric inversion, and low-level inversions are evident on several plots.

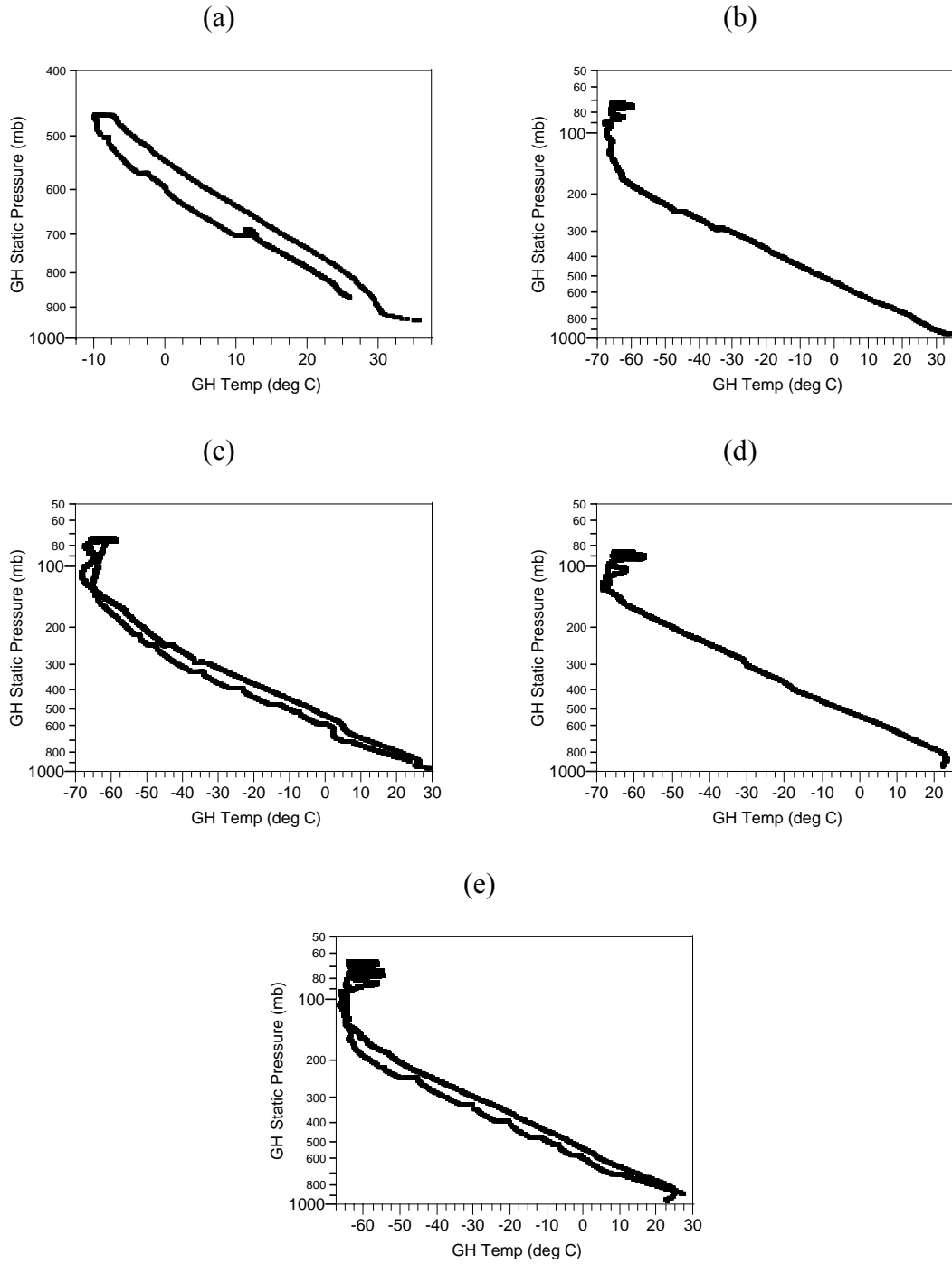


Figure 38. Atmospheric sounding plots of temperature versus pressure from Global Hawk missions (a-e) 1 through 5.

b. Recommendations

The RQ-4A Global Hawk is a proven asset to the intelligence and operational communities and could benefit the meteorological community as well, if the atmospheric data from the system were made available. Weather data are measured and transmitted regularly by the Global Hawk during all phases of its operation so efforts must be made to acquire this readily abundant information. Additional sensors or meteorological payloads are not required to make use of this valuable data. Thus, it appears the only thing preventing the use of this atmospheric intelligence is coordination between the affected agencies to determine an acquisition and communications systems strategy, while maintaining an awareness of the classified nature of the majority of Global Hawk flight routes and missions.

1) FOR AIR FORCE WEATHER

Steps should be taken to obtain Global Hawk environmental intelligence in near real time from the mission control elements or the airframe itself. Coordination with the Global Hawk System Program Office and the 88th Weather Squadron at Wright-Patterson AFB is paramount to ensure acquisition of this valuable weather intelligence, especially in data-sparse battlefield environments. Atmospheric information are available in numerous data-sparse regions during Global Hawk operations and this intelligence could be used to enhance model initialization, improve forecast products, and provide additional data points for analysis.

2) FOR GLOBAL HAWK SPO

Correspond with Air Force weather agencies to make Global Hawk weather data available to meteorologists and mission planners. Doing so would not only improve the weather support provided to Global Hawk operators but also allow trained technicians to evaluate the atmospheric reports and ensure operations are completed successfully.

Analyze the datasets used in this research along with data from other missions to possibly determine the causes of the bias in the data. Research the information provided in Appendix D to resolve any possible measurement or transmission problems within the Global Hawk system.

3) FOR FUTURE RESEARCH

Several additional tests and techniques were contemplated during this research but time was a major impact not only on the methodology but also the final thesis product. More intense regression analysis of all datasets should be explored as well as other possible statistical tests. Further investigation into circular data analysis could provide useful information as well as a new approach to verifying environmental data. Colleagues and professors had very interesting ideas and the question, “Have you considered...?” was asked on several occasions. This meteorologist leaves many considerations and unanswered questions to future students and fellow researchers.

Appendix A: Acronyms

ACARS	Aircraft Communications Addressing and Reporting System
ADS	Air Data System
AFB	Air Force Base
AFCCC	Air Force Combat Climatology Center
AFIT	Air Force Institute of Technology
AIREPS	Aircraft REPortS
AMDAR	Aircraft Meteorological DAta Relay
ANOVA	Analysis of Variance
ARINC	Aeronautical Radio, Inc
ASPAM	Atmospheric Slant Path Analysis Model
AV7	Air Vehicle 7
COAMPS	Coupled Ocean/Atmospheric Mesoscale Prediction System
CONUS	CONTinental United States
CWSU	Center Weather Service Unit
DEVG	Derived Equivalent Vertical Gust
DoD	Department of Defense
DTED	Digital Terrain Elevation Data
EDR	Eddy Dissipation Rate
FLTS	FLight Test Squadron
FNMOC	Fleet Numerical Meteorology and Oceanography Center
FSL	Forecast Systems Laboratory
IMMC	Integrated Mission Management Computer
MSE	Mean Square Error
MSL	Mean Sea Level
MVOI	Multivariate Optimal Interpolation
NOAA	National Oceanic and Atmospheric Administration
NOGAPS	Navy Operational Global Atmospheric Prediction System
NWP	Numerical Weather Prediction
NWSFO	National Weather Service Forecast Offices
PIREPS	PIlot REPortS
RAOB	RAwinsonde OBServation
RMSE	Root Mean Square Error
RTNEPH	Real-Time NEPHanalysis
SPC	Storm Prediction Center
SPO	System Program Office
TDY	Temporary DutY
WPAFB	Wright-Patterson Air Force Base
WRF	Weather Research and Forecasting model
UAV	Unmanned Aerial Vehicle
US	United States
UTC	Universal Time Code

Appendix B: Upper-Level Wind Analyses

Following are upper-level wind analyses corresponding with the five Global Hawk missions used in this research. Charts are centered over California, represent both 300-mb and 200-mb analyses, and are valid at 1200 and 0000 UTC on the dates of the Global Hawk flights (National Weather Service Storm Prediction Center 2003).

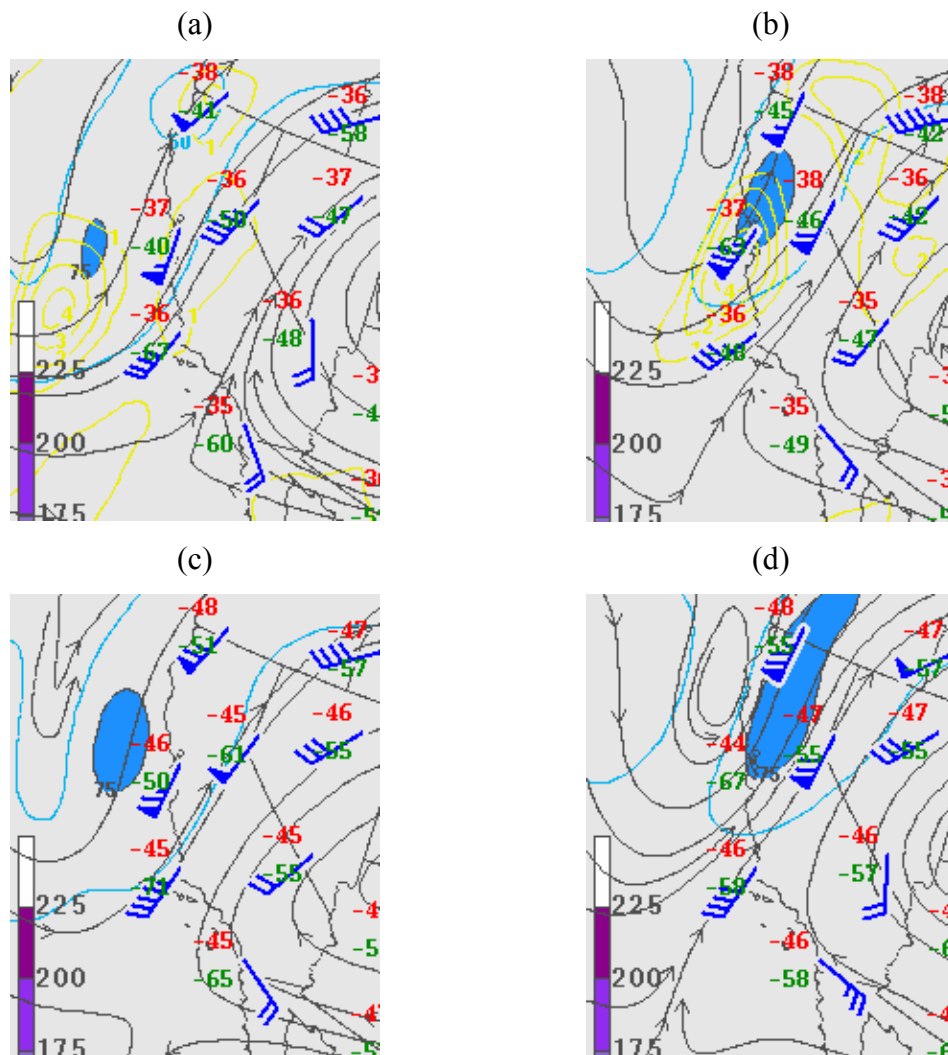


Figure B-1. Upper-level wind analyses for 29 – 30 May 2003. (a) 300 mb at 29/1200 UTC, (b) 300 mb at 30/0000 UTC, (c) 250 mb at 29/1200 UTC, (d) 250 mb at 30/0000 UTC (National Weather Service Storm Prediction Center 2003).

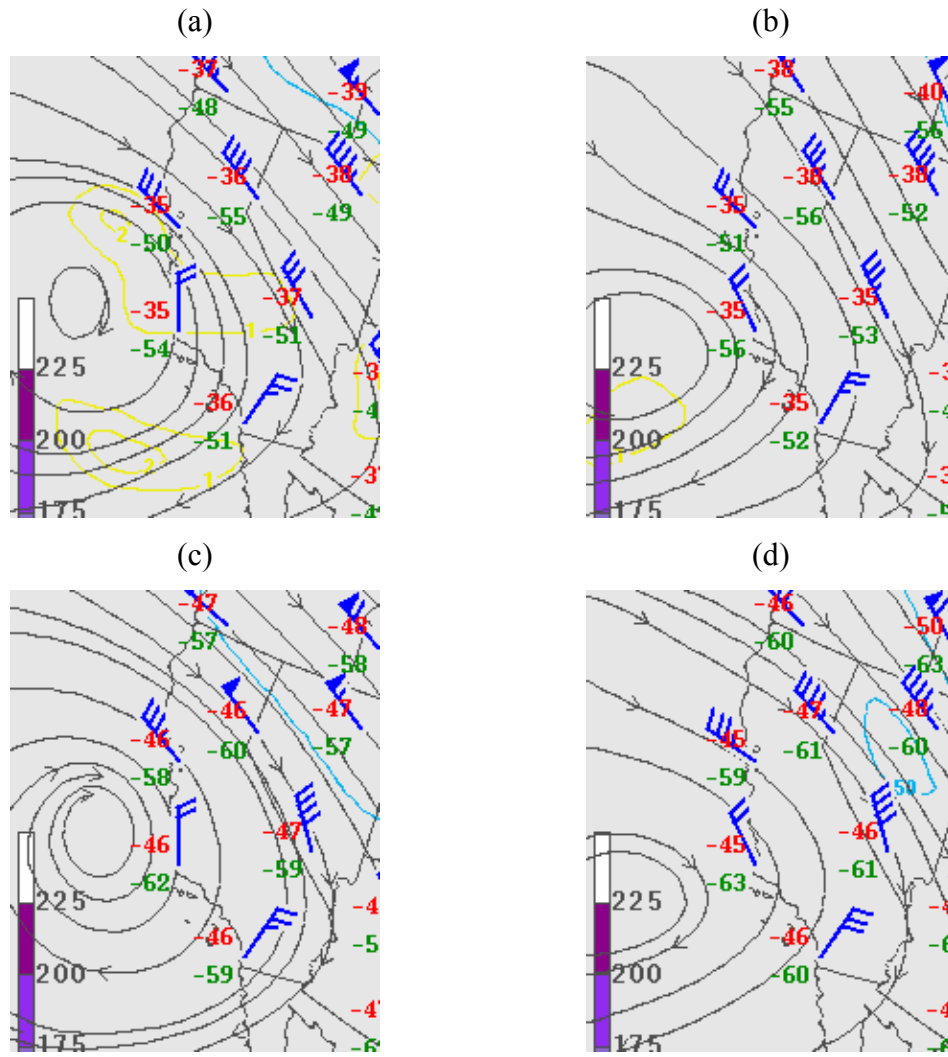


Figure B-2. Upper-level wind analyses for 03 – 04 June 2003. (a) 300 mb at 03/1200 UTC, (b) 300 mb at 04/0000 UTC, (c) 250 mb at 03/1200 UTC, (d) 250 mb at 04/0000 UTC (National Weather Service Storm Prediction Center 2003).

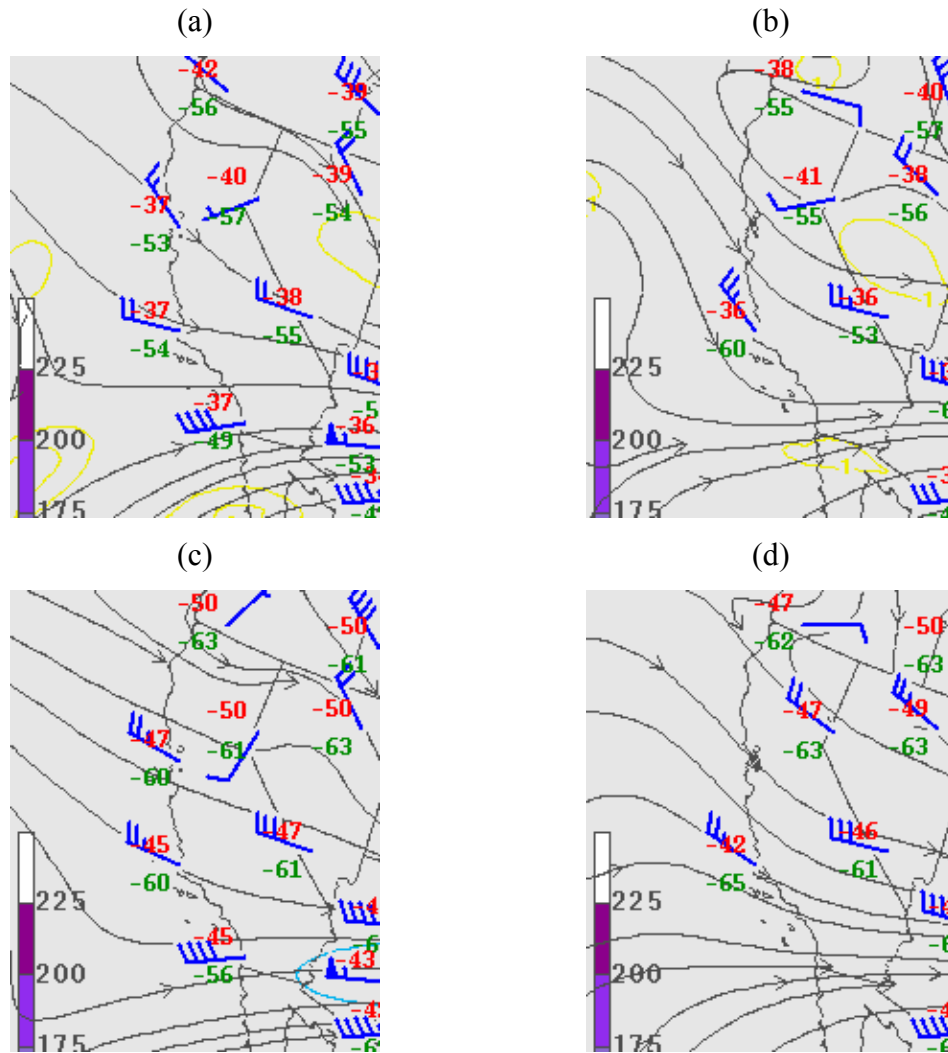


Figure B-3. Upper-level wind analyses for 26 – 27 June 2003. (a) 300 mb at 26/1200 UTC, (b) 300 mb at 27/0000 UTC, (c) 250 mb at 26/1200 UTC, (d) 250 mb at 27/0000 UTC (National Weather Service Storm Prediction Center 2003).

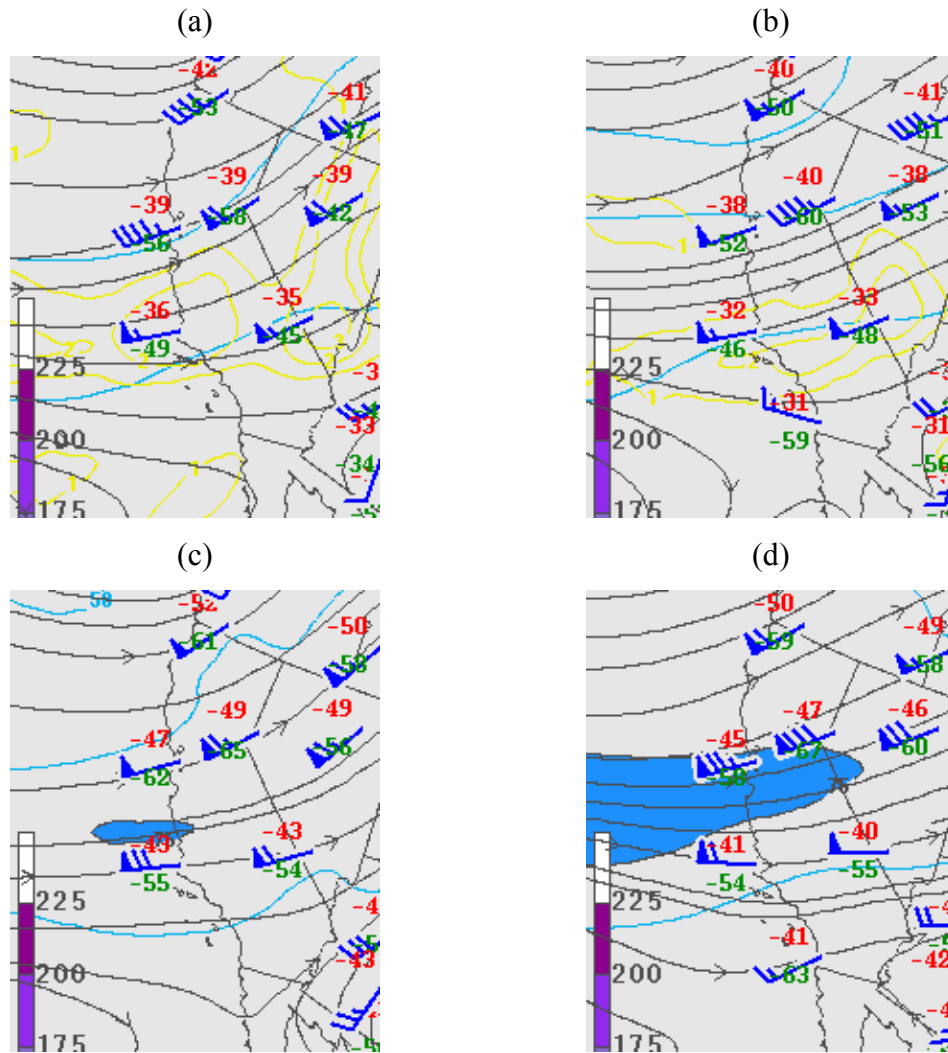


Figure B-4. Upper-level wind analyses for 08 – 09 August 2003. (a) 300 mb at 08/1200 UTC, (b) 300 mb at 09/0000 UTC, (c) 250 mb at 08/1200 UTC, (d) 250 mb at 09/0000 UTC (National Weather Service Storm Prediction Center 2003).

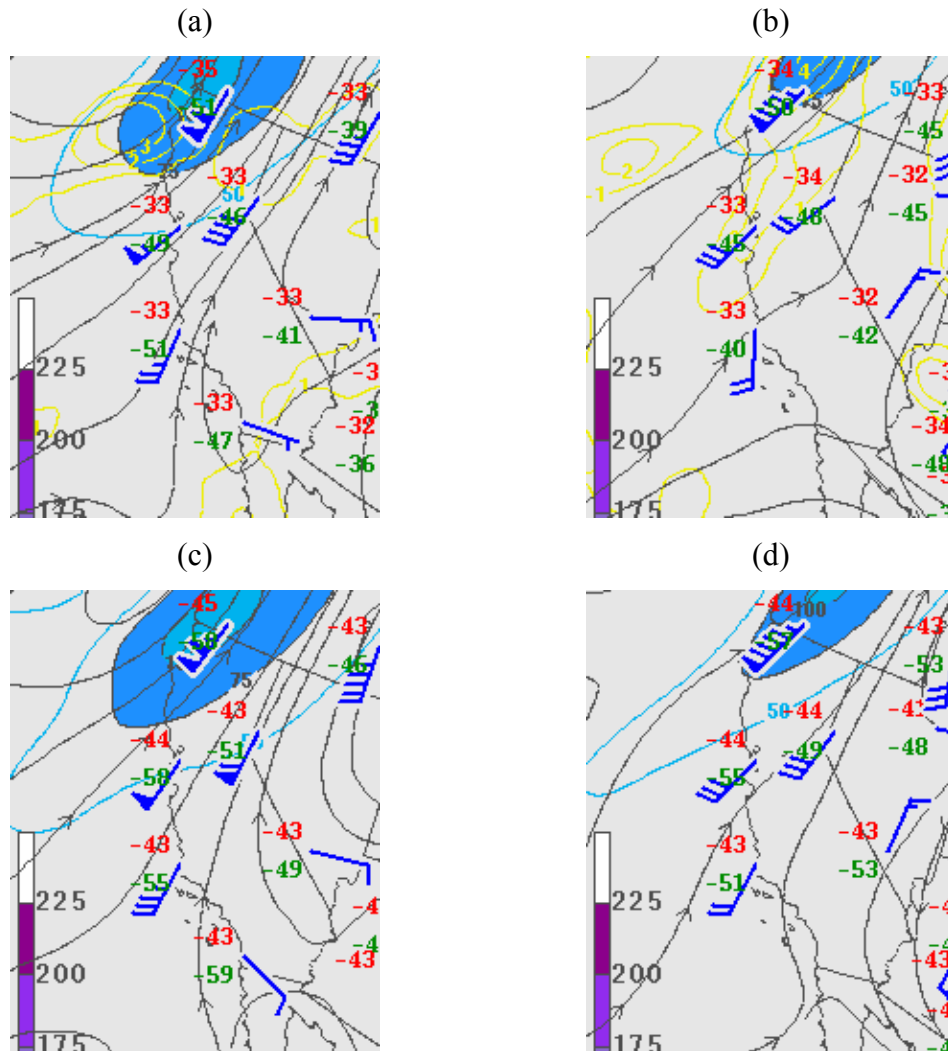


Figure B-5. Upper-level wind analyses for 15 – 16 August 2003. (a) 300 mb at 15/1200 UTC, (b) 300 mb at 16/0000 UTC, (c) 250 mb at 15/1200 UTC, (d) 250 mb at 16/0000 UTC (National Weather Service Storm Prediction Center 2003).

Appendix C: Global Hawk Flight Level Information

Following are the Global Hawk flight levels used in this study and the difference between the actual Global Hawk altitudes and the corresponding 500-foot levels.

Highlighted rows denote the flight levels with the maximum difference for the ascending and descending segments of each mission.

Global Hawk Mission #	Global Hawk Flight Mode	Global Hawk Flight Level (ft MSL)	500-Foot Flight Level (ft MSL)	Difference (ft MSL)
1	Ascent	2507.35	2500	7.35
1	Ascent	2985.78	3000	14.22
1	Ascent	3507.04	3500	7.04
1	Ascent	3984.49	4000	15.51
1	Ascent	4514.88	4500	14.88
1	Ascent	5002.88	5000	2.88
1	Ascent	5518.91	5500	18.91
1	Ascent	5988.93	6000	11.07
1	Ascent	6504.54	6500	4.54
1	Ascent	7000.45	7000	0.45
1	Ascent	7512.73	7500	12.73
1	Ascent	8024.41	8000	24.41
1	Ascent	8499.48	8500	0.52
1	Ascent	8981.06	9000	18.94
1	Ascent	9518.07	9500	18.07
1	Ascent	10010.34	10000	10.34
1	Ascent	10518.62	10500	18.62
1	Ascent	10981.53	11000	18.47
1	Ascent	11503.16	11500	3.16
1	Ascent	12023.56	12000	23.56
1	Ascent	12480.17	12500	19.83
1	Ascent	12974.53	13000	25.47
1	Ascent	13516.05	13500	16.05
1	Ascent	14006.66	14000	6.66
1	Ascent	14479.17	14500	20.83
1	Ascent	15017.81	15000	17.81
1	Ascent	15501.77	15500	1.77

1	Ascent	15972.29	16000	27.71
1	Ascent	16498.79	16500	1.21
1	Ascent	16983.57	17000	16.43
1	Ascent	17474.67	17500	25.33
1	Ascent	17990.14	18000	9.86
1	Ascent	18503.91	18500	3.91
1	Ascent	19002.34	19000	2.34
1	Ascent	19517.82	19500	17.82
1	Ascent	19993.80	20000	6.20
1	Descent	19988.59	20000	11.41
1	Descent	19505.87	19500	5.87
1	Descent	18991.44	19000	8.56
1	Descent	18528.68	18500	28.68
1	Descent	17996.63	18000	3.37
1	Descent	17512.96	17500	12.96
1	Descent	16986.71	17000	13.29
1	Descent	16502.65	16500	2.65
1	Descent	16016.32	16000	16.32
1	Descent	15497.29	15500	2.71
1	Descent	14992.09	15000	7.91
1	Descent	14499.40	14500	0.60
1	Descent	14023.03	14000	23.03
1	Descent	13521.65	13500	21.65
1	Descent	13019.29	13000	19.29
1	Descent	12515.42	12500	15.42
1	Descent	12020.22	12000	20.22
1	Descent	11521.54	11500	21.54
1	Descent	10975.08	11000	24.92
1	Descent	10516.08	10500	16.08
1	Descent	10012.22	10000	12.22
1	Descent	9503.27	9500	3.27
1	Descent	8989.56	9000	10.44
1	Descent	8503.66	8500	3.66
1	Descent	7996.16	8000	3.84
1	Descent	7505.77	7500	5.77
1	Descent	6990.75	7000	9.25
1	Descent	6493.86	6500	6.14
1	Descent	6006.63	6000	6.63
1	Descent	5494.39	5500	5.61
1	Descent	5009.86	5000	9.86
1	Descent	4502.20	4500	2.20
2	Ascent	2485.44	2500	14.56
2	Ascent	2989.83	3000	10.17
2	Ascent	3492.68	3500	7.32
2	Ascent	4016.26	4000	16.26

2	Ascent	4497.97	4500	2.03
2	Ascent	5028.65	5000	28.65
2	Ascent	5482.95	5500	17.05
2	Ascent	6009.95	6000	9.95
2	Ascent	6500.60	6500	0.60
2	Ascent	6977.07	7000	22.93
2	Ascent	7527.22	7500	27.22
2	Ascent	7978.51	8000	21.49
2	Ascent	8498.88	8500	1.12
2	Ascent	9009.58	9000	9.58
2	Ascent	9520.53	9500	20.53
2	Ascent	10026.01	10000	26.01
2	Ascent	10503.98	10500	3.98
2	Ascent	10998.33	11000	1.67
2	Ascent	11474.93	11500	25.07
2	Ascent	11983.53	12000	16.47
2	Ascent	12517.46	12500	17.46
2	Ascent	13015.16	13000	15.16
2	Ascent	13502.74	13500	2.74
2	Ascent	13996.69	14000	3.31
2	Ascent	14518.93	14500	18.93
2	Ascent	14982.53	15000	17.47
2	Ascent	15506.25	15500	6.25
2	Ascent	15979.88	16000	20.12
2	Ascent	16517.32	16500	17.32
2	Ascent	16985.93	17000	14.07
2	Ascent	17522.55	17500	22.55
2	Ascent	18021.79	18000	21.79
2	Ascent	18477.52	18500	22.48
2	Ascent	18982.21	19000	17.79
2	Ascent	19499.04	19500	0.96
2	Ascent	19989.47	20000	10.53
2	Ascent	20485.54	20500	14.46
2	Ascent	21006.30	21000	6.30
2	Ascent	21508.17	21500	8.17
2	Ascent	22011.40	22000	11.40
2	Ascent	22487.58	22500	12.42
2	Ascent	22984.24	23000	15.76
2	Ascent	23518.99	23500	18.99
2	Ascent	24001.08	24000	1.08
2	Ascent	24520.87	24500	20.87
2	Ascent	24982.20	25000	17.80
2	Ascent	25483.69	25500	16.31
2	Ascent	26000.69	26000	0.69
2	Ascent	26500.16	26500	0.16

2	Ascent	27005.39	27000	5.39
2	Ascent	27509.81	27500	9.81
2	Ascent	27981.07	28000	18.93
2	Ascent	28495.59	28500	4.41
2	Ascent	29002.04	29000	2.04
2	Ascent	29503.48	29500	3.48
2	Ascent	30006.91	30000	6.91
2	Ascent	30502.23	30500	2.23
2	Ascent	30993.97	31000	6.03
2	Ascent	31484.43	31500	15.57
2	Ascent	32005.32	32000	5.32
2	Ascent	32498.60	32500	1.40
2	Ascent	32991.54	33000	8.46
2	Ascent	33496.66	33500	3.34
2	Ascent	33998.75	34000	1.25
2	Ascent	34506.27	34500	6.27
2	Ascent	34999.97	35000	0.03
2	Ascent	35486.53	35500	13.47
2	Ascent	35993.27	36000	6.73
2	Ascent	36503.06	36500	3.06
2	Ascent	36989.82	37000	10.18
2	Ascent	37508.25	37500	8.25
2	Ascent	38007.46	38000	7.46
2	Ascent	38504.95	38500	4.95
2	Ascent	38996.73	39000	3.27
2	Ascent	39496.74	39500	3.26
2	Ascent	39997.79	40000	2.21
2	Ascent	40493.89	40500	6.11
2	Ascent	41004.08	41000	4.08
2	Ascent	41508.91	41500	8.91
2	Ascent	42005.59	42000	5.59
2	Ascent	42503.83	42500	3.83
2	Ascent	43001.27	43000	1.27
2	Ascent	43504.22	43500	4.22
2	Ascent	43992.31	44000	7.69
2	Ascent	44494.45	44500	5.55
2	Ascent	45004.24	45000	4.24
2	Ascent	45504.79	45500	4.79
2	Ascent	45992.61	46000	7.39
2	Ascent	46497.27	46500	2.73
2	Ascent	46996.07	47000	3.93
2	Ascent	47501.73	47500	1.73
2	Ascent	48000.67	48000	0.67
2	Ascent	48506.21	48500	6.21
2	Ascent	49004.06	49000	4.06

2	Ascent	49502.25	49500	2.25
2	Ascent	50006.58	50000	6.58
2	Ascent	50495.42	50500	4.58
2	Ascent	50996.03	51000	3.97
2	Ascent	51495.92	51500	4.08
2	Ascent	51994.73	52000	5.27
2	Ascent	52498.96	52500	1.04
2	Ascent	53001.66	53000	1.66
2	Ascent	53502.43	53500	2.43
2	Ascent	53997.13	54000	2.87
2	Ascent	54496.34	54500	3.66
2	Ascent	55000.10	55000	0.10
2	Ascent	55500.52	55500	0.52
2	Ascent	56001.12	56000	1.12
2	Ascent	56501.59	56500	1.59
2	Ascent	57001.64	57000	1.64
2	Ascent	57500.93	57500	0.93
2	Ascent	57999.11	58000	0.89
2	Ascent	58500.37	58500	0.37
2	Ascent	59004.63	59000	4.63
2	Ascent	59502.23	59500	2.23
2	Ascent	60002.20	60000	2.20
2	Descent	60002.20	60000	2.20
3	Ascent	2483.95	2500	16.05
3	Ascent	3024.69	3000	24.69
3	Ascent	3479.86	3500	20.14
3	Ascent	3977.73	4000	22.27
3	Ascent	4514.88	4500	14.88
3	Ascent	4985.18	5000	14.82
3	Ascent	5502.02	5500	2.02
3	Ascent	5991.15	6000	8.85
3	Ascent	6506.22	6500	6.22
3	Ascent	7003.30	7000	3.30
3	Ascent	7527.80	7500	27.80
3	Ascent	7986.75	8000	13.25
3	Ascent	8504.85	8500	4.85
3	Ascent	9005.94	9000	5.94
3	Ascent	9505.12	9500	5.12
3	Ascent	10000.32	10000	0.32
3	Ascent	10495.71	10500	4.29
3	Ascent	10986.70	11000	13.30
3	Ascent	11498.56	11500	1.44
3	Ascent	12004.87	12000	4.87
3	Ascent	12482.21	12500	17.79
3	Ascent	13000.69	13000	0.69

3	Ascent	13524.46	13500	24.46
3	Ascent	13974.66	14000	25.34
3	Ascent	14489.28	14500	10.72
3	Ascent	15013.40	15000	13.40
3	Ascent	15476.39	15500	23.61
3	Ascent	15995.06	16000	4.94
3	Ascent	16508.06	16500	8.06
3	Ascent	17000.83	17000	0.83
3	Ascent	17478.66	17500	21.34
3	Ascent	17976.36	18000	23.64
3	Ascent	18489.07	18500	10.93
3	Ascent	18993.12	19000	6.88
3	Ascent	19502.45	19500	2.45
3	Ascent	19979.92	20000	20.08
3	Ascent	20512.90	20500	12.90
3	Ascent	21017.98	21000	17.98
3	Ascent	21517.31	21500	17.31
3	Ascent	21981.66	22000	18.34
3	Ascent	22483.80	22500	16.20
3	Ascent	23014.06	23000	14.06
3	Ascent	23510.17	23500	10.17
3	Ascent	24014.03	24000	14.03
3	Ascent	24515.79	24500	15.79
3	Ascent	25009.02	25000	9.02
3	Ascent	25518.35	25500	18.35
3	Ascent	26018.87	26000	18.87
3	Ascent	26509.95	26500	9.95
3	Ascent	26992.09	27000	7.91
3	Ascent	27491.76	27500	8.24
3	Ascent	27998.30	28000	1.70
3	Ascent	28503.77	28500	3.77
3	Ascent	29013.96	29000	13.96
3	Ascent	29501.06	29500	1.06
3	Ascent	29982.20	30000	17.80
3	Ascent	30508.52	30500	8.52
3	Ascent	31000.38	31000	0.38
3	Ascent	31505.32	31500	5.32
3	Ascent	31990.68	32000	9.32
3	Ascent	32483.68	32500	16.32
3	Ascent	33006.74	33000	6.74
3	Ascent	33489.61	33500	10.39
3	Ascent	33985.83	34000	14.17
3	Ascent	34509.20	34500	9.20
3	Ascent	35002.96	35000	2.96
3	Ascent	35494.13	35500	5.87

3	Ascent	36007.22	36000	7.22
3	Ascent	36493.53	36500	6.47
3	Ascent	37004.46	37000	4.46
3	Ascent	37514.91	37500	14.91
3	Ascent	38000.63	38000	0.63
3	Ascent	38490.97	38500	9.03
3	Ascent	39002.10	39000	2.10
3	Ascent	39505.91	39500	5.91
3	Ascent	39999.67	40000	0.33
3	Ascent	40509.29	40500	9.29
3	Ascent	40994.23	41000	5.77
3	Ascent	41494.77	41500	5.23
3	Ascent	42003.53	42000	3.53
3	Ascent	42501.71	42500	1.71
3	Ascent	42996.93	43000	3.07
3	Ascent	43490.89	43500	9.11
3	Ascent	44008.25	44000	8.25
3	Ascent	44499.12	44500	0.88
3	Ascent	45004.24	45000	4.24
3	Ascent	45499.89	45500	0.11
3	Ascent	46000.13	46000	0.13
3	Ascent	46502.41	46500	2.41
3	Ascent	46996.07	47000	3.93
3	Ascent	47504.43	47500	4.43
3	Ascent	48000.67	48000	0.67
3	Ascent	48500.55	48500	0.55
3	Ascent	48998.27	49000	1.73
3	Ascent	49505.21	49500	5.21
3	Ascent	49997.46	50000	2.54
3	Ascent	50501.64	50500	1.64
3	Ascent	50999.21	51000	0.79
3	Ascent	51499.18	51500	0.82
3	Ascent	51998.08	52000	1.92
3	Ascent	52502.38	52500	2.38
3	Ascent	53008.68	53000	8.68
3	Ascent	53498.83	53500	1.17
3	Ascent	53997.13	54000	2.87
3	Ascent	54503.88	54500	3.88
3	Ascent	54996.24	55000	3.76
3	Ascent	55500.52	55500	0.52
3	Ascent	56001.12	56000	1.12
3	Ascent	56501.59	56500	1.59
3	Ascent	57001.64	57000	1.64
3	Ascent	57500.93	57500	0.93
3	Ascent	57999.11	58000	0.89

3	Ascent	58500.37	58500	0.37
3	Ascent	58999.95	59000	0.05
3	Ascent	59502.23	59500	2.23
3	Ascent	60002.20	60000	2.20
3	Descent	60002.20	60000	2.20
3	Descent	59502.23	59500	2.23
3	Descent	59004.63	59000	4.63
3	Descent	58495.80	58500	4.20
3	Descent	57999.11	58000	0.89
3	Descent	57487.87	57500	12.13
3	Descent	57001.64	57000	1.64
3	Descent	56509.90	56500	9.90
3	Descent	56013.28	56000	13.28
3	Descent	55492.61	55500	7.39
3	Descent	54996.24	55000	3.76
3	Descent	54477.50	54500	22.50
3	Descent	53997.13	54000	2.87
3	Descent	53473.69	53500	26.31
3	Descent	52987.63	53000	12.37
3	Descent	52526.38	52500	26.38
3	Descent	52004.77	52000	4.77
3	Descent	51518.78	51500	18.78
3	Descent	51015.16	51000	15.16
3	Descent	50520.32	50500	20.32
3	Descent	50018.73	50000	18.73
3	Descent	49514.11	49500	14.11
3	Descent	49009.85	49000	9.85
3	Descent	48503.38	48500	3.38
3	Descent	47973.09	48000	26.91
3	Descent	47507.13	47500	7.13
3	Descent	46969.80	47000	30.20
3	Descent	46512.68	46500	12.68
3	Descent	45975.07	46000	24.93
3	Descent	45473.00	45500	27.00
3	Descent	45016.19	45000	16.19
3	Descent	44499.12	44500	0.88
3	Descent	44017.36	44000	17.36
3	Descent	43510.89	43500	10.89
3	Descent	43005.61	43000	5.61
3	Descent	42520.79	42500	20.79
3	Descent	42018.01	42000	18.01
3	Descent	41502.85	41500	2.85
3	Descent	41004.08	41000	4.08
3	Descent	40490.04	40500	9.96
3	Descent	39982.77	40000	17.23

3	Descent	39476.58	39500	23.42
3	Descent	39005.68	39000	5.68
3	Descent	38504.95	38500	4.95
3	Descent	38000.63	38000	0.63
3	Descent	37499.91	37500	0.09
3	Descent	37015.85	37000	15.85
3	Descent	36498.29	36500	1.71
3	Descent	35999.46	36000	0.54
3	Descent	35489.56	35500	10.44
3	Descent	34999.97	35000	0.03
3	Descent	34507.73	34500	7.73
3	Descent	34024.62	34000	24.62
3	Descent	33503.71	33500	3.71
3	Descent	32977.72	33000	22.28
3	Descent	32493.17	32500	6.83
3	Descent	31989.35	32000	10.65
3	Descent	31477.89	31500	22.11
3	Descent	31014.50	31000	14.50
3	Descent	30502.23	30500	2.23
3	Descent	29988.38	30000	11.62
3	Descent	29496.20	29500	3.80
3	Descent	28978.23	29000	21.77
3	Descent	28500.26	28500	0.26
3	Descent	27969.59	28000	30.41
3	Descent	27522.23	27500	22.23
3	Descent	26978.80	27000	21.20
3	Descent	26478.39	26500	21.61
3	Descent	25971.83	26000	28.17
3	Descent	25471.09	25500	28.91
3	Descent	24977.04	25000	22.96
3	Descent	24489.43	24500	10.57
3	Descent	23992.12	24000	7.88
3	Descent	23509.19	23500	9.19
3	Descent	23026.58	23000	26.58
3	Descent	22504.60	22500	4.60
3	Descent	21982.59	22000	17.41
3	Descent	21499.94	21500	0.06
3	Descent	21021.58	21000	21.58
3	Descent	20492.60	20500	7.40
3	Descent	19987.73	20000	12.27
3	Descent	19505.02	19500	5.02
3	Descent	19001.51	19000	1.51
3	Descent	18489.89	18500	10.11
3	Descent	17922.89	17900	22.89
3	Descent	17521.75	17500	21.75

3	Descent	17006.33	17000	6.33
3	Descent	16509.60	16500	9.60
3	Descent	15973.06	16000	26.94
3	Descent	15494.31	15500	5.69
3	Descent	15014.13	15000	14.13
3	Descent	14508.08	14500	8.08
3	Descent	14000.96	14000	0.96
3	Descent	13478.95	13500	21.05
3	Descent	12978.65	13000	21.35
3	Descent	12480.86	12500	19.14
3	Descent	11988.20	12000	11.80
3	Descent	11502.50	11500	2.50
3	Descent	10982.83	11000	17.17
3	Descent	10474.73	10500	25.27
3	Descent	10015.35	10000	15.35
3	Descent	9484.16	9500	15.84
3	Descent	9004.73	9000	4.73
3	Descent	8509.64	8500	9.64
3	Descent	8012.64	8000	12.64
3	Descent	7504.04	7500	4.04
3	Descent	6998.17	7000	1.83
3	Descent	6492.17	6500	7.83
3	Descent	5995.01	6000	4.99
3	Descent	5486.22	5500	13.78
3	Descent	4991.07	5000	8.93
3	Descent	4508.01	4500	8.01
4	Ascent	3013.57	3000	13.57
4	Ascent	3502.94	3500	2.94
4	Ascent	3979.81	4000	20.19
4	Ascent	4512.24	4500	12.24
4	Ascent	5012.01	5000	12.01
4	Ascent	5487.31	5500	12.69
4	Ascent	6011.06	6000	11.06
4	Ascent	6496.67	6500	3.33
4	Ascent	6978.20	7000	21.80
4	Ascent	7505.77	7500	5.77
4	Ascent	7989.69	8000	10.31
4	Ascent	8476.78	8500	23.22
4	Ascent	8994.41	9000	5.59
4	Ascent	9502.03	9500	2.03
4	Ascent	9980.29	10000	19.71
4	Ascent	10483.63	10500	16.37
4	Ascent	10986.05	11000	13.95
4	Ascent	11495.94	11500	4.06
4	Ascent	12028.23	12000	28.23

4	Ascent	12526.28	12500	26.28
4	Ascent	12998.63	13000	1.37
4	Ascent	13483.85	13500	16.15
4	Ascent	14015.91	14000	15.91
4	Ascent	14510.25	14500	10.25
4	Ascent	14984.00	15000	16.00
4	Ascent	15512.24	15500	12.24
4	Ascent	16007.21	16000	7.21
4	Ascent	16502.65	16500	2.65
4	Ascent	17003.19	17000	3.19
4	Ascent	17516.96	17500	16.96
4	Ascent	18017.73	18000	17.73
4	Ascent	18516.30	18500	16.30
4	Ascent	18996.47	19000	3.53
4	Ascent	19493.07	19500	6.93
4	Ascent	19992.94	20000	7.06
4	Ascent	20507.61	20500	7.61
4	Ascent	20990.14	21000	9.86
4	Ascent	21491.72	21500	8.28
4	Ascent	22010.47	22000	10.47
4	Ascent	22492.30	22500	7.70
4	Ascent	22982.31	23000	17.69
4	Ascent	23494.50	23500	5.50
4	Ascent	23992.12	24000	7.88
4	Ascent	24509.71	24500	9.71
4	Ascent	25010.05	25000	10.05
4	Ascent	25499.43	25500	0.57
4	Ascent	26017.80	26000	17.80
4	Ascent	26493.62	26500	6.38
4	Ascent	26989.88	27000	10.12
4	Ascent	27506.43	27500	6.43
4	Ascent	28000.60	28000	0.60
4	Ascent	28503.77	28500	3.77
4	Ascent	28998.47	29000	1.53
4	Ascent	29494.99	29500	5.01
4	Ascent	29995.79	30000	4.21
4	Ascent	30504.75	30500	4.75
4	Ascent	31001.67	31000	1.67
4	Ascent	31489.64	31500	10.36
4	Ascent	32010.64	32000	10.64
4	Ascent	32510.80	32500	10.80
4	Ascent	32992.91	33000	7.09
4	Ascent	33492.43	33500	7.57
4	Ascent	34008.80	34000	8.80
4	Ascent	34498.95	34500	1.05

4	Ascent	34991.02	35000	8.98
4	Ascent	35507.82	35500	7.82
4	Ascent	36001.02	36000	1.02
4	Ascent	36495.12	36500	4.88
4	Ascent	36991.45	37000	8.55
4	Ascent	37498.25	37500	1.75
4	Ascent	38000.63	38000	0.63
4	Ascent	38503.20	38500	3.20
4	Ascent	39002.10	39000	2.10
4	Ascent	39491.24	39500	8.76
4	Ascent	39999.67	40000	0.33
4	Ascent	40497.74	40500	2.26
4	Ascent	40996.20	41000	3.80
4	Ascent	41502.85	41500	2.85
4	Ascent	42001.46	42000	1.46
4	Ascent	42505.95	42500	5.95
4	Ascent	43001.27	43000	1.27
4	Ascent	43504.22	43500	4.22
4	Ascent	44001.41	44000	1.41
4	Ascent	44503.78	44500	3.78
4	Ascent	45001.85	45000	1.85
4	Ascent	45499.89	45500	0.11
4	Ascent	45997.62	46000	2.38
4	Ascent	46497.27	46500	2.73
4	Ascent	47001.33	47000	1.33
4	Ascent	47499.04	47500	0.96
4	Ascent	47997.91	48000	2.09
4	Ascent	48497.73	48500	2.27
4	Ascent	49004.06	49000	4.06
4	Ascent	49496.32	49500	3.68
4	Ascent	49997.46	50000	2.54
4	Ascent	50501.64	50500	1.64
4	Ascent	50999.21	51000	0.79
4	Ascent	51502.45	51500	2.45
4	Ascent	52001.43	52000	1.43
4	Ascent	52495.53	52500	4.47
4	Ascent	52998.15	53000	1.85
4	Ascent	53498.83	53500	1.17
4	Ascent	53997.13	54000	2.87
4	Ascent	54500.11	54500	0.11
4	Ascent	55000.10	55000	0.10
4	Ascent	55500.52	55500	0.52
4	Ascent	55997.06	56000	2.94
4	Ascent	56497.44	56500	2.56
4	Descent	56501.59	56500	1.59

4	Descent	55997.06	56000	2.94
4	Descent	55508.44	55500	8.44
4	Descent	54996.24	55000	3.76
4	Descent	54500.11	54500	0.11
4	Descent	54000.81	54000	0.81
4	Descent	53491.64	53500	8.36
4	Descent	53008.68	53000	8.68
4	Descent	52485.26	52500	14.74
4	Descent	51994.73	52000	5.27
4	Descent	51495.92	51500	4.08
4	Descent	51008.78	51000	8.78
4	Descent	50479.88	50500	20.13
4	Descent	49982.28	50000	17.72
4	Descent	49511.14	49500	11.14
4	Descent	48989.59	49000	10.41
4	Descent	48500.55	48500	0.55
4	Descent	48017.23	48000	17.23
5	Ascent	2514.32	2500	14.32
5	Ascent	2986.79	3000	13.21
5	Ascent	3496.27	3500	3.73
5	Ascent	4519.11	4500	19.11
5	Ascent	5005.57	5000	5.57
5	Ascent	5503.65	5500	3.65
5	Ascent	5989.48	6000	10.52
5	Ascent	6509.03	6500	9.03
5	Ascent	7013.57	7000	13.57
5	Ascent	7488.39	7500	11.61
5	Ascent	7986.75	8000	13.25
5	Ascent	8493.51	8500	6.49
5	Ascent	8979.25	9000	20.75
5	Ascent	9511.90	9500	11.90
5	Ascent	9981.54	10000	18.46
5	Ascent	10498.89	10500	1.11
5	Ascent	10995.74	11000	4.26
5	Ascent	11518.92	11500	18.92
5	Ascent	11985.53	12000	14.47
5	Ascent	12525.60	12500	25.60
5	Ascent	12996.55	13000	3.45
5	Ascent	13497.15	13500	2.85
5	Ascent	14028.72	14000	28.72
5	Ascent	14481.33	14500	18.67
5	Ascent	14994.29	15000	5.71
5	Ascent	15504.02	15500	4.02
5	Ascent	15990.51	16000	9.49
5	Ascent	16505.74	16500	5.74

5	Ascent	17000.83	17000	0.83
5	Ascent	17482.65	17500	17.35
5	Ascent	17988.52	18000	11.48
5	Ascent	18485.77	18500	14.23
5	Ascent	19008.22	19000	8.22
5	Ascent	19500.74	19500	0.74
5	Ascent	19985.13	20000	14.88
5	Ascent	20521.74	20500	21.74
5	Ascent	21008.10	21000	8.10
5	Ascent	21510.91	21500	10.91
5	Ascent	22004.90	22000	4.90
5	Ascent	22499.86	22500	0.14
5	Ascent	23011.17	23000	11.17
5	Ascent	23508.21	23500	8.21
5	Ascent	24013.04	24000	13.04
5	Ascent	24479.30	24500	20.70
5	Ascent	25011.08	25000	11.08
5	Ascent	25485.79	25500	14.21
5	Ascent	26004.96	26000	4.96
5	Ascent	26499.07	26500	0.93
5	Ascent	26995.41	27000	4.59
5	Ascent	27497.39	27500	2.61
5	Ascent	28012.08	28000	12.08
5	Ascent	28483.89	28500	16.11
5	Ascent	29010.39	29000	10.39
5	Ascent	29494.99	29500	5.01
5	Ascent	29993.32	30000	6.68
5	Ascent	30492.15	30500	7.85
5	Ascent	30991.40	31000	8.60
5	Ascent	31502.71	31500	2.71
5	Ascent	31998.66	32000	1.34
5	Ascent	32499.95	32500	0.05
5	Ascent	33012.27	33000	12.27
5	Ascent	33500.89	33500	0.89
5	Ascent	33998.75	34000	1.25
5	Ascent	34509.20	34500	9.20
5	Ascent	35010.42	35000	10.42
5	Ascent	35497.17	35500	2.83
5	Ascent	35994.82	36000	5.18
5	Ascent	36501.46	36500	1.46
5	Ascent	37007.71	37000	7.71
5	Ascent	37498.25	37500	1.75
5	Ascent	37988.69	38000	11.31
5	Ascent	38490.97	38500	9.03
5	Ascent	38993.14	39000	6.86

5	Ascent	39502.24	39500	2.24
5	Ascent	39997.79	40000	2.21
5	Ascent	40509.29	40500	9.29
5	Ascent	41004.08	41000	4.08
5	Ascent	41506.89	41500	6.89
5	Ascent	42007.66	42000	7.66
5	Ascent	42505.95	42500	5.95
5	Ascent	42992.59	43000	7.41
5	Ascent	43504.22	43500	4.22
5	Ascent	43999.14	44000	0.86
5	Ascent	44503.78	44500	3.78
5	Ascent	44999.46	45000	0.54
5	Ascent	45499.89	45500	0.11
5	Ascent	45997.62	46000	2.38
5	Ascent	46499.84	46500	0.16
5	Ascent	47003.96	47000	3.96
5	Ascent	47496.35	47500	3.65
5	Ascent	47997.91	48000	2.09
5	Ascent	48506.21	48500	6.21
5	Ascent	48998.27	49000	1.73
5	Ascent	49496.32	49500	3.68
5	Ascent	49997.46	50000	2.54
5	Ascent	50498.54	50500	1.46
5	Ascent	50999.21	51000	0.79
5	Ascent	51499.18	51500	0.82
5	Ascent	51998.08	52000	1.92
5	Ascent	52502.38	52500	2.38
5	Ascent	53001.66	53000	1.66
5	Ascent	53498.83	53500	1.17
5	Ascent	53997.13	54000	2.87
5	Ascent	54496.34	54500	3.66
5	Ascent	55000.10	55000	0.10
5	Ascent	55500.52	55500	0.52
5	Ascent	56001.12	56000	1.12
5	Ascent	56501.59	56500	1.59
5	Ascent	57001.64	57000	1.64
5	Ascent	57500.93	57500	0.93
5	Ascent	57994.65	58000	5.35
5	Ascent	58500.37	58500	0.37
5	Ascent	58999.95	59000	0.05
5	Ascent	59502.23	59500	2.23
5	Ascent	60002.20	60000	2.20
5	Ascent	60499.37	60500	0.63
5	Ascent	61003.55	61000	3.55
5	Ascent	61509.70	61500	9.70

5	Ascent	62001.41	62000	1.41
5	Descent	62001.41	62000	1.41
5	Descent	61499.14	61500	0.86
5	Descent	60998.40	61000	1.60
5	Descent	60504.40	60500	4.40
5	Descent	60002.20	60000	2.20
5	Descent	59497.44	59500	2.56
5	Descent	59014.00	59000	14.00
5	Descent	58509.51	58500	9.51
5	Descent	57985.73	58000	14.27
5	Descent	57483.52	57500	16.48
5	Descent	56980.39	57000	19.61
5	Descent	56489.14	56500	10.86
5	Descent	56017.34	56000	17.34
5	Descent	55468.89	55500	31.11
5	Descent	55038.77	55000	38.77
5	Descent	54515.20	54500	15.20
5	Descent	54030.29	54000	30.29
5	Descent	53520.41	53500	20.41
5	Descent	53033.27	53000	33.27
5	Descent	52516.09	52500	16.09
5	Descent	52004.77	52000	4.77
5	Descent	51486.13	51500	13.87
5	Descent	51034.30	51000	34.30
5	Descent	50529.67	50500	29.67
5	Descent	49973.18	50000	26.82
5	Descent	49472.61	49500	27.39
5	Descent	48969.34	49000	30.66
5	Descent	48520.35	48500	20.35
5	Descent	48006.19	48000	6.19
5	Descent	47515.21	47500	15.21
5	Descent	47001.33	47000	1.33
5	Descent	46479.31	46500	20.69
5	Descent	46005.14	46000	5.14
5	Descent	45536.63	45500	36.63
5	Descent	45030.54	45000	30.54
5	Descent	44468.82	44500	31.18
5	Descent	43980.93	44000	19.07
5	Descent	43519.79	43500	19.79
5	Descent	42966.58	43000	33.42
5	Descent	42497.48	42500	2.52
5	Descent	41974.59	42000	25.41
5	Descent	41478.63	41500	21.37
5	Descent	41025.77	41000	25.77
5	Descent	40501.59	40500	1.59

5	Descent	40022.22	40000	22.22
5	Descent	39520.59	39500	20.59
5	Descent	38984.20	39000	15.80
5	Descent	38483.98	38500	16.02
5	Descent	37968.23	38000	31.77
5	Descent	37508.25	37500	8.25
5	Descent	37019.11	37000	19.11
5	Descent	36504.64	36500	4.64
5	Descent	35996.37	36000	3.63
5	Descent	35474.36	35500	25.64
5	Descent	34996.98	35000	3.02
5	Descent	34487.24	34500	12.76
5	Descent	33971.48	34000	28.52
5	Descent	33516.39	33500	16.39
5	Descent	33012.27	33000	12.27
5	Descent	32498.60	32500	1.40
5	Descent	32018.65	32000	18.65
5	Descent	31506.63	31500	6.63
5	Descent	30999.10	31000	0.90
5	Descent	30511.04	30500	11.04
5	Descent	29980.96	30000	19.04
5	Descent	29511.99	29500	11.99
5	Descent	28980.60	29000	19.40
5	Descent	28500.27	28500	0.27
5	Descent	27974.18	28000	25.82
5	Descent	27501.91	27500	1.91
5	Descent	27008.72	27000	8.72
5	Descent	26505.60	26500	5.60
5	Descent	26012.45	26000	12.45
5	Descent	25484.74	25500	15.26
5	Descent	25000.77	25000	0.77
5	Descent	24509.71	24500	9.71
5	Descent	24036.97	24000	36.97
5	Descent	23504.30	23500	4.30
5	Descent	23027.54	23000	27.54
5	Descent	22477.19	22500	22.81
5	Descent	22006.75	22000	6.75
5	Descent	21520.05	21500	20.05
5	Descent	21007.20	21000	7.20
5	Descent	20491.72	20500	8.28
5	Descent	20005.96	20000	5.96
5	Descent	19495.63	19500	4.37
5	Descent	19010.74	19000	10.74
5	Descent	18497.31	18500	2.69
5	Descent	17982.03	18000	17.97

5	Descent	17518.55	17500	18.55
5	Descent	17019.68	17000	19.68
5	Descent	16483.36	16500	16.64
5	Descent	15988.99	16000	11.01
5	Descent	15519.71	15500	19.71
5	Descent	14988.41	15000	11.59
5	Descent	14494.35	14500	5.65
5	Descent	13988.87	14000	11.13
5	Descent	13464.97	13500	35.03
5	Descent	12984.17	13000	15.83
5	Descent	12529.67	12500	29.67
5	Descent	12006.21	12000	6.21
5	Descent	11507.75	11500	7.75
5	Descent	10980.24	11000	19.76
5	Descent	10481.73	10500	18.27
5	Descent	10029.76	10000	29.76
5	Descent	9502.03	9500	2.03
5	Descent	9012.01	9000	12.01
5	Descent	8488.12	8500	11.88
5	Descent	8009.10	8000	9.10
5	Descent	7500.56	7500	0.56
5	Descent	6999.30	7000	0.70
5	Descent	6493.30	6500	6.70
5	Descent	5992.25	6000	7.75
5	Descent	5494.93	5500	5.07
5	Descent	5009.86	5000	9.86

Appendix D: Global Hawk Data Reports & Flight Mode

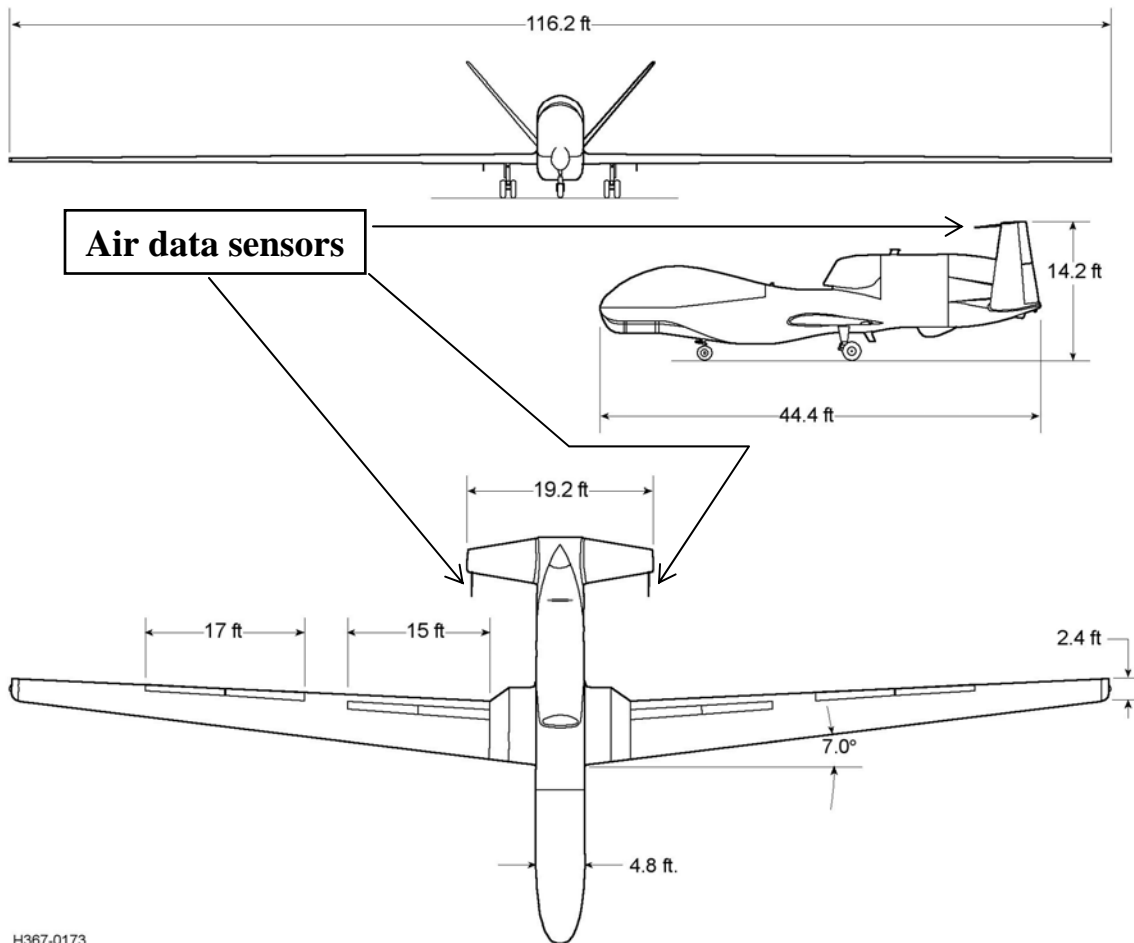
The following are notes pertaining to the Global Hawk data reports based on indicated flight mode (Climb, Altitude Hold, and Descend). Approximate Flight Level is reported in thousands of feet. Actual Flight Mode indicates any possible discrepancies in Global Hawk data reports based on differences from Indicated Flight Mode. Any data reports used in the statistical analysis of this research are indicated in the last column.

Mission #	Indicated Flight Mode	Time (sec)	Approximate Flight Levels (Kft)	Actual Flight Mode	Data Used
1	Climb	57898-58238	2.3-19.7		Yes
1	Alt Hold	58239-58617	18.3-20.2	Climb & Descend	Yes
1	Descend	58631-58698	18.3-15.5		Yes
1	Alt Hold	58699-58769	15.5-14.3	Descend	Yes
1	Descend	58770-58854	14.3-10.2		Yes
1	Alt Hold	58855-59500	10.2-4.3	Descend	Yes
2	Climb	60668-61254	2.4-30.5		Yes
2	Alt Hold	61255-61533	30.5-31.0	Climb & Descend	Yes
2	Climb	61534-61583	31.0-32.5		Yes
2	Alt Hold	61584-61702	32.5-35.0	Climb	Yes
2	Alt Hold	61703-62016	35.0-35.07	Climb & Descend	No
2	Climb	62017-63559	35.07-55.0		Yes
2	Climb	63560-64926	55.0-59.0	Slow; Climb	Yes
2	Climb	64927-66791	59.0-60.0	Slow; Climb & Descend	Yes
2	Climb	66792-72190	59.7-60.4	Climb & Descend	No
2	Descend	72192-72344	59.6-60.4		Yes
3	Climb	56236-56831	2.1-30.5		Yes
3	Alt Hold	56832-57137	30.5-31.1	Climb & Descend	Yes
3	Climb	57138-57250	31.0-34.5		Yes
3	Alt Hold	57251-57520	34.5-35.0	Climb & Descend	Yes
3	Climb	57521-59898	35.0-58.0		Yes
3	Climb	59899-60260	58.0-59.0	Slow; Climb	Yes
3	Climb	60261-66256	59.0-60.0	Slow; Climb & Descend	Yes
3	Climb	66257-67446	59.9-60.1	Climb & Descend	Yes
3	Descend	67447-68213	37.7-59.9		Yes

3	Alt Hold	68214-68412	37.5-37.7	Climb & Descend	Yes
3	Descend	68413-68461	35.2-37.5		Yes
3	Alt Hold	68462-68577	35.0-35.2	Climb & Descend	Yes
3	Descend	68578-68700	28.7-35.0		Yes
3	Alt Hold	68701-68887	28.5-28.7	Climb & Descend	Yes
3	Descend	68888-68954	24.7-28.5		Yes
3	Alt Hold	68955-69054	24.4-24.7	Climb & Descend	Yes
3	Descend	69055-69127	20.4-24.4		Yes
3	Alt Hold	69128-69381	18.3-20.3	Climb & Descend	Yes
3	Descend	69382-69435	15.3-18.3		Yes
3	Alt Hold	69436-69535	14.2-15.3	Climb & Descend	Yes
3	Descend	69536-69614	10.1-14.1		Yes
3	Alt Hold	69615-69928	4.3-10.0	Climb & Descend	Yes
4	Climb	52017-55314	2.2-54.0		Yes
4	Climb	55315-56585	54.0-55.0	Slow; Climb & Descend	Yes
4	Climb	56586-56767	54.9-55.0	Climb & Descend	No
4	Climb	56768-58244	55.0-56.0	Slow; Climb & Descend	Yes
4	Climb	58245-66218	55.6-56.9	Climb & Descend	Yes
4	Descend	66219-66258	56.8-56.8	Climb & Descend	Yes
4	Descend	66259-66614	47.9-56.8		Yes
5	Climb	53210-56095	2.2-57.0		Yes
5	Climb	56096-56489	57.0-58.0	Slow; Climb & Descend	Yes
5	Climb	56490-58041	58.0-59.0	Slow; Climb & Descend	Yes
5	Climb	58042-63062	59.0-60.0	Slow; Climb & Descend	Yes
5	Climb	63063-85216	59.7-62.3	Slow; Climb & Descend	Yes
5	Descend	85217-85634	60.0-62.1	Slow; Climb & Descend	Yes
5	Descend	85635-86094	35.2-60.0	Climb & Descend	Yes
5	Alt Hold	86095-86223	35.0-35.2	Climb & Descend	No
5	Descend	86224-86335	28.7-35.0		Yes
5	Alt Hold	86336-86488	28.5-28.7	Climb & Descend	No
5	Descend	86489-86551	24.6-28.5		Yes
5	Alt Hold	86552-86649	24.4-24.6	Climb & Descend	Yes
5	Descend	86650-86714	20.4-24.4		Yes
5	Alt Hold	86715-86834	20.1-20.4	Climb & Descend	No
5	Alt Hold	86835-86904	18.3-20.1	Descend	Yes
5	Alt Hold	86905-86999	18.3-18.4	Climb & Descend	No
5	Descend	87000-87049	15.4-18.3		Yes
5	Alt Hold	87050-87120	15.2-15.4	Climb & Descend	No
5	Alt Hold	87121-87156	14.2-15.2	Descend	Yes
5	Descend	87157-87231	10.0-14.2		Yes
5	Alt Hold	87232-87316	9.8-10.0	Climb & Descend	No
5	Alt Hold	87317-87573	4.3-9.8	Descend	Yes

Appendix E: Global Hawk Dimensions

The following diagram illustrates the overall dimensions of the Global Hawk airframe. The location of the air data sensors on the tails of the aircraft are denoted (Northrop Grumman 2001).



Bibliography

- 88th Weather Squadron, 2002: AFIT Meteorology Thesis Topic Proposal—Accuracy of Meteorological Data Obtained from Sensors on Non-Traditional Platforms, 2 pp. [Available from 88 WS/WES, 2049 Monahan Way, Bldg 91, Area B, Wright-Patterson AFB, OH 45433-7204.]
- Allen, M.S., 2003: Evaluation of the Mountain Wave Forecast Model's Stratospheric Turbulence Simulations. M.S. thesis, Department of Engineering Physics, Air Force Institute of Technology, 81 pp.
- AMS, 2002: *A Brief Guide for Authors*. American Meteorological Society (AMS), Boston, Massachusetts.
- Axford, D.N., 1968: On the accuracy of Wind Measurements Using an Inertial Platform in an Aircraft, and an Example of a Measurement of the Vertical Mesostructure of the Atmosphere. *Journal of Applied Meteorology*, **7**, 645-666.
- Benjamin, S.G., B.E. Schwartz, and R.E. Cole, 1999: Accuracy of ACARS wind and temperature observations determined by collocation. *Weather and Forecasting*, **14**, 1032-1038.
- Bisiaux, M., M.E. Cox, D.A. Forrester, and T.J. Storey, 1983: Possible improvements in meteorology for aircraft navigation. *Journal of Navigation*, **36**, 54-63.
- Caterinicchia, Dan, 2002: Air Force chief derides 'tribes'. *Federal Computer Week*. [Available on-line at <http://www.fcw.com/fcw/articles/2002/0826/web-afitc-08-27-02.asp> .]
- Fisher, N.I., 1993: *Statistical Analysis of Circular Data*. Cambridge University Press, 277 pp.
- Forecast Systems Laboratory, cited 2003: FSL's Aircraft Data Web. [Available on-line at <http://acweb.fsl.noaa.gov/> .]
- _____, cited 2003: FSL Aircraft Data (ACARS/AMDAR) Information. [Available on-line at <http://acweb.fsl.noaa.gov/FAQ.html> .]
- Golden J.H., R. Serafin, V. Lally, and J. Facundo, 1986: Atmospheric Sounding Systems. *Mesoscale Meteorology and Forecasting*, P.S. Ray, Ed., American Meteorological Society, 50-70.

- Mamrosh, R.D., 1998: The use of high-frequency ACARS soundings in forecasting convective storms. *16th Conf. on Weather Analysis and Forecasting*, Phoenix, AZ, Amer. Meteor. Soc., 106-108.
- _____, R. Decker, and C. Weiss, 2001: Field Forecaster Evaluation of ACARS data: Results of the NAOS ACARS Assessment. *Fifth Symposium on Integrated Observing Systems*, Albuquerque, NM Amer. Meteor. Soc., 184-190.
- Maptech Inc., cited 2003: Maptech MapServer [Available on-line at <http://mapserver.maptech.com/>.]
- Moninger, W.R., R.D. Mamrosh, and P.M. Pauley, 2003: Automated meteorological reports from commercial aircraft. *Bulletin of the American Meteorological Society*, **84**, 203-216.
- Montgomery, D.C., and G.C. Runger, 2003: *Applied Statistics and Probability for Engineers*. John Wiley & Sons, Inc., 706 pp.
- Morone, L.L., 1986: The observational error of automated wind reports from aircraft. *Bulletin of the American Meteorological Society*, **67**, 177-185.
- Nash, J., 1994: Upper wind observing systems used for meteorological operations. *Annales de Geophysicae*, **12**, 691-710.
- National Weather Service Storm Prediction Center, cited 2003: Surface and Upper Air Maps [Available on-line at <http://www.spc.noaa.gov/obswx/maps/>.]
- Northrop Grumman, 2001: *Preliminary Contractor Flight Operations Manual – Global Hawk Unmanned Aerial Vehicle, RQ4A*. Revision C. RAC Number: 367-3000-206. Northrop Grumman, 10 Oct 2001.
- Painting, D.J., 2002: AMDAR Reference Manual. [Unpublished WMO document]
- Pauley, P.M., 2003: Operational Aircraft Data for Numerical Weather Prediction- Characteristics and Quality Control. [In preparation for *Monthly Weather Review*.]
- Richner, H., and T. Gutermann, 1987: Vertical air motion and other meteorological parameters from commercial aircraft. Preprints, *Sixth Symposium on Meteorological Observations and Instrumentation*. New Orleans, LA, American Meteorological Society, 269-272.
- Schwartz, B.E., and S.C. Benjamin, 1995: A Comparison of Temperature and Wind Measurements from ACARS-Equipped Aircraft and Rawinsondes. *Weather and Forecasting*, **10**, 528-544.

Wilks, D.S., 1995: *Statistical Methods in the Atmospheric Sciences*. Academic Press, 467 pp.

Vita

Captain Steven M. Callis graduated from Eastern Wayne High School in Goldsboro, North Carolina. He entered undergraduate studies at North Carolina State University in Raleigh, North Carolina where he graduated with a Bachelor of Science degree in Meteorology and was commissioned through the Detachment 595 Air Force Reserve Officer Training Corps.

His first assignment was at Charleston AFB as a Wing Weather Officer. He was then assigned to the 607th Weather Squadron, Yongsan AIN, Seoul, Republic of Korea and served as the 17th Aviation Brigade Staff Weather Officer and Combat Weather Team OIC. He later became a Staff Weather Officer in the Air Force Operations Group at the Pentagon. While assigned to the Pentagon, he also served as a White House Social Aide. He entered the Graduate School of Engineering and Physics, Air Force Institute of Technology and upon graduation will be assigned to the USAFE Operational Weather Squadron, Sembach AB, Germany.

REPORT DOCUMENTATION PAGE

Form Approved
OMB No. 074-0188

The public reporting burden for this collection of information is estimated to average 1 hour per response, including the time for reviewing instructions, searching existing data sources, gathering and maintaining the data needed, and completing and reviewing the collection of information. Send comments regarding this burden estimate or any other aspect of the collection of information, including suggestions for reducing this burden to Department of Defense, Washington Headquarters Services, Directorate for Information Operations and Reports (0704-0188), 1215 Jefferson Davis Highway, Suite 1204, Arlington, VA 22202-4302. Respondents should be aware that notwithstanding any other provision of law, no person shall be subject to a penalty for failing to comply with a collection of information if it does not display a currently valid OMB control number.

PLEASE DO NOT RETURN YOUR FORM TO THE ABOVE ADDRESS.

1. REPORT DATE (DD-MM-YYYY) March 2004		2. REPORT TYPE Master's Thesis		3. DATES COVERED (From - To) Jun 2003 - Mar 2004	
4. TITLE AND SUBTITLE VERIFICATION OF METEOROLOGICAL DATA REPORTS FROM THE RQ-4A GLOBAL HAWK UNMANNED AERIAL VEHICLE				5a. CONTRACT NUMBER	
				5b. GRANT NUMBER	
				5c. PROGRAM ELEMENT NUMBER	
6. AUTHOR(S) Callis, Steven M., Captain, USAF				5d. PROJECT NUMBER	
				5e. TASK NUMBER	
				5f. WORK UNIT NUMBER	
7. PERFORMING ORGANIZATION NAMES(S) AND ADDRESS(S) Air Force Institute of Technology Graduate School of Engineering and Management (AFIT/ENP) 2950 Hobson Way, Bldg 640 WPAFB OH 45433-7765				8. PERFORMING ORGANIZATION REPORT NUMBER AFIT/GM/ENP/04-03	
9. SPONSORING/MONITORING AGENCY NAME(S) AND ADDRESS(ES) 88 th Weather Squadron 2049 Monahan Way Bldg 91, Area B Wright-Patterson AFB, OH 45433-7204				10. SPONSOR/MONITOR'S ACRONYM(S)	
Global Hawk System Program Office ASC/RAV 2640 Loop Road West Wright-Patterson AFB, OH 45433-7106					
12. DISTRIBUTION/AVAILABILITY STATEMENT APPROVED FOR PUBLIC RELEASE; DISTRIBUTION UNLIMITED					
13. SUPPLEMENTARY NOTES					
14. ABSTRACT Unmanned aerial vehicles (UAVs) have onboard sensors that continuously record weather data during their missions. This information is extremely valuable to both the meteorological and UAV communities with numerous potential benefits, which include improved weather forecast products and additional weather intelligence for military planners. The value of any dataset is directly related to its accuracy and this research determined the accuracy of weather data obtained from a particular UAV, the RQ-4A Global Hawk. This was accomplished through statistical analysis and comparisons with upper-air data and Atmospheric Slant Path Analysis Model (ASPAM) profiles of the atmosphere. Recommendations are provided for the use of this valuable environmental intelligence source to multiple user communities. Similar sensors exist on commercial aircraft using the Aircraft Communications Addressing and Reporting System (ACARS). Data from ACARS-equipped aircraft are compiled and quality controlled by the National Weather Service Forecast Systems Laboratory, then processed and made available to numerous agencies. Personnel use the information not only to enhance their forecast products but also as a data source for ingest into numerical weather prediction models. ACARS data are more spatially and temporally available than rawinsonde data, thus potentially having a more significant impact on upper-air analysis models. Forecasters also use this near-real-time data to enhance their products such as weather warnings and advisories. ACARS information is a proven asset to the weather community as well as mission planners. Methods analogous to the implementation and quality control of ACARS data can also be applied to the information obtained from UAVs since its accuracy is demonstrated in this research. This study illustrates the utility of the UAVs to create on-demand upper-air soundings for any location worldwide, whereas ACARS data are limited to commercial aircraft routes. The use of this data can greatly enhance forecast models and products especially in data-sparse regions, as well as provide a weather reconnaissance capability to military planners.					
15. SUBJECT TERMS Global Hawk, UAV, Verification, Meteorological, Weather, Data					
16. SECURITY CLASSIFICATION OF:			17. LIMITATION OF ABSTRACT	18. NUMBER OF PAGES	19a. NAME OF RESPONSIBLE PERSON
a. REPORT	b. ABSTRACT	c. THIS PAGE			Lt Col Ronald P. Lowther, ENP
U	U	U	UU	120	19b. TELEPHONE NUMBER (Incl area code) (937) 255-3636, ext 4645

Standard Form 298 (Rev. 8-98)
Prescribed by ANSI Std. Z39-18